European air quality maps of PM and ozone for 2010 and their uncertainty

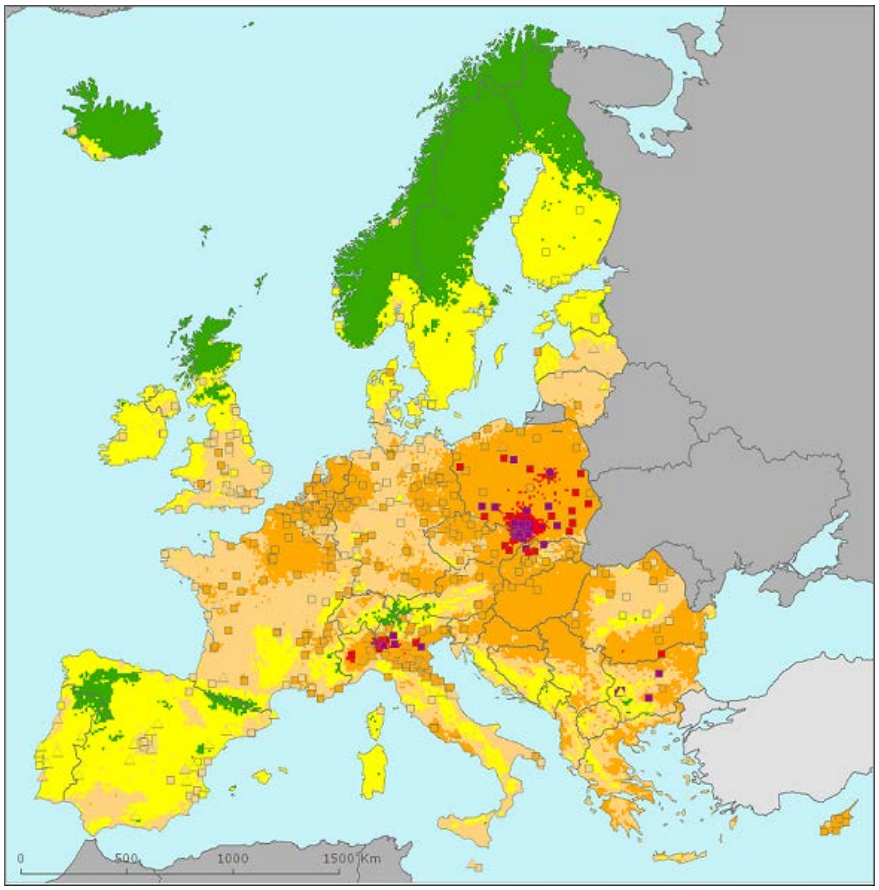

ETC/ACM Technical Paper 2012/12
March 2013

Jan Horálek, Peter de Smet, Linton Corbet,
Pavel Kurfürst, Frank de Leeuw

European Topic Centre
on Air Pollution and
Climate Change Mitigation

The European Topic Centre on Air Pollution and Climate Change Mitigation (ETC/ACM)
is a consortium of European institutes under contract of the European Environment Agency
RIVM UBA-V ÖKO AEAT EMISIA CHMI NILU INERIS PBL CSIC

Front-page picture:
Annual mean PM2.5 concentration in µg.m^{-3} for both rural and urban areas, combined into one final map for the year 2010. Its target value is 25 µg.m^{-3}. (Figure 5.1 of this paper).

Author affiliation:
Jan Horálek, Linton Corbet, Pavel Kurfürst: Czech Hydrometeorological Institute (CHMI), Prague, Czech Republic
Peter de Smet, Frank de Leeuw: National Institute for Public Health and the Environment (RIVM), Bilthoven, The Netherlands

Refer to this document as:
Horálek J, De Smet P, Corbet L,Kurfürst P, De Leeuw F (2013). European air quality maps of PM and ozone for 2010 and analysis of their uncertainty. ETC/ACM Technical paper 2012/12 http://acm.eionet.europa.eu/reports/ETCACC_TP_2012_12_spatAQmaps_2010

DISCLAIMER

This ETC/ACM Technical Paper has not been subjected to European Environment Agency (EEA) member country review. It does not represent the formal views of the EEA.

ETC/ACM Technical Paper 2012/12
European Topic Centre on Air Pollution and Climate Change Mitigation
PO Box 303
3720 AH Bilthoven
The Netherlands
Phone +31 30 2743562
Fax +31 30 2744433
Email etcacm@rivm.nl
Website http://acm.eionet.europa.eu/

Contents

1 Introduction

This paper provides an update of European air quality concentrations, probabilities of exceeding relevant thresholds and population exposure estimates for another consecutive year, 2010. The analysis is based on interpolation of annual statistics of observational data from 2010, reported by EEA Member countries in 2011. The paper presents mapping results and includes an uncertainty analysis of the interpolated maps, adopting the latest methodological developments of Horálek et al. (2007, 2008, 2010) and De Smet et al. (2009, 2010, 2011, 2012).

We again consider in this paper PM_{10} and ozone as being the most relevant pollutants for annual updating. Additionally and for the first time, $PM_{2.5}$ is presented as a third important policy-relevant pollutant and health-impact indicator based on the mapping methodology developed by Denby et al. (2011a, 2011b).

The analysis method for the year 2010 was similar to that for the year 2009. In this paper, we summarise the methodological and data updates applied to the 2010 data.

Next to annual indicator maps, we present in tables the population exposure to PM_{10}, $PM_{2.5}$ and ozone and the exposure of vegetation to ozone. These tables of population exposure are prepared using combined final maps and the population density map of 1x1 km grid resolution. The tables of the exposure of vegetation are prepared with a 2x2 km grid resolution.

For all the maps, we include a quantitative estimate of their interpolation uncertainty, using cross-validation parameters and scatter-plots. In addition, the paper contains the maps with probability estimates of limit/target value exceedances. For presentational purposes at the European scale, we aggregated the maps at 1x1 km grid resolution into maps at 10x10 km grid resolution, leading to considerably smaller figure file sizes.

Chapter 2 describes briefly the applied changes in methodology. Chapter 3 documents the updated input data. Chapters 4, 5 and 6 present the calculations, the mapping, the exposure estimates and the uncertainty results for PM_{10}, $PM_{2.5}$ and ozone respectively. Chapter 7 summarizes the conclusions on exposure estimates and their interpolation uncertainties involved with the interpolated mapping of the air pollutant indicators.

2 Used methodology

2.1 Mapping method

Previous technical papers prepared by the ETC/ACC (Technical Papers 2011/11, 2011/5, 2010/10, 2010/9, 2009/16, 2009/9, 2008/8, 2007/7, 2006/6, 2005/8 and 2005/7) discuss methodological developments and details on spatial interpolations and their uncertainties. No changes took place in the methodology in comparison with the two preceeding reports (De Smet et al., 2011, 2012), resp. with $PM_{2.5}$ mapping methodology paper (Denby et al., 2011b). In this chapter a summary on the currently applied methods is given.

2.1.1 Pseudo $PM_{2.5}$ station data estimation

To supplement measured $PM_{2.5}$ data, we also use data from so-called *pseudo $PM_{2.5}$ stations*. These data are estimates based on measured PM_{10} data and supplementary data at the locations of real $PM_{2.5}$ stations, using linear regression:

$$Z_{PM\,2.5}(s) = c + b.Z_{PM10}(s) + a_1.X_1(s) + ... + a_n.X_n(s) + \varepsilon(s) \quad (2.1)$$

where $Z_{PM\,2.5}(s)$ is the measured value of $PM_{2.5}$ at the station *s*,

$Z_{PM10}(s)$ is the measured value of PM_{10} at the station *s*,

$X_1(s),\ldots, X_n(s)$ are the *n* number of other supplementary variables at the station *s*,

$c, b, a_1,,\ldots, a_n$ are the parameters of the linear regression model calculated at the points of both $PM_{2.5}$ and PM_{10} measurements,

$\varepsilon(s)$ is the random error.

When applying the estimation method, rural and urban/suburban background stations are handled together. For details, see Denby et al. (2011b).

2.1.2 Interpolation

The mapping method used is a linear regression model followed by kriging of the residuals produced from that model (residual kriging). Interpolation is therefore carried out according to the relation:

$$\hat{Z}(s_0) = c + a_1.X_1(s_0) + a_2.X_2(s_0) + ... + a_n.X_n(s_0) + \eta(s_0) \quad (2.2)$$

where $\hat{Z}(s_0)$ is the estimated value of the air pollution indicator at the point s_o,

$X_1(s_0), X_2(s_0),\ldots, X_n(s_0)$ are the *n* number of individual supplementary variables at the point s_o

$c, a_1, a_2,,\ldots, a_n$ are the *n+1* parameters of the linear regression model calculated at the points of measurement,

$\eta(s_0)$ is the spatial interpolation of the residuals of the linear regression model at point of measurement s_o.

Ordinary kriging based on variogram estimates using a spherical function (with parameters: *nugget, sill, range*) is used to interpolate the residuals. For different pollutants and area types (rural, urban), different supplementary data are used, depending on their improvement to the fit of the regression.

For the PM_{10} and $PM_{2.5}$ indicators we apply, prior to linear regression and interpolation, a logarithmic transformation to measurement and EMEP model concentrations. In the case of $PM_{2.5}$ rural data, population is also log-transformed. After interpolation, we apply a back-transformation. For details, see De Smet et al. (2011). In the case of urban $PM_{2.5}$ map, we do not use any supplementary data – we apply just lognormal kriging.

For the vegetation related indicators (AOT40 for crops and forests) we only construct rural maps based on rural background stations, based on the assumption that no vegetation is located in urban areas. For the health related indicators we construct the rural and urban maps separately and then merge them.

2.1.3 Merging of rural and urban maps

Health related indicator maps are constructed (using linear regression with kriging of its residuals) for the rural and urban areas separately on a grid at 10x10 km resolution. The rural map is based on rural background stations and the urban map on urban and suburban background stations. Subsequent to this, the rural and urban maps are merged into one combined air quality indicator map using a European-wide population density grid at 1x1 km resolution. For the 1x1 km grid cells with a population density less than a defined value of α_1, we select the rural map value and for grid cells with a population density greater than a defined value α_2, we select the urban map value. For areas with population density within the interval (α_1, α_2) a weighting function of α_1 and α_2 is applied (for details and the setting of the parameters α_1 and α_2, see Horálek et al., 2010, 2007 and 2005). This applies to the grid cells where the estimated rural value is lower in the case of PM_{10} and $PM_{2.5}$ or higher in the case of ozone, than the estimated urban map value. In the minor areas with grid values for which this criterion does not hold, we apply a joint urban/rural map (created using all background stations regardless their type), as far as its value lies in between the rural and urban map value. For details, see De Smet et al. (2011).

Summarising, the separate rural, urban and joint urban/rural maps are constructed at a resolution of 10x10 km; their merging takes place on basis of the 1x1 km resolution population density grid, resulting in a final combined pollutant indicator map on this 1x1 km resolution grid. This map is then used for population exposure estimates. At times we indicate the applied chain of optimised combinations of spatial resolutions, the process of *interpolation -> merging -> exposure estimate*, as the '10-1-1' (in km). For presentational purposes of European map pictures a spatial aggregation to 10x10 km resolution is sufficient. In all calculations and map presentations the EEA standard projection and datum defined as EEA ETRS89-LAEA5210 is used.

For further details and discussion on subjects briefly addressed in this section, refer to De Smet et al. (2011), chapter 2.

2.2 Calculation of population and vegetation exposure

Population and vegetation exposure estimates are based on the interpolated concentration maps, population density data and land cover data.

2.2.1 Population exposure

Population exposure for individual countries and for Europe as a whole is calculated from the air quality maps and population density data, both at 1x1 km resolution. For each concentration class, the total population per country as well as the European-wide total is determined. In addition, we express per-country and European-wide exposure as the population-weighted concentration, i.e. the average concentration weighted according to the population in a grid cell:

$$\hat{c} = \frac{\sum_{i=1}^{N} c_i p_i}{\sum_{i=1}^{N} p_i} \qquad (2.3)$$

where $\hat{c}$ is the population-weighted average concentration in the country or in the whole Europe,
p_i is the population in the i^{th} grid cell,
c_i is the concentration in the i^{th} grid cell,
N is the number of grid cells in the country or in Europe as a whole.

2.2.2 Vegetation exposure

Vegetation exposure for individual countries and for Europe as a whole is calculated based on the air quality maps and land cover data, both in 2x2 km grid resolution. For each concentration class, the total vegetation area per country as well as European-wide is determined.

2.3 Methods for uncertainty analysis

The uncertainty estimation of the European map is based on cross-validation. The cross-validation method computes the quality of the spatial interpolation for each measurement point from all available information except from the point in question, i.e. it withholds one data point and then makes a prediction at the spatial location of that point. This procedure is repeated for all measurement points in the available set. The predicted and measured values at these points are plotted in the form of a scatter plot. With help of statistical indicators the quality of the predictions is demonstrated objectively – no suppositions have to be fulfilled. The advantage of the nature of this cross-validation technique is that it enables evaluation of the quality of the predicted values at locations without measurements, as long as they are within the area covered by the measurements.

In addition, we make a simple comparison between the point measurements and interpolated values of the 10x10 km grid (or the 2x2 km grid in the case of AOT40). Where the 10x10 km grid is used, the grid value is the averaged result of the 1x1 km interpolations in each area. The interpolated value within a grid cell will only approximate the predicted value(s) at the station(s) lying within that cell.

Another method to estimate uncertainties is based on geostatistical theory: together with the prediction, the prediction standard error is computed at all the grid cells, which represents in fact the interpolation uncertainty map (see Cressie, 1993 for a detailed discussion). Based on the concentration and the uncertainty map the exceedance probability map is created.

2.3.1 Cross-validation

The results of cross-validation are described by the statistical indicators and scatter plots. The main indicator used is root mean squared error (RMSE) and additional is the mean prediction error (MPE) or bias:

$$RMSE = \sqrt{\frac{1}{N}\sum_{i=1}^{N}(\hat{Z}(s_i) - Z(s_i))^2} \tag{2.4}$$

$$MPE = \frac{1}{N}\sum_{i=1}^{N}(\hat{Z}(s_i) - Z(s_i)) \tag{2.5}$$

where $Z(s_i)$ is the measured concentration at the i^{th} point, $i = 1, \ldots, N$,

$\hat{Z}(s_i)$ is the estimated concentration at the i^{th} point using other information, without the measured concentration at the i^{th} point,

N is the number of the measuring points.

RMSE should be as small as possible, MPE should be as close to zero as possible.

In the cross-validation of $PM_{2.5}$, only stations with measured $PM_{2.5}$ data are used (not pseudo $PM_{2.5}$ stations).

2.3.2 Comparison of the point measured and interpolated grid values

The comparison of measured and predicted grid values is described by the linear regression equation and its parameters and statistical values. The comparison is executed separately for rural and urban maps. In the case of $PM_{2.5}$, only the stations with measured $PM_{2.5}$ data are used.

The point-point cross-validation analysis (Section 2.3.1) describes interpolation performance at point locations when there is no observation (as it follows the leave-one-out approach). In this case the smoothing effect of the interpolation is most prevalent. The point-grid approach (Section 2.3.2) indicates performance of the value for each 10x10 km grid-cell with respect to the observations that are within such a cell. As such, some variability is due to smoothing but it also includes smoothing due to spatial averaging into the 10x10 km cells. Therefore, the point-grid approach tells us how well our interpolated and aggregated values approximate the measurements where there are measurements and the point-point approach tells us how well our interpolated values estimate the indicator when there are no measurements.

2.3.3 Exceedance probability mapping

The maps with the probability of exceedance (PoE) of a specific threshold value (e.g. limit or target value) are constructed using the concentration and uncertainty maps:

$$PoE(x) = 1 - \Phi\left(\frac{LV - C_c(x)}{\delta_c(x)}\right) \tag{2.6}$$

where $PoE(x)$ is the probability of limit/target value (*LV/TV*) exceedance in the grid cell *x*,
$\Phi(\,)$ is the cumulative distribution function of the normal distribution,
LV is the limit or target value of the relevant indicator,
$C_c(x)$ is the interpolated concentration in the grid cell *x*,
$\delta_c(x)$ is the standard error of the estimation in the grid cell *x*.

The standard error of the probability map of the combined (rural and urban) map is calculated from the standard errors of the separate rural and urban maps, see Horálek et al. (2008) and De Smet et al. (2011). The maps with the probability of threshold value exceedance (PoE) are constructed in 10x10 km grid resolution.

3 Input data

The types of input data in this paper are not different from that of De Smet et al. (2012). The air quality, meteorological and, where possible, the supplementary data has been updated. No further changes in selecting and processing the input data have been implemented. For readability of this paper, we reproduce here the list of the input data. The key data is the air quality measurements at the monitoring stations extracted from AirBase, including geographical coordinates (*latitude, longitude*). The supplementary data cover the whole mapping domain and are converted into the EEA reference projection ETRS89-LAEA5210 on a grid of 10x10 km resolution. The data for the AOT40 maps, however, were converted – like last year – into a 2x2 km resolution to allow accurate land cover exposure estimates to be prepared for use in Core Set Indicator 005 of the EEA.

3.1 Measured air quality data

Air quality station monitoring data for the relevant year are extracted from the European monitoring database AirBase (Mol et al. 2012). This data set is supplemented by several rural stations from the database EBAS (http://ebas.nilu.no) not reported to AirBase. Only data from stations classified by AirBase and/or EBAS of the type *background* for the areas *rural*, *suburban* and *urban* are used. *Industrial* and *traffic* station types are not considered; they represent local scale concentration levels not applicable at the mapping resolution employed. The following substances and their indicators are considered:

PM_{10} – annual average [µg.m^{-3}], year 2010
– 36th highest daily average value [µg.m^{-3}], year 2010

$PM_{2.5}$ – annual average [µg.m^{-3}], year 2010

Ozone – 26th highest daily maximum 8-hour average value [µg.m^{-3}], year 2010
– SOMO35 [µg.m^{-3}.day], year 2010
– AOT40 for crops [µg.m^{-3}.hour], year 2010
– AOT40 for forests [µg.m^{-3}.hour], year 2010

SOMO35 is the annual sum of maximum daily 8-hour concentrations above 70 µg.m^{-3} (i.e. 35 ppb). AOT40 is the sum of the differences between hourly concentrations greater than 80 µg.m^{-3} (i.e. 40 ppb) and 80 µg.m^{-3}, using only observations between 7:00 and 19:00 UTC, calculated over the three months from May to July (AOT40 for crops), respectively over the six months from April to September (AOT40 for forests). Note that the term *vegetation* as used in the ozone directive is not further defined. Comparing the definitions in the Mapping Manual (UNECE, 2004) and those in the ozone directive suggests that we have to interpret the term *vegetation* in the ozone directive as agricultural crops. The exposure of *agricultural crops* has been evaluated here on basis of the AOT40 for vegetation as defined in the ozone directive.

For the indicators relevant to human health (i.e. PM_{10}, $PM_{2.5}$ and for ozone the 26th highest daily maximum 8-hour average and SOMO35) data from *rural*, *urban* and *suburban background* stations are considered. For the indicators relevant to vegetation damage (both AOT40 parameters for ozone) only *rural background* stations are considered.

Only the stations with annual data coverage of at least 75 percent are used. We excluded the stations from French overseas areas (departments), Svalbard, Azores, Madeira and Canary Islands and also eastern Turkey (which is outside the EEA map extent *Map_1c* (EEA 2011)). These areas we excluded from the interpolation and mapping domain. To reach a more extended spatial coverage by measurement data we use, in addition to the AirBase data, seven additional rural background PM_{10} stations and nine rural background $PM_{2.5}$ stations from the EBAS database. Table 3.1 shows the number of the measurement stations selected for the individual pollutants and their respective indicators. Compared to 2009, the number of stations selected for 2010 increased for the PM_{10} health indicators by approximately 14 % for rural and 1 % for urban background stations. For ozone, both for health and vegetation related indicators, the numbers of stations remained approximately the same.

Table 3.1 Number of stations selected for individual indicators and areas. Rural background stations are used for rural areas. Urban and suburban background stations are used for urban areas.

	PM10		PM2.5	ozone			
	annual average	36th daily maximum	annual average	26th highest daily max. 8h	SOMO35	AOT40 for crops	AOT40 for forests
rural	329	329	113	499	499	508	501
urban	1108	1108	378	989	989		

For $PM_{2.5}$ mapping an additional 233 rural background and 789 urban/suburban background PM_{10} stations (in the places with no $PM_{2.5}$ measurement) were also used for the purpose of calculating the pseudo $PM_{2.5}$ station data.

3.2 Unified EMEP model output

The chemical dispersion model used was the Unified EMEP model (revision rv4.0), which is an Eulerian model with a resolution of 50x50 km. Information from this model was sampled at 10x10 km grid resolution for the interpolation process.

As per the previous year, we received the EMEP data in the form of daily means for PM_{10} and $PM_{2.5}$ and hourly means for ozone. We aggregated these primary data according annex B of Mol et al. (2012) to the same set of parameters as we have them for the air quality observations:

PM_{10} – annual average [µg.m^{-3}], year 2010 (aggregated from daily values)
– 36th highest daily average value [µg.m^{-3}], year 2010 (aggregated from daily values)

$PM_{2.5}$ – annual average [µg.m^{-3}], year 2010 (aggregated from daily values)

Ozone – 26th highest daily maximum 8-hour average value [µg.m^{-3}], year 2010 (aggregated from hourly values)
– SOMO35 [µg.m^{-3}.day], year 2010
– AOT40 for crops [µg.m^{-3}.hour], year 2010 (aggregated from hourly values)
– AOT40 for forests [µg.m^{-3}.hour], year 2010 (aggregated from hourly values)

Simpson et al. (2003, 2012) and http://www.emep.int/OpenSource/index.html (EMEP web site) describe the model in more detail. Emissions for the relevant year (Mareckova et al. 2012) are used and the model is driven by ECMWF meteorology. Fagerli et al. (2012) provides details on the EMEP modelling for 2010.

In the original format, a point represents the centre of a grid cell (in 50x50 km resolution). The data are imported into *ArcGIS* as a point shapefile, subsequently converted into a 200x200 m resolution raster grid and spatially aggregated into the reference EEA 10x10 km grid.

3.3 Altitude

We use the altitude data field (in meters) of GTOPO30 that covers the European continent, with an original grid resolution of 30 x 30 arcseconds. The field is converted into a resolution of 200x200 m and spatially aggregated into the reference EEA 10x10 km grid and 2x2 km grid. For details, see Horálek et al. (2007).

3.4 Meteorological parameters

Actual meteorological surface layer parameters we extracted from the Meteorological Archival and Retrieval System (MARS) of the ECMWF (European Centre for Medium-range Weather Forecasts). Currently we use the following ECMWF variables (details specified in Horálek et al. 2007, Section 4.5) as supplementary data in the regressions:

Wind speed – annual average [m.s^{-1}], year 2010
Surface solar radiation – annual average [MWs.m^{-2}], year 2010

3.5 Population density and population totals

Population density (in inhbs.km^{-2}, census 2001) is based on JRC data for the majority of countries (JRC, 2009) – source: EEA, pop01clcv5.tif, official version 5, 24 Sep. 2009, resolution 100x100 m.

For countries (Andorra, Albania, Bosnia-Herzegovina, Iceland, Liechtenstein, FYR of Macedonia, Montenegro, Norway, Serbia, Switzerland and Turkey) and regions (Faroe Islands, Jersey, Guernsey, Man and northern part of Cyprus) which are not included in this map we used population density data from an alternative source: ORNL LandScan Global Population Dataset (ORNL, 2008).

The ORNL data is reprojected and converted from its original WGS1984 30x30 arcsec grids into EEA's reference projection ETRS89-LAEA5210 at 1x1 km resolution by EEA (eea_r_3035_1_km_landscan-eurmed_2008, EEA (2008)). The ORNL data was compared with JRC data for countries covered by both data sources and when this was not possible Eurostat national population data for 2010 (Eurostat, 2012) was used. Figure 3.1 presents this comparison based on the national population totals of the individual countries.

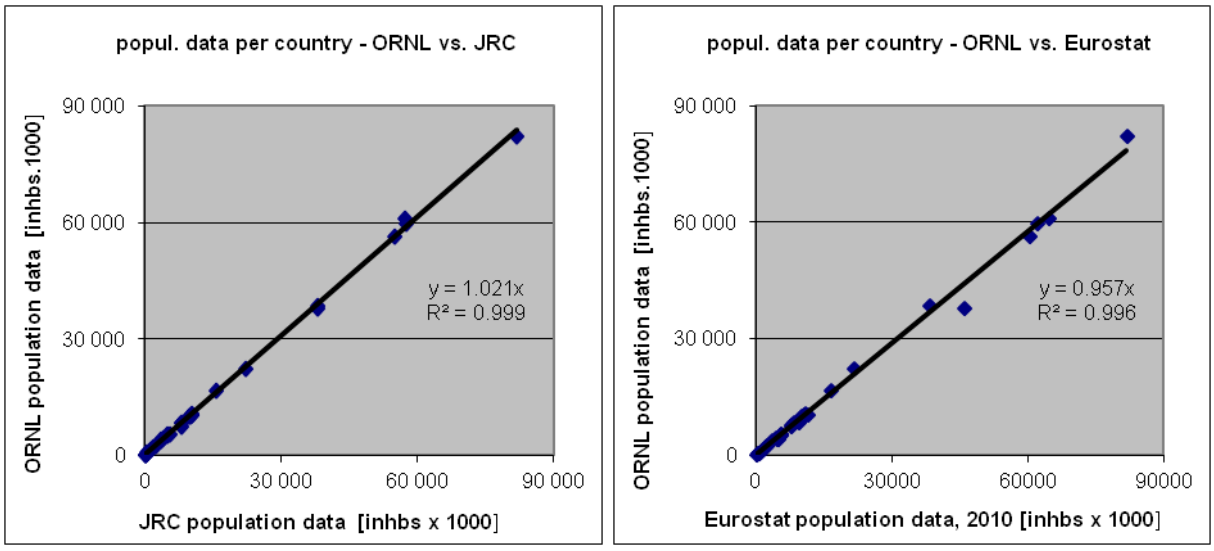

Figure 3.1 Correlation between ORNL (y-axis) and JRC (x-axis, left), respectively Eurostat 2010 revision (x-axis, right) national population totals.

Population density data can be used to classify the spatial distribution of each type of area (rural, urban or mixed population density) in Europe. We use this information to select and weight the air quality value, grid cell by grid cell. Furthermore, we use it to estimate population health exposure and exceedance numbers per country and for Europe as a whole, including involved uncertainties. These activities take place on the 1x1 km resolution grid in accordance with the recommendations of Horálek et al. (2010). For presentational purposes, we construct maps on the 10x10 km resolution grid. To facilitate all this, we aggregated the JRC 100x100 m population density data into a 1x1 km grid, merged that with the ORNL dataset and aggregated the result into the 10x10 km resolution map.

Population totals for individual countries presented in exposure tables in Sections 4.2, 5.2 and 6.2 are based on Eurostat national population data for 2010 (Eurostat, 2012). For countries (Andorra, Albania, Bosnia-Herzegovina, Monaco, San Marino and Serbia) which are not included in the Eurostat database, the population totals are based on UN (2010) for 2010.

3.6 Land cover

CORINE Land Cover 2000 – grid 100 x 100 m, version 16 (04/2012) is used (CLC2000 – 100m, g100_00.zip; EEA, 2012). The countries missing in this database are Andorra and Turkey.

4 PM_{10} maps

This chapter presents the 2010 updates (for the interpolated map and exposures) of the two PM_{10} health indicators: annual average and 36th highest daily average. The separate urban and rural concentration maps were calculated on the 10x10 km resolution grid and the subsequent combined concentration map was based on the 1x1 km gridded population density map. The population exposure tables were calculated at 1x1 km grid resolution. All maps here are presented using the 10x10 km grid resolution. The standard EEA ETRS89-LAEA5210 coordinate reference system was applied.

4.1 Annual average

4.1.1 Concentration map

Figure 4.1 presents the combined final map for the 2010 PM_{10} annual averages as the result of interpolation and merging of the separate maps as described in detail in De Smet et al. (2011) and Horálek et al. (2007). Red and purple areas and stations exceed the limit value (LV) of 40 µg.m^{-3}. Supplementary data in the regression used for rural areas consisted of EMEP model output, altitude, wind speed and surface solar radiation and for urban areas it was EMEP model output only. (The relevant linear regression submodels have been identified earlier in Horálek et al. (2008) and De Smet et al. (2009, 2010, 2011) as P.Eawr and UP.E, respectively.)

As one can observe, in a few areas of the map (Bulgaria, Poland) the high urban background measurement values do not seem to influence the interpolation results despite their clustering. The main reason is that the map presented here is an aggregation of 1 km^2 grid values to a 10 km^2 resolution and this aggregation smoothes out the elevated values one would more likely be able to distinguish in the higher resolution map, especially in the case of urban background stations representing the urban areas. (Therefore, the exposure estimates of Table 4.2 are derived just from the 1x1 km grid map.) Another less prominent reason is the smoothing effect kriging has in general. However, kriging would in the case of clustering not mask these elevations in the separate 1x1 km urban and rural maps.

Table 4.1 presents the estimated parameters of the linear regression models (c, a_1, a_2,…) and of the residual kriging (*nugget, sill, range*) and includes the statistical indicators of both the regression and the kriging. The adjusted R^2 and standard error are indicators for the fit of the regression relationship, where the adjusted R^2 should be as close to 1 as possible and the standard error should be as small as possible. The adjusted R^2 was 0.44 for the rural areas and 0.38 for urban areas. The R^2 values show a better fit of the regression than observed at all previous years, i.e. 2009 (0.38 and 0.06), 2008 (0.29 and 0.00), 2007 (0.40 and 0.10), 2006 (0.29 and 0.03) and 2005 (0.28 and 0.06) (De Smet et al. 2012, 2011, 2010 and 2009, Table 4.1; Horálek et al. 2008, Tables A.21 and A2.6). Obvious improvement of the regression fit in the urban areas compared to previous years was detected. The reason probably is the improvement of the EMEP model. RMSE and MPE are the cross-validation indicators, showing the quality of the resulting map; the MPE indicates to what extent the estimation is un-biased. Sections 4.1.2 and 4.1.3 deal with a more detailed analysis and compares with results of 2009, 2008, 2007, 2006 and 2005.

As indicated in Table 4.1, surface solar radiation was, in contrast to previous years, found to be statistically non-significant and thus it was not used in 2010 mapping.

Table 4.1 Parameters of the linear regression models (Eq. 2.2) and of the ordinary kriging variograms (nugget, sill, range) - and their statistics - of PM_{10} indicator annual average for 2010 in rural (left) and urban (right) areas as used for the combined final map. The linear regression models were P.Eawr (rural areas) and UP.E (urban areas). Interpolation of regression residuals using ordinary kriging (OK) is indicated by '-a').

linear regr. model + OK on its residuals	rural areas (lnP.Eawr-a) coeff.	urban areas (lnUP.E-a) coeff.
c (constant)	2.02	1.59
a1 (log. EMEP model 2010)	0.585	0.66
a2 (altitude GTOPO)	-0.00045	
a3 (wind speed 2010)	-0.107	
a4 (s. solar radiation 2010)	n. sign.	
adjusted R^2	**0.44**	**0.38**
standard error [µg.m^{-3}]	**0.30**	**0.29**
nugget	0.035	0.010
sill	0.052	0.062
range [km]	520	770
RMSE [µg.m^{-3}]	**4.50**	**6.60**
MPE [µg.m^{-3}]	**0.20**	**-0.15**

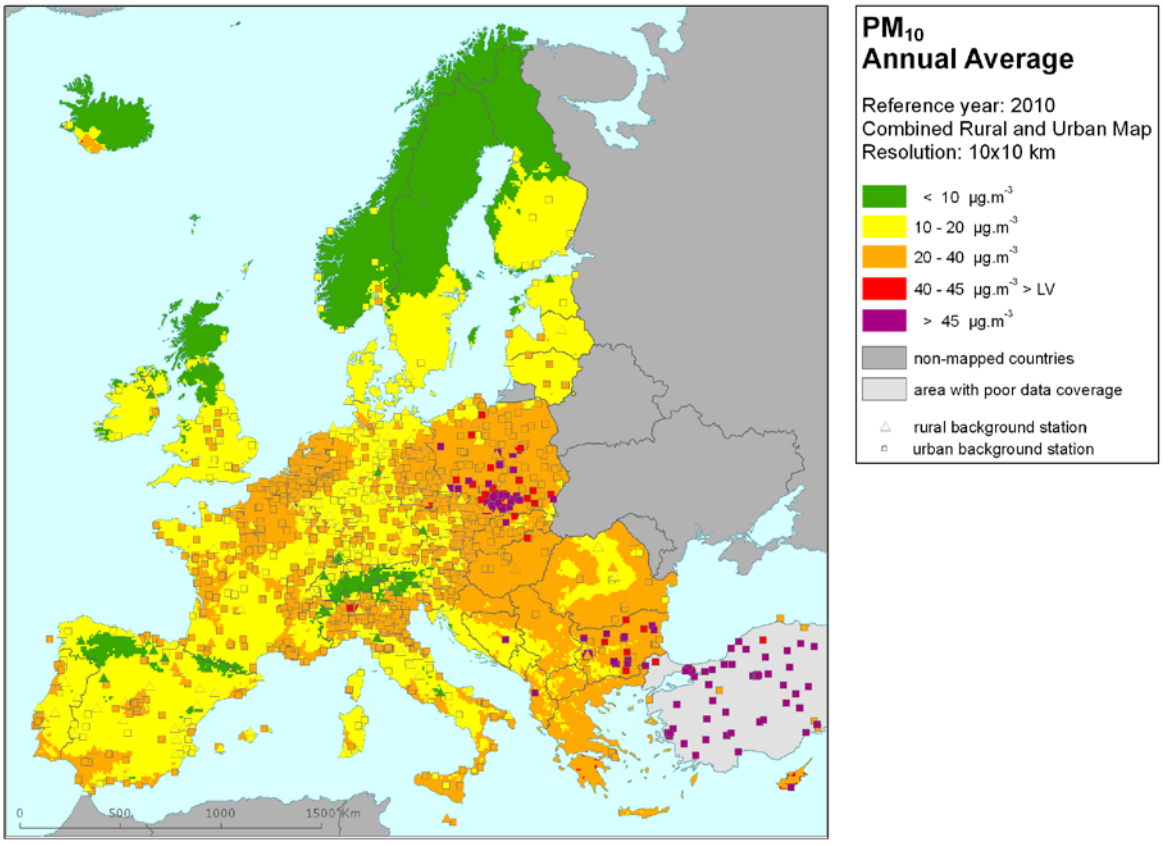

Figure 4.1 Combined rural and urban concentration map of PM_{10} – annual average, year 2010. Spatial interpolated concentration field (10x10 km grid resolution, excluding Turkey due to lack of rural air quality data) and the measured values in the measuring points. Units: µg.m^{-3}.

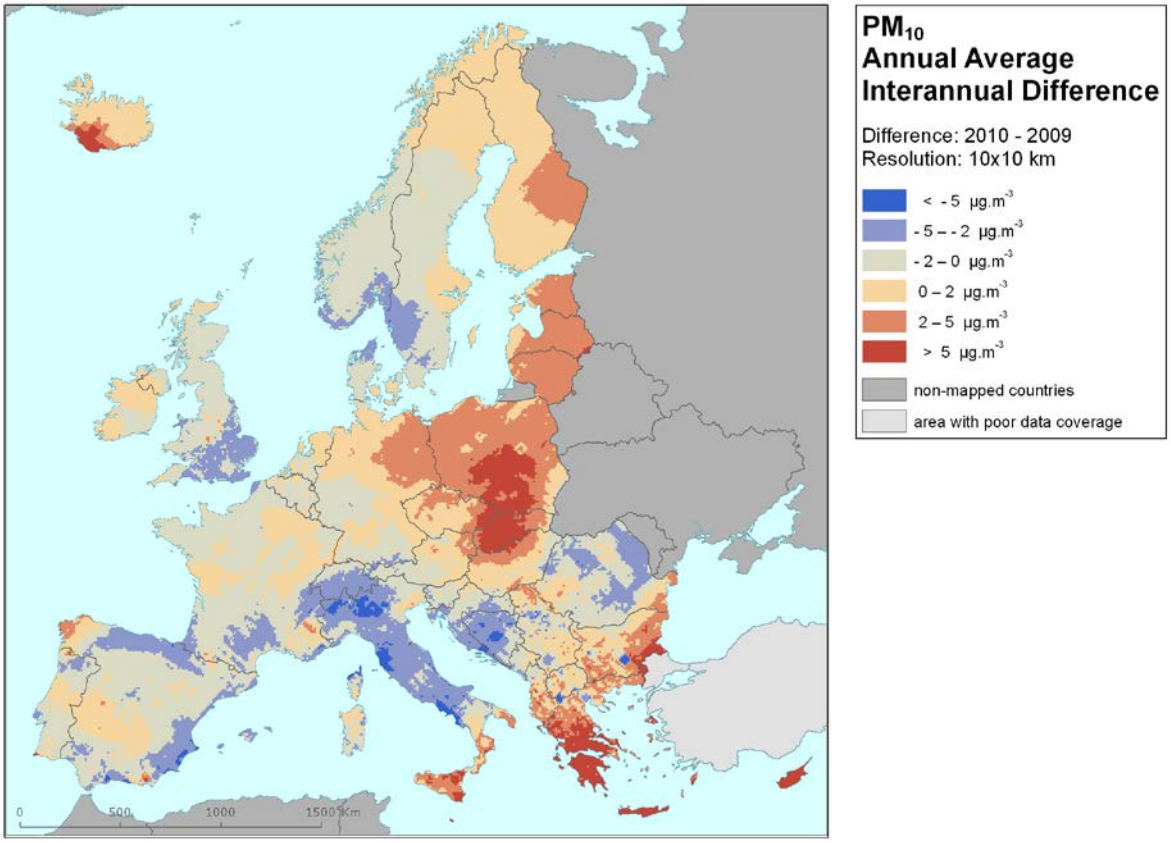

Figure 4.2 Interannual difference between mapped concentrations for 2010 and 2009 – PM_{10}, annual average. Units: $\mu g.m^{-3}$.

Figure 4.2 presents the interannual difference between 2010 and 2009 for annual average PM_{10}. Red areas show an increase of PM_{10} concentration, while blue areas show a decrease. The highest increases can be seen in southern Poland, Slovakia, south-eastern Iceland (caused by the volcanic activity of Eyjafjallajökull), southern Greece and Cyprus.

4.1.2 Population exposure

Table 4.2 gives the population frequency distribution for a limited number of exposure classes calculated at the 1x1 km grid resolution, as well as the population-weighted concentration for individual countries and for Europe as a whole according to Equation 2.2 of De Smet et al. (2010).

Almost 30 % of the European population has been exposed to annual average concentrations below 20 $\mu g.m^{-3}$, the WHO (World Health Organization) air quality guideline. De Leeuw and Ruyssenaars (2011) estimate that 80-90 % of the urban population is exposed to levels above the WHO guideline reference level, i.e. 10-20 % is below the WHO reference level. This lower amount specifically accounts only for the urban population in the larger cities of Europe. It therefore represents areas where, in general, considerably higher PM_{10} concentrations occur throughout the year. The estimate of Table 4.2 (29.3%) includes the total European population, including inhabitants in the rural areas, the smaller cities and the villages which are, in general, exposed to lower levels of PM_{10} throughout the year. It is important to note that this difference in WHO reference level exposure estimates is explained by the use of different population characteristics and area representation in the calculations. Two-thirds of the European population in 2010 lived in areas where the PM_{10} annual mean

concentration was estimated to be between 20 and 40 $\mu g.m^{-3}$. About 5 % of the population lived in areas where the PM_{10} annual limit value was exceeded, with Albania, Cyprus and FYR of Macedonia showing a population-weighted concentration and a median above the LV. However, as the next Section 4.1.3 discusses, the current mapping methodology tends to underestimate high values. Therefore, the exceedance percentage would most likely be higher and precipitate exceedances at additional countries, for example Bulgaria.

The merging of the separate rural and urban maps takes place on a 1x1 km resolution grid of population density. The application of this high resolution merging process, now for the third consecutive year, induces a shift in the distribution of population over the different exposure classes as well as in the population-weighted concentrations. In order to enable the comparison of the results also with the earlier years, the results for the year 2007 were re-calculated, using this new methodology.

The evolution of population exposure in the last five years is presented in Table 4.3, based on results presented in previous reports (De Smet et al., 2012, 2011) for the years 2009 and 2008, based on the recalculated results for 2007 and based on the paper with the tests of new methodology (Horálek et al., 2010) for 2006.

The frequency distribution shows large variability over Europe, with many countries showing exposures above the limit value both in 2009 as well as in 2010; some with considerable increase, others with a decrease. Cyprus and FYR of Macedonia, with about 66% or more exposure in 2008 and 2009, still have similar percentages of their populations exposed to levels above the LV (CY 83%, MK 70%). Romania's exceedance exposure reduced considerably from about one-third in 2007 and one-fifth in 2008 to approximately 4% in 2009 and 2% in 2010.

Several countries with hardly any or no exceedances in 2007 did show elevated PM_{10} annual averages well above the limit value in 2008 and beyond. For example, in Cyprus this situation continues with 87 % in 2008, 73% in 2009 and 83 % in 2010. The values in Cyprus are influenced by the limited number of the stations reported (two). Similarly, Albania shows 7 % in 2008, 52 % in 2009 and 63 % in 2010, likely caused by the limited number of stations (two in 2009, one in 2010).

Bosnia and Herzegovina (0 % in 2008, 52 % in 2009 and 17 % in 2010), Serbia (62 % in 2008, 55 % in 2009 and 21 % in 2010) and Montenegro (36 % in 2008, 60 % in 2009 and 42 % in 2010) had limited numbers of stations. The strong fluctuation between the three years may have its cause in this limited number of stations as well as inter-annual variability induced by different dispersion conditions.

The area in exceedance in Poland increased steeply from the 12 - 15 % in 2007 – 2009 to about 30 % in 2010. The Czech Republic increased from 3 % in 2009 to 9% in 2010, Slovakia from 1% to 3%. Italy and Croatia are the only two countries with exceedances in 2009 and no exceedance in 2010.

In a number of countries in northern and north-western Europe, the LV of 40 μg.m^{-3} seems to continue to not be exceeded. When comparing between years the population exposed to the low levels, i.e. below 20 μg.m^{-3}, it is found that the percentage for 2010 (29 %) is roughly the same as in 2009 (29 %) and 2008 (31 %) but that it is higher than for the years 2007 with 24 % and 2006 with 20 %. This tendency of reducing exposure of the population living in areas with concentrations above the limit value, established in previous years (from 10.3 % in 2006 to 6.8 % in 2007 and 5.8 % in 2008) seems to continue with a value of 5.2 % in 2010. The tendency comes with a degree of uncertainty however as an increase in 2009 (to 6.0%) occurred.

Table 4.2 Population exposure and population-weighted concentration – PM_{10}, annual average, year 2010. Resolution: 1x1 km.

Country		Population	2010 Percent [%]					Population-weighted conc.
			< LV			> LV		
			< 10	10 - 20	20 - 40	40 - 45	> 45	
		x 1000	μg.m^{-3}	μg.m^{-3}	μg.m^{-3}	μg.m^{-3}	μg.m^{-3}	μg.m^{-3}
Albania	AL	3 204	0	4.8	32.6	4.4	58.2	45.5
Andorra	AD	85	9.8	90.2	0	0	0	17.9
Austria	AT	8 375	1.0	23.7	75.3	0	0	22.7
Belgium	BE	10 840	0	3.3	96.7	0	0	25.7
Bosnia-Herzegovina	BA	3 760	0.0	15.8	67.0	17.0	0.1	30.8
Bulgaria	BG	7 564	0	1.8	49.1	19.5	29.5	38.0
Croatia	HR	4 426	0.0	10.1	89.9	0	0	27.3
Cyprus	CY	819	0	0	17.3	5.3	77.4	50.2
Czech Republic	CZ	10 507	0	6.6	83.9	2.1	7.3	28.3
Denmark	DK	5 535	0.3	99.3	0.4	0	0	15.7
Estonia	EE	1 340	1.1	98.9	0	0	0	14.1
Finland	FI	5 351	9.7	90.3	0	0	0	12.2
France	FR	64 694	0.0	18.4	81.6	0	0	23.0
Germany	DE	81 802	0.0	35.5	64.5	0	0	21.2
Greece	GR	11 305	0	0.2	78.9	12.2	8.8	37.3
Hungary	HU	10 014	0	0.0	100.0	0	0	28.1
Iceland	IS	318	21.0	78.3	0.6	0.1	0	10.7
Ireland	IE	4 468	1.7	98.1	0.2	0	0	13.7
Italy	IT	60 340	0.2	13.9	85.8	0	0	26.4
Latvia	LV	2 248	0	38.1	61.9	0	0	21.5
Liechtenstein	LI	36	0.2	99.8	0	0	0	17.3
Lithuania	LT	3 329	0	39.7	60.3	0	0	22.0
Luxembourg	LU	502	0	39.5	60.5	0	0	19.4
Macedonia, FYR of	MK	2 053	0	3.8	26.2	9.5	60.5	43.9
Malta	MT	414	0	0	100	0	0	32.5
Monaco	MC	35	0	0	100	0	0	24.0
Montenegro	ME	616	0.0	23.2	34.7	40.5	1.6	32.8
Netherlands	NL	16 575	0	0.1	99.9	0	0	24.3
Norway	NO	4 858	28.3	51.0	20.8	0	0	14.7
Poland	PL	38 167	0	1.8	68.2	14.7	15.3	35.2
Portugal	PT	10 638	0.2	35.2	64.6	0	0	21.7
Romania	RO	21 462	0	13.6	84.5	2.0	0	25.2
San Marino	SM	32	0	11.0	89.0	0	0	25.0
Serbia (incl. Kosovo)	RS	9 856	0	2.6	76.6	6.1	14.6	33.1
Slovakia	SK	5 425	0	0.7	96.4	2.8	0.2	30.2
Slovenia	SI	2 047	0	9.0	91.0	0	0	26.0
Spain	ES	45 989	0.9	31.3	67.8	0	0	21.4
Sweden	SE	9 341	9.0	91.0	0	0	0	12.8
Switzerland	CH	7 786	1.7	34.6	63.7	0	0	19.8
United Kingdom	UK	62 027	1.7	73.3	25.0	0	0	18.2
Total		**538 185**	**0.9**	**28.4**	**65.6**	**2.2**	**3.0**	**24.3**
			29.3			**5.2**		

Note: Turkey is not included in the calculation due to lacking air quality data.

Table 4.3 Evolution of percentage population living in above limit value (left) and population-weighted concentration (right) in the years 2006-2010 – PM_{10}, annual average. Resolution: 1x1 km.

Country		Population above LV 40 µg.m^{-3} [%]						Population-weighted conc. [µg.m^{-3}]					
		2006	2007	2008	2009	2010	diff. '10 - '09	2006	2007	2008	2009	2010	diff. '10 - '09
Albania	AL	3.1	0.1	6.5	52.1	62.6	10.5	31.8	31.6	33.3	35.3	45.5	10.1
Andorra	AD	0	0	0	0	0	0	22.5	20.5	18.7	17.7	17.9	0.2
Austria	AT	0	0	0	0	0	0	26.0	22.1	21.3	21.6	22.7	1.1
Belgium	BE	0	0	0	0	0	0	31.3	24.8	23.9	26.5	25.7	-0.8
Bosnia-Herzegovina	BA	6.9	3.3	0.0	51.6	17.2	-34.4	33.1	32.4	29.3	37.2	30.8	-6.4
Bulgaria	BG	49.9	42.1	62.1	53.8	49.0	-4.8	41.6	40.2	44.2	39.8	38.0	-1.9
Croatia	HR	0.1	0	0	3.0	0	-3.0	31.5	30.0	28.1	29.0	27.3	-1.7
Cyprus	CY	0	0	87.0	73.0	82.7	9.7	35.4	33.9	76.1	41.0	50.2	9.2
Czech Republic	CZ	13.8	1.8	1.7	3.3	9.4	6.1	33.5	25.6	24.2	25.3	28.3	2.9
Denmark	DK	0	0	0	0	0	0	23.5	20.8	18.8	16.3	15.7	-0.5
Estonia	EE	0	0	0	0	0	0	19.7	15.7	12.9	13.4	14.1	0.6
Finland	FI	0	0	0	0	0	0	17.0	13.7	12.5	11.7	12.2	0.5
France	FR	0	0	0	0	0	0	20.4	24.6	22.6	24.0	23.0	-1.0
Germany	DE	0	0	0	0	0	0	24.2	20.7	19.6	20.7	21.2	0.6
Greece	GR	3.6	1.5	37.0	23.4	20.9	-2.5	33.6	33.5	39.7	35.3	37.3	2.0
Hungary	HU	2.2	0	0	0	0	0	32.9	28.7	26.8	27.6	28.1	0.5
Iceland	IS	0	0	0	0	0.1	0.1	17.4	12.2	15.2	9.0	10.7	1.7
Ireland	IE	0	0	0	0	0	0	14.9	14.7	15.4	12.8	13.7	0.9
Italy	IT	24.2	19.8	2.7	8.8	0	-8.8	33.9	33.2	30.1	28.7	26.4	-2.3
Latvia	LV	0	0	0	0	0	0	21.9	17.8	19.1	18.8	21.5	2.8
Liechtenstein	LI	0	0	0	0	0	0	24.9	20.7	20.6	18.3	17.3	-1.0
Lithuania	LT	0	0	0	0	0	0	22.5	18.5	17.3	19.0	22.0	3.1
Luxembourg	LU	0	0	0	0	0	0	20.8	19.5	18.2	21.0	19.4	-1.6
Macedonia, FYR of	MK	61.3	52.1	67.8	74.5	70.0	-4.5	39.3	38.5	41.6	45.4	43.9	-1.6
Malta	MT	0	0	0	0	0	0	29.4	27.0	27.5	27.2	32.5	5.4
Monaco	MC	0	0	0	0	0	0	36.7	34.5	29.5	26.8	24.0	-2.8
Montenegro	ME	9.7	1.3	38.7	61.1	42.1	-19.0	33.1	33.1	33.6	35.0	32.8	-2.2
Netherlands	NL	0	0	0	0	0	0	29.1	25.8	24.0	24.3	24.3	0.0
Norway	NO	0	0	0	0	0	0	19.6	15.6	15.7	14.1	14.7	0.7
Poland	PL	28.5	13.4	12.4	14.7	30.0	15.3	37.0	28.8	28.3	30.8	35.2	4.4
Portugal	PT	0	0	0	0	0	0	28.4	27.0	21.8	22.9	21.7	-1.2
Romania	RO	47.0	32.0	19.6	4.0	2.0	-2.0	39.1	35.0	30.8	28.9	25.2	-3.8
San Marino	SM	0	0	0	0	0	0	33.9	31.2	29.6	26.0	25.0	-1.0
Serbia (incl. Kosovo)	RS	66.0	59.1	61.8	55.5	20.7	-34.8	41.8	39.4	40.1	39.5	33.1	-6.3
Slovakia	SK	16.3	2.4	1.7	1.2	3.0	1.8	33.8	29.1	26.7	26.9	30.2	3.2
Slovenia	SI	0	0	0	0	0	0	29.0	27.2	25.0	25.2	26.0	0.8
Spain	ES	7.5	2.6	1.3	0	0	0	31.4	29.6	25.2	23.7	21.4	-2.2
Sweden	SE	0	0	0	0	0	0	19.0	15.7	16.3	13.8	12.8	-1.0
Switzerland	CH	0.9	0	0	0	0	0	23.2	21.4	20.5	21.0	19.8	-1.2
United Kingdom	UK	0	0	0	0	0	0	23.2	21.6	19.5	18.4	18.2	-0.2
Total		**10.3**	**6.8**	**5.8**	**6.0**	**5.2**	**-0.8**	**28.5**	**26.2**	**24.8**	**24.6**	**24.3**	**-0.3**

Considering the average for the whole of Europe, the overall population-weighted annual mean PM_{10} concentration in 2010 was 24.3 µg.m^{-3}. This is slightly lower than previous years: 0.3 µg.m^{-3} lower than in 2009, 0.5 µg.m^{-3} lower than in 2008, 1.9 µg.m^{-3} lower than in 2007 and 4.2 µg.m^{-3} lower than in 2006 (Table 4.3). The slight decrease of the population-weighted concentration in comparison with 2009, 2008, 2007 and 2006 occured mainly in EU countries with few to no limit value exceedances.

4.1.3 Uncertainties

Uncertainty estimated by cross-validation

Using RMSE as the most common indicator, the *absolute mean uncertainty* of the combined final map at areas 'in between' the station measurements can be expressed in µg.m^{-3}. Table 4.1 shows that the absolute mean uncertainty of the combined final map of PM_{10} annual average expressed by RMSE is 4.5 µg.m^{-3} for the rural areas and 6.6 µg.m^{-3} for the urban areas. That is the lowest absolute uncertainty for rural areas, but the second highest for the urban areas of the years 2005 - 2010. Alternatively, one could express this uncertainty in relative terms by relating the absolute RMSE uncertainty to the mean air pollution indicator value for all stations. This *relative mean uncertainty* of the combined final map of PM_{10} annual average is 22.7% for rural areas and 22.5% for urban areas. This is, for rural areas, the lowest of all in the period 2005 - 2010. The higher uncertainty levels for urban areas in the years 2008 - 2010, compared to the years 2007 - 2005, are caused specifically by addition of Turkish urban background stations reported only since 2008. (Turkish urban stations show high concentrations, uncertainty statistics are sensitive to such values.) These data have been used in the calculations since 2008 (although the interpolation result for Turkey is not present in the map due to lack of rural air quality data for Turkey). These relative uncertainty values fulfil the data quality objectives for models as set in Annex I of the air quality directive 2008/50/EC (EC, 2008). Table 7.5 summarises both the absolute and relative uncertainties over these past six years.

Figure 4.3 shows the cross-validation scatter plots, obtained according Section 2.3 of De Smet et al. (2010), for both rural and urban areas. The R^2 indicates that for the rural areas about 62 % and for the urban areas about 75 % of the variability is attributable to the interpolation. Corresponding values of the map of 2005 (52 % and 71 %), 2006 (52 % and 69 %), 2007 (59 % and 66 %), 2008 (48 % and 82 %) and 2009 (54% and 73%) help illustrate that for 2010 interpolation performance at both the rural and urban locations is slightly above the average of the earlier five years.

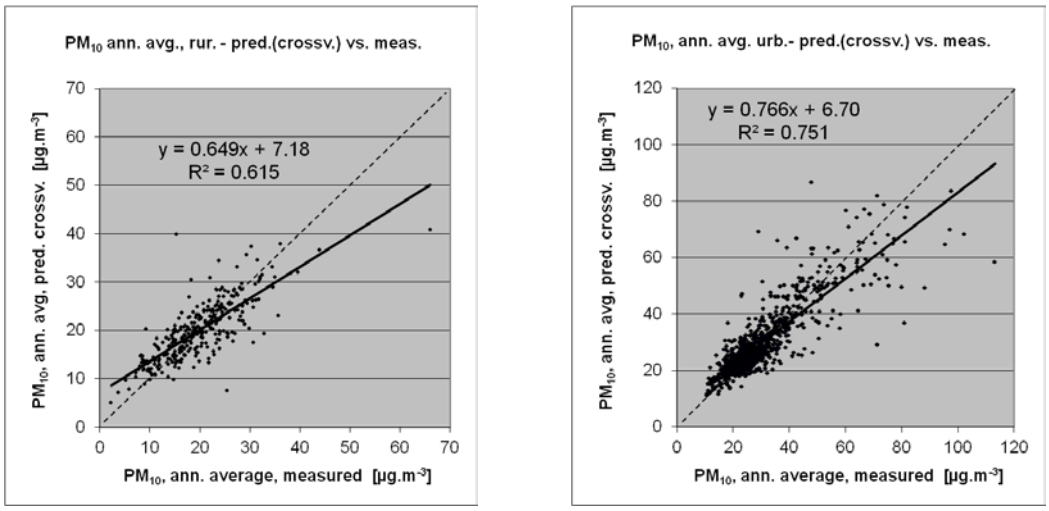

Figure 4.3 Correlation between cross-validation predicted values (y-axis) and measurements (x-axis) for the PM_{10} annual average for 2010 for rural (left) and urban (right) areas. R^2 and the slope a (from the linear regression equation $y = a \cdot x + c$) should be as close 1 as possible, the intercept c should be as close 0 as possible

The scatter plots indicate that in areas with high concentrations the interpolation methods tend to underestimate the levels. For example, in rural areas an observed value of 40 µg.m^{-3} is estimated in the interpolations to be about 33 µg.m^{-3}, about 18 % too low. This underestimation at high values is natural to all spatial interpolations. It can be reduced by either using a higher number of the stations at improved spatial distribution, or introducing a closer regression by using other supplementary data.

Comparison of point measurement values with the predicted grid value

In addition to the point observation - point prediction cross-validation discussed in the previous subsection, a simple comparison has been made between the point observation values and interpolated prediction values averaged at 10x10 km grid resolution for the separate rural and urban maps. This *point-grid* comparison indicates to what extent the predicted value of a grid cell represents the corresponding measured values at stations located in that cell. The results of the point observation - point prediction cross-validation of Figure 4.3 compared to those of the point-grid validation are summarised in Table 4.4. The table shows a better correlated relation between station measurements and the interpolated values of the corresponding grid cells (i.e. higher R^2, smaller intercept and slope closer to 1) at both rural and urban map areas than it does at the point cross-validation predictions. That is because the simple comparison between point measurements and the gridded interpolated values shows the uncertainty at the actual station locations (points), while the point observation – point prediction cross-validation simulates the behaviour of the interpolation at positions without actual measurements within the area covered by measurements. The uncertainty at measurement locations is caused partly by the smoothing effect of the interpolation and partly by the spatial averaging of the values in the 10x10 km grid cells. The level of the smoothing effect leading to underestimation at areas with high values is there smaller than it is in situations where no measurement is represented in such areas. For example, in urban areas the predicted interpolation gridded value will be about 59 $\mu g.m^{-3}$ at the corresponding station point with the measured value of 65 $\mu g.m^{-3}$, i.e. an underestimation of about 9 %.

Table 4.4 Linear regression equation and coefficient of determination R^2 from the scatter plots of (i) the predicted point values based on cross-validation and (ii) the aggregated predictions into 10x10 km grid cells versus the measured point values for PM_{10} indicator annual average for rural and urban areas of 2010.

	rural areas		urban areas	
	equation	R^2	equation	R^2
i) cross-validation prediction (Fig 4.3)	y = 0.649x + 7.18	0.615	y = 0.766x + 6.70	0.751
ii) 10x10 km grid prediction	y = 0.733x + 5.02	0.799	y = 0.843x + 4.27	0.903

Probability of Limit Value exceedance map

Next to the point cross-validation analysis, we constructed the map of probability of limit value exceedance. For this purpose, we aggregated the 1x1 km gridded combined final concentration map into a 10x10 km grid resolution map. Then we derived, with support of the 10x10 km uncertainty map and the limit value (40 $\mu g.m^{-3}$), the probability of exceedance (PoE) map at that same resolution (Figure 4.4). It is important to emphasize that the exceedance of the spatial average of a 10x10 km grid cell can show low probability even though some smaller (e.g. urban) areas inside such a grid cell show high probability of exceedance (using finer grid cell resolution).

The map demonstrates areas with a probability of limit value exceedance above 75 % marked in red (*high* probability) and areas below 25 % in green (*low* probability). Red indicates areas for which exceedance is *very likely* to occur due to either high concentrations close to or already above the LV accompanied with such uncertainty that exceedance is very likely, or areas with lower concentrations accompanied with high uncertainty levels reaching above the LV that excess is very likely. Vice versa, in the green areas it is *not likely* to have predicted concentrations and accompanying uncertainties at levels that do reach above the LV.

In the probability maps, the areas with 25-50 % and 50-75 % probability of LV exceedance are marked in yellow and orange respectively. The yellow colour indicates the areas with the estimated concentrations below limit value, but for which there exists a *modest* probability of exceeding the limit. On the contrary, the orange areas have estimated concentrations above the limit value, but with a chance of non-exceedance caused by its accompanying uncertainty. Table 4.5 summarises the classes and terminology for probability (i.e. likelihood) that are distinguished in this paper.

The patterns in the spatial distribution of the different PoE classes over Europe differ in 2010 from those of 2009 in limited areas only. The region of southern Poland – north-eastern Czech Republic with the industrial zones of Krakow, Katowice (PL) and Ostrava (CZ) shows a larger area with the highest probability of exceedance (75-100 %) in comparison with 2009. Contrary to that, the Po valley in Italy shows a lower probability of exceedance, in comparison with 2009. In south-eastern Europe, where relatively few measurement stations are located, especially at some larger cities with mostly high traffic density and heavy industry, elevated PoE do show up. In comparison with 2009, more (and larger) such areas occur in Albania and Greece, while less (and smaller) occur in Bulgaria and Serbia. Furthermore, some moderate PoE occurs in a large part of Cyprus. In other parts of Europe there exists just little likelihood of exceedance. In general, it can be concluded that the likelihood of exceedance in 2010 is slightly higher, but in a more restricted area when compared to the levels of 2009.

Table 4.5 Probability mapping classes and terminology use in this paper.

Map class colour	Percentage probability of threshold exceedance	Degree of probability (/ likelihood) of exceedance	Likelihood of exceedance
Green	0 – 25	Low/ Little	Not likely
Yellow	25 – 50	Modest	Somewhat likely
Orange	50 – 75	Moderate	Rather Likely
Red	75 – 100	High / Large	Very likely

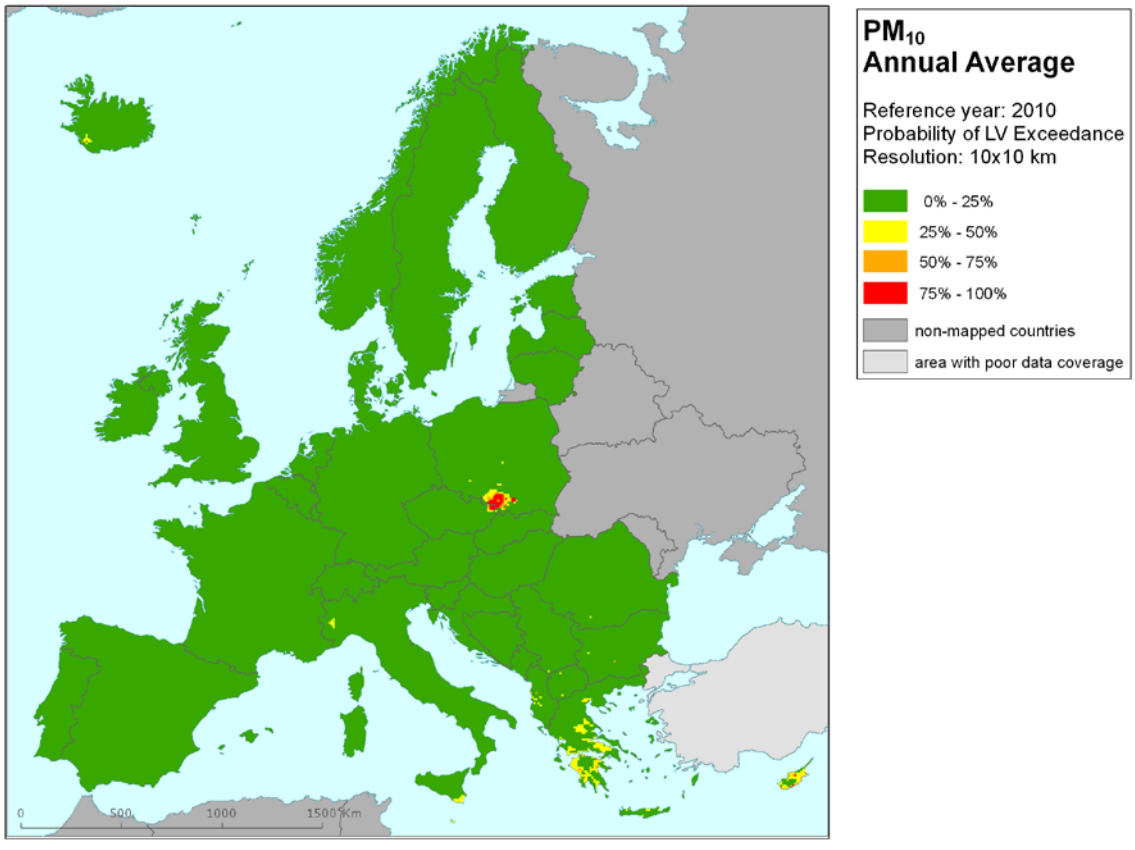

Figure 4.4 Map with the probability of the limit value exceedance for PM_{10} annual average ($\mu g.m^{-3}$) for 2010 on European scale calculated on the 10 x 10 km grid resolution. Interpolation uncertainty is considered only, no other sources of uncertainty.

4.2 36^{th} highest daily average

4.2.1 Concentration map

Similar to the PM_{10} annual average map, the combined final map of 36^{th} highest daily values has been derived from the separate rural, urban and joint rural/urban maps, using the same set of supplementary data parameters (Section 4.1.1) in the regression models and interpolation of residuals. Table 4.6 presents the estimated parameters of the linear regression models and of the residual kriging, including its statistical indicators. As in the case of annual average mapping, surface solar radiation was this year found to be statistically non-significant and thus it was not used in 2010 mapping.

Table 4.6 Parameters of the linear regression models (Eq.2.1) and of the ordinary kriging variograms (nugget, sill, range) - and their statistics - of PM_{10} indicator 36^{th} highest daily mean for 2010 in the rural (left) and urban (right) areas as used for final mapping, i.e. rural linear regression model P.Eawr (left), resp. urban UP.E (right), followed by the interpolation on its regression residuals using ordinary kriging (OK, coded with 'a').

linear regr. model + OK on its residuals	**rural areas (lnP.Eawr-a)**	**urban areas (lnUP.E-a)**
	coeff.	**coeff.**
c (constant)	2.47	1.97
a1 (lnEMEP model 2010)	0.536	0.58
a2 (altitude GTOPO)	-0.00045	
a3 (wind speed 2010)	-0.128	
a4 (s. solar radiation 2010)	n. sign.	
adjusted R^2	**0.39**	**0.34**
standard error [$\mu g.m^{-3}$]	**0.32**	**0.32**
nugget	0.030	0.012
sill	0.076	0.071
range [km]	620	650
RMSE [$\mu g.m^{-3}$]	**8.64**	**12.17**
MPE [$\mu g.m^{-3}$]	**0.27**	**-0.29**

The regressions on the 2010 data have an adjusted R^2 of 0.39 for rural areas and 0.34 for urban areas. Such a fit for rural areas is similar to 2009 (0.40) and 2007 (0.41) and better than in 2008, 2006 and 2005 (0.26, 0.27, 0.29). In urban areas the fit was much better than for all of the previous years – 2005, 0.0; 2006, 0.02; 2007, 0.09; 2008, 0.06 (De Smet et al. 2012, 2011, 2010, 2009 and Horálek et al. 2008). RMSE and MPE are the cross-validation indicators for the quality of the resulting map. Section 4.2.3 discusses in more detail the RMSE analysis and the comparison with 2005 - 2009.

Figure 4.5 presents the combined final map, where areas and stations exceeding the limit value (LV) of 50 µg.m^{-3} on more than 35 days are coloured red and purple.

As one can observe in a few areas of the map, the high urban background measurement values do not seem to influence the interpolation results despite their clustering. The main reason is that the map presented here is an aggregation of 1 km^2 grid values to a 10 km^2 resolution and this aggregation smoothes out the elevated values one would more likely be able to distinguish in the higher resolution map, especially in the case of urban background stations representing the urban areas. Another less prominent reason is the smoothing effect kriging has in general. However, kriging would in the case of clustering, not mask these elevations in the separate 1x1 km urban and rural maps.

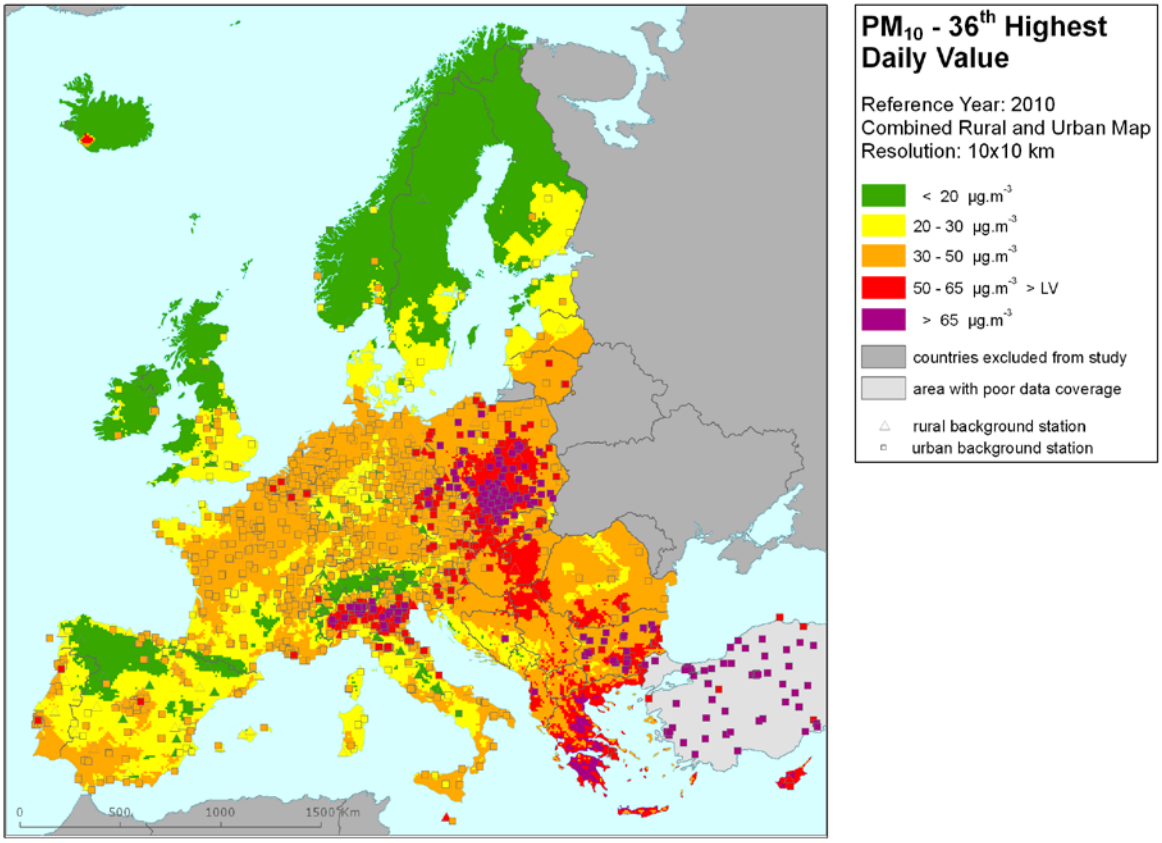

Figure 4.5 Combined rural and urban concentration map of PM_{10} – 36th highest daily average values, year 2010. Spatial interpolated concentration field (10x10 km grid resolution, excluding Turkey due to lack of rural air quality data) and the measured values in the measuring points. Units: µg.m^{-3}.

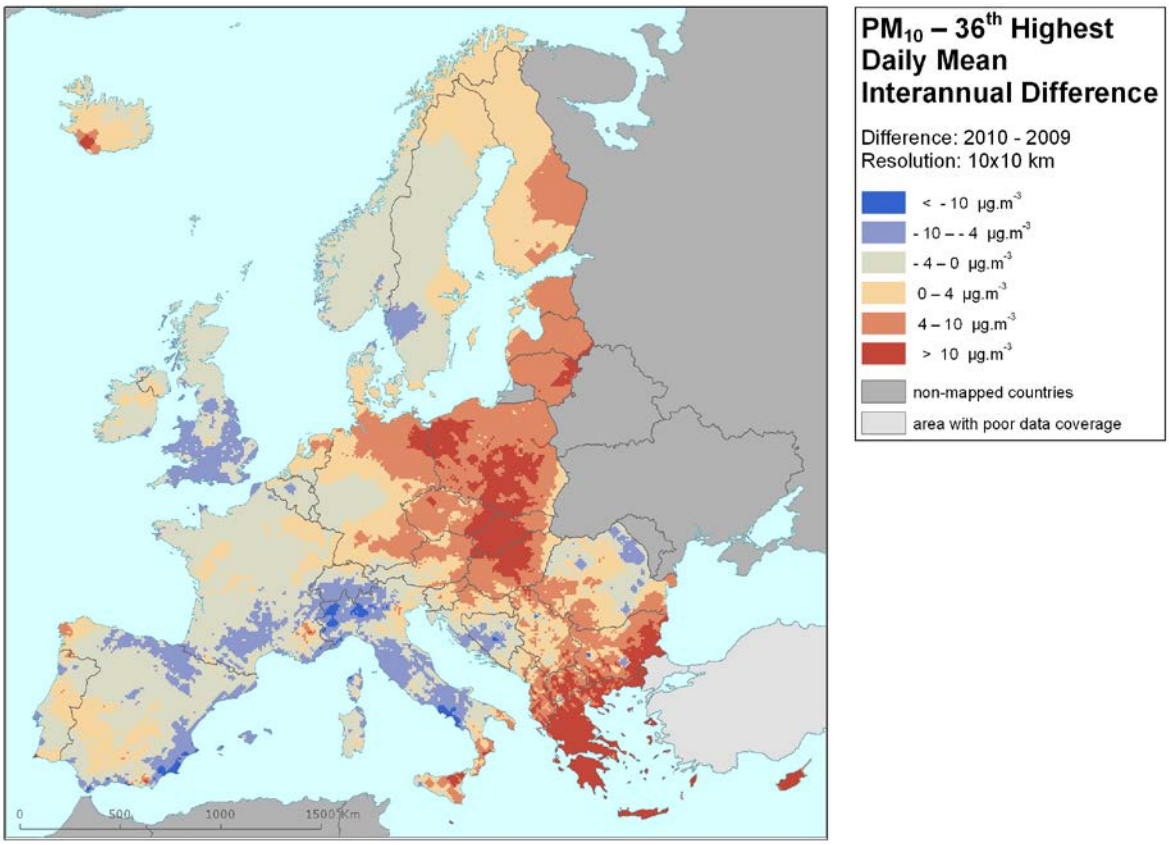

Figure 4.6 Interannual difference between mapped concentrations for 2010 and 2009 – PM_{10}, 36th highest daily average values. Units: µg.m^{-3}. Resolution: 10x10 km.

Figure 4.6 presents the interannual difference between 2010 and 2009 for 36th highest daily mean. Red areas show an increase of PM_{10} concentration, while blue areas show a decrease. The highest increase can be seen in Poland, Slovakia, Hungary, Bulgaria, Greece and Cyprus.

4.2.2 Population exposure

Table 4.7 gives the population frequency distribution for a limited number of exposure classes calculated at 1x1 km grid resolution, as well as the population-weighted concentration for individual countries and for Europe as a whole. Table 4.8 shows the evolution of the population exposure in the last five years.

Table 4.7 Population exposure and population-weighted concentration – PM_{10}, 36th highest daily average value, year 2010. Resolution: 1x1 km.

Country		Population	2010 Percent [%]					Population-weighted conc. [µg.m^{-3}]
			< LV			> LV		
		x 1000	< 20 µg.m^{-3}	20 - 30 µg.m^{-3}	30 - 50 µg.m^{-3}	50 - 65 µg.m^{-3}	> 65 µg.m^{-3}	
Albania	AL	3 204		0.6	21.0	16.1	62.3	69.5
Andorra	AD	85	13.5	8.0	78.4			28.5
Austria	AT	8 375	1.0	5.7	69.4	23.8		42.8
Belgium	BE	10 840		1.3	98.7			42.7
Bosnia & Herzegovina	BA	3 760	0.1	8.3	26.7	45.9	19.1	53.7
Bulgaria	BG	7 564		0.2	19.7	21.8	58.4	69.2
Croatia	HR	4 426	0.0	5.0	36.3	58.6		50.5
Cyprus	CY	819			1.0	17.1	81.9	74.5
Czech Republic	CZ	10 507		0.7	52.1	33.7	13.4	53.7
Denmark	DK	5 535	1.0	92.9	6.1			25.5
Estonia	EE	1 340	6.2	79.0	14.9			25.8
Finland	FI	5 351	24.5	75.5				22.7
France	FR	64 694	0.3	9.1	90.6			37.1
Germany	DE	81 802	0.0	6.6	92.9	0.5		37.2
Greece	GR	11 305			4.3	51.9	43.8	64.8
Hungary	HU	10 014			30.6	69.1	0.3	52.3
Iceland	IS	318	98.5	1.5	0.0		0.0	16.8
Ireland	IE	4 468	35.8	56.0	8.2			23.2
Italy	IT	60 340	0.3	9.8	58.6	15.8	15.3	45.2
Latvia	LV	2 248	0.0	14.8	85.2			37.8
Liechtenstein	LI	36	0.2	12.0	87.8			33.6
Lithuania	LT	3 329		3.4	96.6			39.5
Luxembourg	LU	502		20.9	79.1			31.9
Macedonia, FYR of	MK	2 053		0.6	11.7	10.5	77.2	80.1
Malta	MT	414			96.7	3.3		49.4
Monaco	MC	35			100			36.1
Montenegro	ME	616	0.6	17.7	14.8	29.7	37.2	54.0
Netherlands	NL	16 575			100			40.2
Norway	NO	4 858	35.6	33.3	31.0			25.7
Poland	PL	38 167		0.1	28.6	22.7	48.6	65.7
Portugal	PT	10 638	1.4	17.5	81.0	0.2		35.6
Romania	RO	21 462	0.0	1.4	70.4	24.6	3.6	45.2
San Marino	SM	32		5.0	95.0			44.0
Serbia (incl. Kosovo)	RS	9 856		0.9	18.6	54.7	25.8	60.1
Slovakia	SK	5 425		0.1	17.6	67.6	14.7	56.0
Slovenia	SI	2 047		1.2	60.2	38.6		47.2
Spain	ES	45 989	3.8	22.1	73.9	0.1		33.4
Sweden	SE	9 341	18.4	81.6	0.0			22.1
Switzerland	CH	7 786	1.7	11.0	87.2			36.3
United Kingdom	UK	62 027	5.3	47.2	47.6			28.8
Total		**538 185**	**2.3**	**15.2**	**61.9**	**11.4**	**9.3**	**41.9**
			79.4			**20.6**		

Note: Turkey is not included in the calculation due to lacking air quality data.

Table 4.8 Evolution of percentage population living in above limit value (left) and population-weighted concentration (right) in the years 2006-2010 – PM_{10}, 36th highest daily average value. Resolution: 1x1 km.

Country		Population above LV 50 µg.m^{-3} [%]						Population-weighted conc. [µg.m^{-3}]					
		2006	2007	2008	2009	2010	diff. '10 - '09	2006	2007	2008	2009	2010	diff. '10 - '09
Albania	AL	70.6	74.5	76.6	62.4	78.4	16.0	54.0	53.3	55.7	51.3	69.5	18.2
Andorra	AD	0	0	0	0	0	0	35.7	32.1	29.3	29.4	28.5	-0.9
Austria	AT	43.9	3.4	0	0	23.8	23.8	47.1	39.9	36.9	36.7	42.8	6.0
Belgium	BE	73.1	4.2	0	3.3	0	-3.3	51.3	43.5	38.4	45.8	42.7	-3.1
Bosnia-Herzegovina	BA	80.0	68.8	68.0	65.7	64.9	-0.8	57.4	52.7	50.6	57.8	53.7	-4.1
Bulgaria	BG	81.8	76.6	75.4	73.4	80.2	6.8	74.2	67.5	78.2	70.3	69.2	-1.1
Croatia	HR	80.2	46.2	35.0	27.7	58.6	30.9	53.7	49.6	48.6	46.9	50.5	3.7
Cyprus	CY	81.5	91.8	98.3	80.6	99.0	18.4	58.2	54.4	130.7	68.6	74.5	5.8
Czech Republic	CZ	76.6	20.9	13.1	14.7	47.2	32.5	57.5	46.2	42.5	43.6	53.7	10.0
Denmark	DK	0	0	0	0	0	0	37.0	32.5	29.0	26.0	25.5	-0.5
Estonia	EE	0	0	0	0	0	0	34.1	28.0	22.4	22.4	25.8	3.4
Finland	FI	0	0	0	0	0	0	29.5	23.9	21.9	19.4	22.7	3.3
France	FR	1.7	5.0	0.6	3.0	0	-3.0	32.9	41.0	36.3	39.2	37.1	-2.1
Germany	DE	2.0	0	0	0	0.5	0.4	41.3	35.7	31.7	34.4	37.2	2.8
Greece	GR	78.6	79.5	84.9	38.2	95.7	57.5	54.3	53.0	64.9	54.7	64.8	10.1
Hungary	HU	96.9	44	35.4	24.4	69.4	45.0	58.5	48.5	47.5	46.4	52.3	6.0
Iceland	IS	0.1	0	0	0	0.0	0.0	27.2	21.4	25.4	15.8	16.8	1.1
Ireland	IE	0	0	0	0	0	0	24.1	24.8	25.8	21.7	23.2	1.6
Italy	IT	58.4	63.3	46.2	31.9	31.2	-0.7	58.6	57.4	51.7	48.6	45.2	-3.5
Latvia	LV	0	0	0	0	0	0	40.0	31.9	32.7	33.4	37.8	4.4
Liechtenstein	LI	0	0	0	0	0	0	47.5	39.3	38.5	31.5	33.6	2.1
Lithuania	LT	0	0	0	0	0	0	39.7	33.2	29.5	32.7	39.5	6.8
Luxembourg	LU	0	0	0	0	0	0	35.9	32.5	29.1	34.3	31.9	-2.4
Macedonia, FYR of	MK	74.5	78.3	73.8	80.3	87.7	7.4	69.9	57.8	71.5	75.6	80.1	4.6
Malta	MT	0	0	0	0	3.3	3	44.8	42.6	40.3	38.7	49.4	10.7
Monaco	MC	100	0	0	0	0	0	59.7	46.2	46.0	41.5	36.1	-5.4
Montenegro	ME	69.5	71.6	70.8	65.7	66.9	1.2	57.9	53.6	56.7	51.8	54.0	2.2
Netherlands	NL	3.9	0	0	0	0	0	46.1	41.9	37.7	39.0	40.2	1.2
Norway	NO	0	0	0	0	0	0	31.9	26.3	26.1	24.0	25.7	1.7
Poland	PL	75.2	47.1	38.3	60.5	71.3	10.8	64.0	50.8	48.6	55.4	65.7	10.3
Portugal	PT	57.2	24	0	0	0.2	0	48.3	45.0	35.5	38.5	35.6	-2.9
Romania	RO	91.2	73.0	53.5	39.8	28.2	-11.6	65.4	57.7	53.1	49.0	45.2	-3.8
San Marino	SM	84.8	100	25.9	0	0	0	57.4	54.1	48.9	40.6	44.0	3.5
Serbia (incl. Kosovo)	RS	87.5	81.5	77.5	77.8	80.5	2.7	73.1	61.8	68.6	67.6	60.1	-7.4
Slovakia	SK	83.8	43.7	38.2	33.5	82.3	48.9	58.5	50.5	47.5	46.2	56.0	9.7
Slovenia	SI	63.3	40	5.5	0	38.6	38.6	49.2	46.1	42.7	41.9	47.2	5.3
Spain	ES	55.6	40.5	12.5	1.0	0.1	-0.8	49.3	46.9	40.1	38.0	33.4	-4.6
Sweden	SE	0	0	0	0	0	0	32.0	25.8	26.4	23.3	22.1	-1.2
Switzerland	CH	8.3	2	1.9	0.9	0	-1	43.9	39.9	36.5	37.1	36.3	-0.8
United Kingdom	UK	0	0	0	0	0	0	35.5	34.7	32.1	30.1	28.8	-1.2
Total		**35.7**	**26.2**	**19.4**	**16.5**	**20.6**	**4.2**	**47.8**	**44.1**	**41.3**	**41.2**	**41.9**	**0.7**

It has been estimated that in 2010 almost 21% of the European population lived in areas where the 36th highest daily mean of PM_{10} exceeded the limit value of 50 µg.m^{-3}. This is slightly more than in 2009 (17 %) and 2008 (19.4 %). However, in Albania, Bosnia-Herzegovina, Bulgaria, Croatia, Cyprus, FYR of Macedonia, Greece, Hungary, Montenegro, Poland, Serbia and Slovakia both the population-weighted indicator concentration and the median were above the LV, implying that in these countries the average concentration exceeded the LV and more than half of the population was exposed to concentrations exceeding the LV. The Czech Republic has a population-weighted concentration above the LV, but its median dropped below the LV to 47 % of the population.

In comparison with 2009, an increase of both population above the LV and population-weighted concentration especially in Greece, Slovakia, Hungary, Czech Republic and Slovenia can be seen.

The percentage of the total European population living in areas above the LV is 20.6 % in 2010, which is 4.1 % higher than in 2009 and 1.1% higher than in 2008. It is well below the levels of earlier years 2007 and 2006, see Table 4.8.

Such an increase is less obvious in the European-wide population-weighted concentration of the 36th highest daily mean, which is estimated for the year 2010 at 41.9 µg.m^{-3}, being 0.7µg.m^{-3} above that of 2009 and 0.6 µg.m^{-3} above that of 2008. In comparison with earlier years, it is about 2.2 µg.m^{-3} lower than in 2007 and about 6 µg.m^{-3} lower than in 2006.

Comparing observed PM_{10} exceedances in 2010 (annual average of section 4.1.2, with 36th highest daily average) one can conclude that the daily average limit value is the more stringent of the two. This conclusion was also drawn in the earlier reports.

4.2.3 Uncertainties

Uncertainty estimated by cross-validation

Cross-validation analysis determines the uncertainty. For the combined map of PM_{10} indicator 36th highest daily mean in 2010, Table 4.6 shows an absolute mean uncertainty (expressed as the RMSE) of 8.6 µg.m^{-3} for rural areas and 12.2 µg.m^{-3} for urban areas. For previous years, the values were 8.0 µg.m^{-3} and 13.2 µg.m^{-3} (2009), 8.8 and 12.7 µg.m^{-3} (2008), 8.0 and 9.1 µg.m^{-3} (2007), 13.3 and 9.9 µg.m^{-3} (2006) and 9.8 and 11.7 µg.m^{-3} (2005). This indicates that both rural and urban maps may differ from year to year somewhat in their levels of uncertainty. The relative mean uncertainty (absolute RMSE relative to the mean indicator value) of the 2010 map of PM_{10} indicator 36th highest daily mean is 24.4 % for rural areas and 23.7 % for urban areas. The previous years had: 24.1 and 26.7 % (2009), 28.2 and 24.4 % (2008), 23.5 and 19.6 % (2007), 26.3 and 21.4 % (2006) and 26.6 and 23.5 % (2005). In urban areas the higher uncertainty for 2008 - 2010, compared to previous years is caused specifically by Turkish urban background stations reported and used in the calculations for 2008 for the first time. (An interpolation result for Turkey is not presented in the map due to lack of population density data). Table 7.5 summarises both the absolute and relative uncertainties over the past six years.

Figure 4.7 shows the cross-validation scatter plots for both rural and urban areas. The R^2 indicates that for rural areas about 64 % and for urban areas about 77 % of the variability is attributable to the interpolation. Corresponding values with those of the 2009 map (56 % and 72 %), 2008 map (52 and 79 %), the 2007 map (60 and 65 %), the 2006 map (56 and 65 %) and the 2005 map (55 and 75 %) show that the fit is the best for rural and the second best for urban areas in 2010.

The scatter plots indicate that in areas with high concentrations the interpolation methods tend to underestimate the levels. For example, in urban areas (Figure 4.7, right panel) an observed value of 130 µg.m^{-3} would be estimated in the interpolation as about 111 µg.m^{-3}, i.e. about 15 % too low. For rural areas the underestimation is slightly stronger.

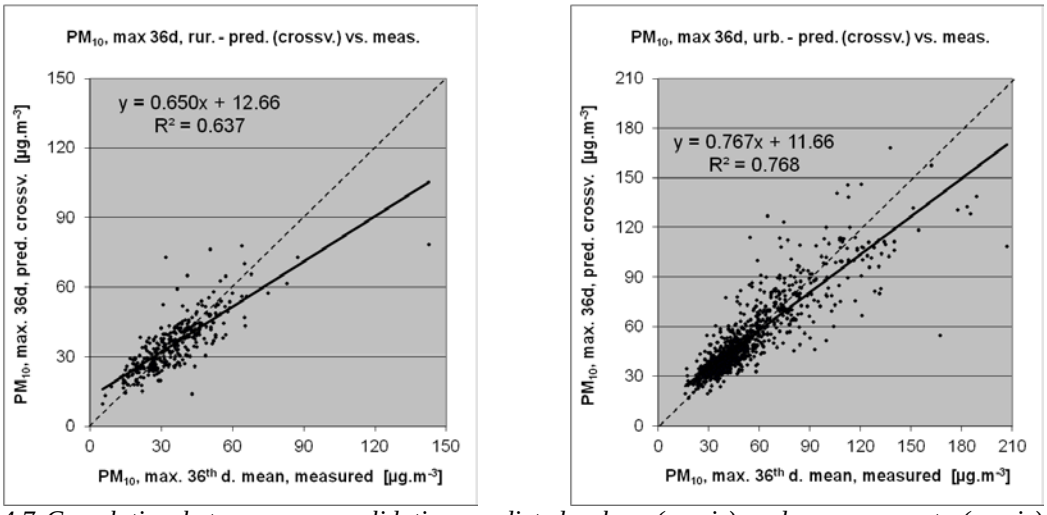

Figure 4.7 Correlation between cross-validation predicted values (y-axis) and measurements (x-axis) for the PM_{10} indicator 36th highest daily mean for 2010 for rural (left) and urban (right) areas. R^2 and the slope a (from the linear regression equation $y = a \cdot x + c$) should be as close 1 as possible, the intercept c should be as close to 0 as possible.

Comparison of point measurement values with the predicted grid value

In addition to the point observation – point prediction cross-validation, a simple comparison was made between the point observation values and interpolation predicted grid values. The results of the cross-validation compared to the gridded validation are summarised in Table 4.9. The uncertainty at measurement locations is caused partly by the smoothing effect of the interpolation and partly by the spatial averaging of the values in the 10x10 km grid cells. The level of smoothing, which leads to underestimation in areas with high values, is weaker in areas where measurements exist than in areas where a measurement point is not available. For example, in urban areas the predicted interpolation gridded value would be about 117 µg.m^{-3} at a corresponding station point with a measurement value of 130 µg.m^{-3}, i.e. an underestimation of 9 %. This is less than the underestimation of 15 % for such a location without a measurement value, discussed in the previous subsection.

Table 4.9 Linear regression equation and coefficient of determination R^2 from the scatter plots of (i) the predicted point values based on cross-validation and (ii) the aggregation into 10x10 km grid cells versus the measured point values for PM_{10} indicator 36th highest daily mean for rural and urban areas in 2010.

	rural areas		urban areas	
	equation	R^2	equation	R^2
i) cross-validation prediction (Fig 4.6)	y = 0.650x + 12.66	0.637	y = 0.767x + 11.66	0.768
ii) 10x10 km grid prediction	y = 0.742x + 8.60	0.834	y = 0.843x + 7.42	0.909

Probability of Limit Value exceedance map

Again, we constructed the map with the probability of the limit value exceedance (PoE), using an aggregated 10x10 km gridded concentration map (based on the 1x1 km combined final map), the 10x10 km gridded uncertainty map and the limit value (LV, 50 µg.m^{-3}). Figure 4.8 presents the probability of exceedance 10x10 km gridded map classifying the areas with probability of limit value exceedance below 25 % (little PoE) in green, between 25-50 % (modest PoE) in yellow, between 50-75 % (moderate PoE) in orange and above 75 % in red (large PoE). Section 4.1.3 explains in more detail the significance of the colour classes in the map.

Comparing the probabilities of exceedance (PoE) of 2008 and 2009 (see de Smet et al., 2011 and 2012) with those of 2010, one can conclude that an increase in the spatial extents and PoE levels throughout central and south-eastern Europe occurred in 2010. In particular, large areas of Poland,

Slovakia, Hungary, Serbia, Bulgaria, Greece and Cyprus have increased PoE, going mostly from green and yellow areas in 2009 to orange and red areas in 2010.

The Po valley in northern Italy has quite a similar PoE pattern to 2009. Western Belgium and north-western France have decreased levels of PoE (at the spatial resolution 10x10 km), going from yellow and some orange in 2009 back to green in 2010 (like in 2008). An increase from green to orange in a limited area of south-west Iceland was caused by the volcanic activity of Eyjafjallajökull.

Keeping in mind that the interpolated maps refer to the rural or (sub)urban background situations only, it cannot be excluded that exceedances of limit values may occur at the many *hotspot* and traffic locations throughout Europe. The PoE in the urbanised regions of Rome and some other Italian and French urban regions decreased in 2010 from yellow to greens.

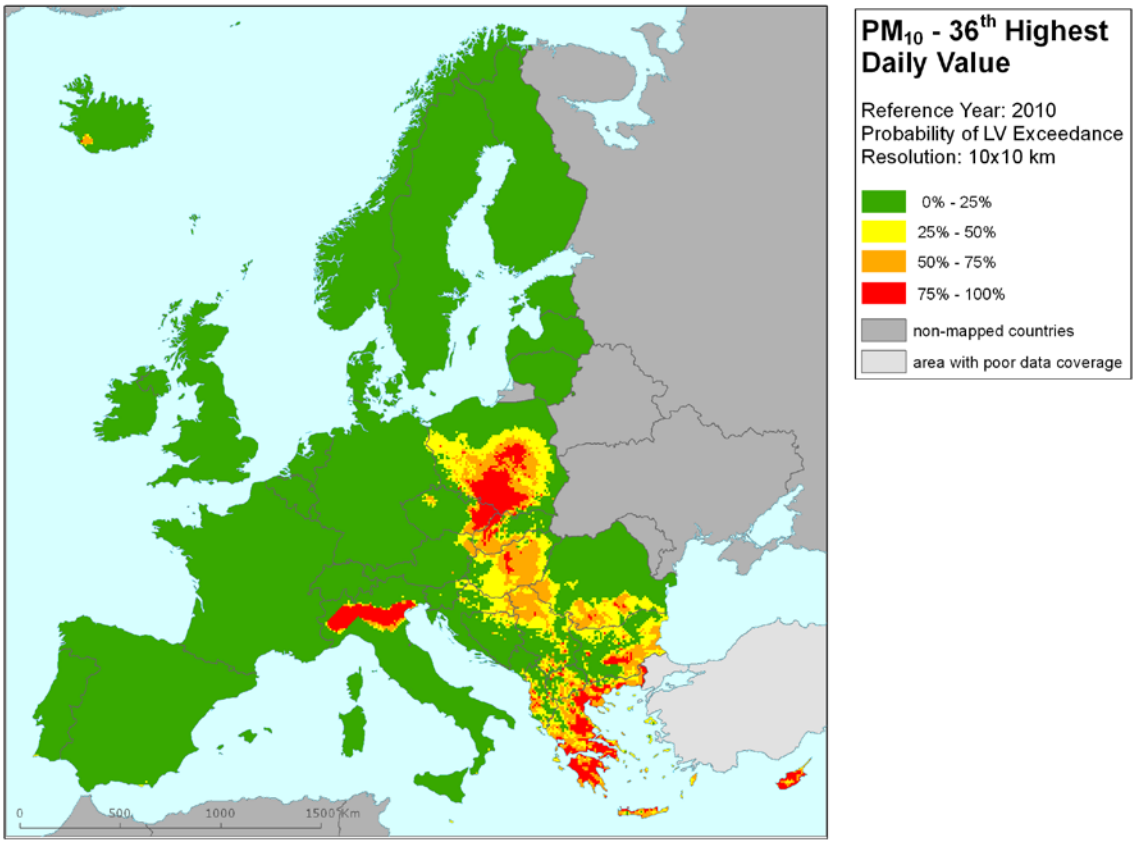

Figure 4.8 Map with the probability of the limit value exceedance for PM_{10} indicators 36th highest daily mean ($\mu g.m^{-3}$) for 2010 on the European scale calculated on the 10 x 10 km grid resolution. Interpolation uncertainty is considered only, no other sources of uncertainty.

5 $PM_{2.5}$ maps

This chapter presents for the first time in this regular report the $PM_{2.5}$ health indicator (annual average). The mapping methodology developed in Denby et. al (2011a, 2011b) was used. To increase the spatial coverage of measurements, pseudo $PM_{2.5}$ stations data were used in addition to measured $PM_{2.5}$ data. The separate urban and rural concentration maps were calculated on a grid of 10x10 km resolution and the subsequent combined concentration map was based on the 1x1 km gridded population density map. Population exposure tables are calculated on a grid of 1x1 km resolution. All maps are presented in at 10x10 km resolution. The standard EEA ETRS89-LAEA5210 coordinate reference system was applied.

5.1 Annual average

5.1.1 Concentration map

Figure 5.1 presents the combined final map for the 2010 $PM_{2.5}$ annual averages as the result of the interpolation and merging of the separate maps as described in detail in De Smet et al. (2011), using both measured $PM_{2.5}$ and pseudo $PM_{2.5}$ station data, as described in Denby (2011b). The red and purple areas and stations exceed the limit value (LV) of 25 $\mu g.m^{-3}$. Pseudo $PM_{2.5}$ stations data are estimated using PM_{10} measured data, surface solar radiation and latitude. Supplementary data in the regression used for rural areas consist of EMEP model output, altitude, wind speed, surface solar radiation and population density and for urban areas, no supplementary data are used . The relevant supplementary data both for pseudo $PM_{2.5}$ station data estimation and for the linear regression submodels used in residual kriging were identified earlier in Denby et al. (2011a, 2011b).

As one can observe in a few areas of the map, the high urban background measurement values do not seem to influence the interpolation results despite their clustering. The main reason is that the map presented here is an aggregation of 1 km^2 grid values to a 10 km^2 resolution and this aggregation smoothes out the elevated values one would more likely be able to distinguish in the higher resolution map, especially in the case of urban stations representing the urban background areas. Another less prominent reason is the smoothing effect kriging has in general. However, kriging would not, in the case of clustering, mask these elevations in the separate 1x1 km urban and rural maps.

Table 5.1 presents the regression coefficients determined for pseudo $PM_{2.5}$ stations data estimation. The same supplementary data as in Denby (2011b) are used. Nevertheless, population and longitude were detected as statistically non-significant. The R^2 values show a better fit of the regression than observed at year 2008 (0.84) and 2007 (0.89). A plausible reason is that there was a larger number of $PM_{2.5}$ stations in 2010.

Table 5.1 Parameters of the linear regression model (Eq. 2.1) and its statistics for generation of pseudo $PM_{2.5}$ stations data, without regard to the rural or urban/suburban type of the stations, for $PM_{2.5}$ 2010 annual average.

linear regr. model	both rural and urban areas
	coeff.
c (constant)	45.02
b (PM_{10} measured data, 2010 annual avg.)	0.635
a1 (population)	n. sign.
a2 (surface solar radiation 2010)	-1.968
a3 (latitude)	-0.474
a4 (longitude)	n. sign.
adjusted R^2	**0.95**
standard error [$\mu g.m^{-3}$]	**1.59**

Table 5.2 presents the estimated parameters of the linear regression models (c, a_1, a_2,…) and of the residual kriging (*nugget*, *sill*, *range*) and includes the statistical indicators of both the regression and the kriging. The adjusted R^2 and standard error are indicators for the fit of the regression relation, where the adjusted R^2 should be as close to 1 as possible and the standard error should be as small as possible. The adjusted R^2 is 0.49 for the rural areas. The R^2 values show a better fit of the regression than observed at year 2008 (0.44) and 2007 (0.48), while the analysis for 2010 was not conducted (Denby et al. 2011b, Table 3). For urban areas, no supplementary data are used, see Denby (2011b). Nevertheless, seeking higher agreement between the measured and modelled data (similar to the case of PM_{10}, Section 4.1) can lead into the use of supplementary data in future years.

RMSE and MPE are the cross-validation indicators, showing the quality of the resulting map; the MPE indicates to what extent the estimation is un-biased. Only stations with measured (not pseudo) $PM_{2.5}$ data are used for calculating RMSE and MPE. Section 5.1.3 deals with a more detailed cross-validation analysis.

Table 5.2 Parameters of the linear regression models (Eq. 2.2) and of the ordinary kriging variograms (nugget, sill, range) - and their statistics - of $PM_{2.5}$ indicator annual average for 2010 in rural areas (left) and urban (right) areas as used for the combined final map, i.e. linear regression model P.Eawrp followed by interpolation of its regression residuals using ordinary kriging (OK), indicated by 'a' (rural areas, left) and lognormal kriging (LK), indicated by 'b' (urban areas, right). For the urban areas no regression on supplementary data was used (see the text).

linear regr. model + OK on its residuals	**rural areas (lnP.Eawrp-a) coeff.**	**urban areas (b) coeff.**
c (constant)	1.06	
a1 (log. EMEP model 2010)	0.642	
a2 (altitude GTOPO)	-0.00019	
a3 (wind speed 2010)	-0.080	
a4 (s. solar radiation 2010)	n. sign.	
a4 (log. population density)	0.054	
adjusted R^2	**0.49**	
standard error [µg.m^{-3}]	**0.30**	
nugget	0.015	0.015
sill	0.060	0.057
range [km]	230	490
RMSE [µg.m^{-3}]	**3.38**	**3.12**
MPE [µg.m^{-3}]	**0.06**	**-0.44**

The merging of the separate rural and urban maps takes place on the 1x1 km resolution map of population density.

According to Figure 5.1, the most polluted areas seem to be the Katowice (PL) and Ostrava (CZ) industrial region, together with the Po valley in Northern Italy.

$PM_{2.5}$ map for 2009 has not been calculated, thus the interannual difference cannot be presented.

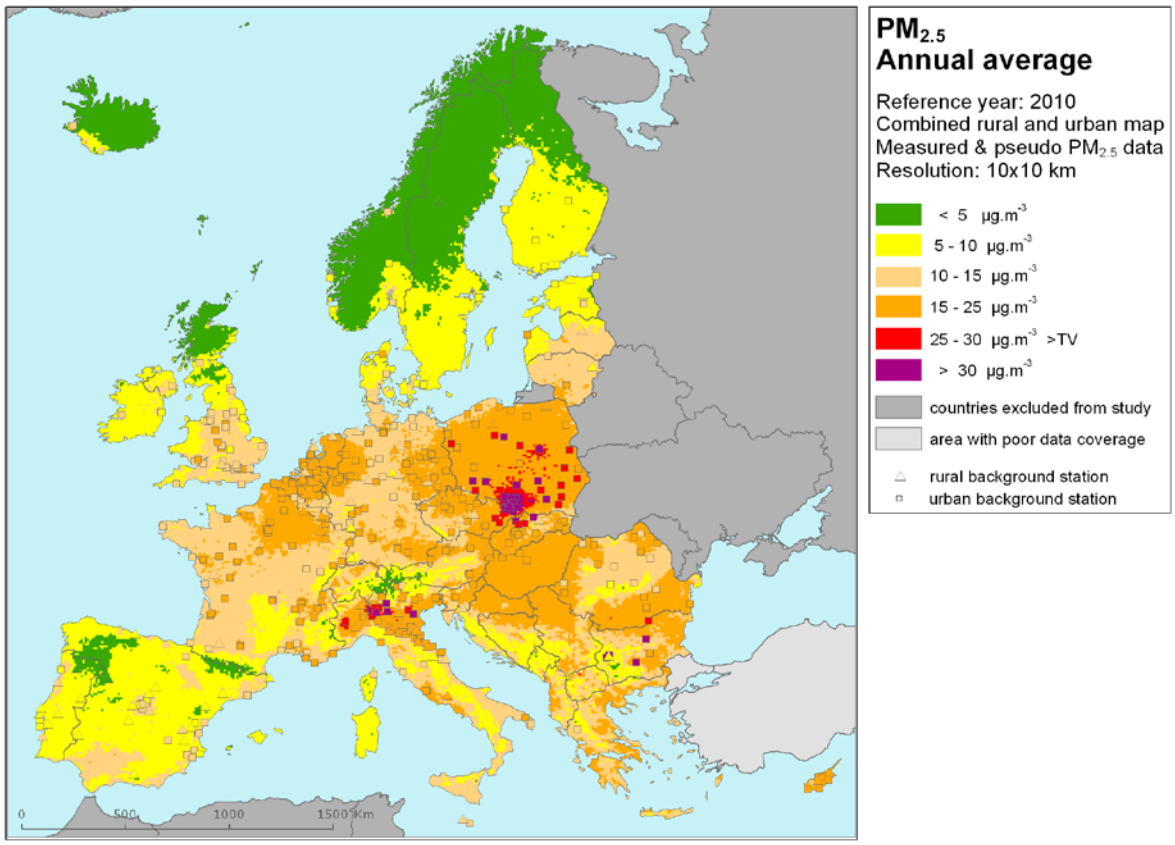

Figure 5.1 Combined rural and urban concentration map of $PM_{2.5}$ – annual average, year 2010. Spatial interpolated concentration field and the measured values in the measuring points. Units: $\mu g.m^{-3}$.

5.1.2 Population exposure

Table 5.3 gives the population frequency distribution for a limited number of exposure classes calculated on a grid of 1x1 km resolution, as well as the population-weighted concentration for individual countries and for Europe as a whole according to Equation 2.2 of De Smet et al. (2010).

Only 8 % of the European population in 2010 has been exposed to $PM_{2.5}$ annual mean concentrations below 10 $\mu g.m^{-3}$, the WHO (World Health Organization) air quality guideline. One third (32 %) of the population lived in areas where the $PM_{2.5}$ annual mean concentration is estimated to be between 10 and 15 $\mu g.m^{-3}$, while about half (52 %) of the population lived in areas with $PM_{2.5}$ values between 15 and 25 $\mu g.m^{-3}$. About 8 % of the population lived in areas where the $PM_{2.5}$ annual target value (TV) is exceeded in 2010, with Albania, Bulgaria, FYR of Macedonia, Montenegro and Poland showing either a population-weighted concentration or a median or both above the target value. However, as the next section discusses, the current mapping methodology tends to underestimate high values. Therefore, the exceedance percentage will most likely be higher and cause exceedance at a few more countries, for example Bosnia-Herzegovina.

The comparison of $PM_{2.5}$ and PM_{10} exposure (see Table 4.2) shows the $PM_{2.5}/PM_{10}$ ratio of

population-weighted concentrations to be about 0.7, for most countries. The exceptions are Cyprus, Malta and Greece; a plausible cause might be the influence of Saharan dust containing there a relative large fraction of coarse particles. (The $PM_{2.5}/PM_{10}$ ratio at the Cypriot rural station CY0002R is 0.52 and at the Maltese rural station MT00007 it is 0.35.)

Considering the average for the whole of Europe, the overall population-weighted annual mean $PM_{2.5}$ concentration in 2010 was 16.8 $\mu g.m^{-3}$. This is slightly higher than in previous years: 0.5 $\mu g.m^{-3}$ higher than in both 2008 and 2007 (16.3 $\mu g.m^{-3}$). The numbers for 2007 and 2008 were calculated using 1x1 km resolution (while preparing the paper Denby et al., 2011b). The ratios for 2009 were not calculated.

Table 5.3 Population exposure and population-weighted concentration – $PM_{2.5}$, annual average, year 2010. Resolution: 1x1 km.

Country		Population	2010 Percent [%]						Population-weighted conc.
			< TV				> TV		
			< 5	5 - 10	10 - 15	15 - 25	25 - 30	> 30	
		x 1000	$\mu g.m^{-3}$	$\mu g.m^{-3}$	$\mu g.m^{-3}$	$\mu g.m^{-3}$	$\mu g.m^{-3}$	$\mu g.m^{-3}$	[$\mu g.m^{-3}$]
Albania	AL	3 204	0	4.3	17.7	24.6	14.4	39.1	25.1
Andorra	AD	85	6.6	9.3	84.1	0	0	0	12.4
Austria	AT	8 375	0.1	2.0	15.0	83.0	0	0	17.7
Belgium	BE	10 840	0	0.0	2.7	97.3	0	0	18.8
Bosnia & Herzegovina	BA	3 760	0	6.7	10.8	35.3	44.6	2.6	22.2
Bulgaria	BG	7 564	0.0	2.9	9.8	26.5	33.1	27.7	24.5
Croatia	HR	4 426	0	2.5	8.6	87.9	1.0	0	20.0
Cyprus	CY	819	0	0	0.9	99.1	0	0	21.8
Czech Republic	CZ	10 507	0	0.2	5.4	78.7	6.5	9.2	21.5
Denmark	DK	5 535	0.4	17.5	82.2	0	0	0	11.4
Estonia	EE	1 340	0.0	81.4	18.6	0	0	0	8.9
Finland	FI	5 351	1.2	98.8	0	0	0	0	7.8
France	FR	64 694	0.0	2.2	28.8	68.9	0	0	16.2
Germany	DE	81 802	0.0	0.3	20.9	78.7	0	0	16.3
Greece	GR	11 305	0	0.5	11.6	81.6	5.1	1.2	20.0
Hungary	HU	10 014	0	0	0.0	93.2	6.7	0	20.3
Iceland	IS	318	16.2	83.3	0.5	0.0	0	0	6.9
Ireland	IE	4 468	0.1	36.0	63.9	0	0	0	10.3
Italy	IT	60 340	0.0	4.9	32.2	56.8	4.2	1.7	17.5
Latvia	LV	2 248	0	7.8	38.9	53.3	0	0	14.7
Liechtenstein	LI	36	0	1.4	20.4	78.2	0	0	15.3
Lithuania	LT	3 329	0	0.8	45.5	53.7	0	0	15.6
Luxembourg	LU	502	0	0	15.6	84.4	0	0	15.8
Macedonia, FYR of	MK	2 053	0	3.5	12.0	10.7	17.6	56.1	27.5
Malta	MT	414	0	0	100	0	0	0	13.8
Monaco	MC	35	0	0	100	0	0	0	14.9
Montenegro	ME	616	0.0	20.3	8.0	7.0	9.3	55.3	24.6
Netherlands	NL	16 575	0	0.0	0.9	99.1	0	0	17.6
Norway	NO	4 858	17.9	42.9	39.2	0	0	0	8.8
Poland	PL	38 167	0	0.0	1.1	45.8	26.6	26.6	26.4
Portugal	PT	10 638	1.7	24.1	74.2	0	0	0	10.5
Romania	RO	21 462	0	0.4	29.3	62.6	7.8	0	17.0
San Marino	SM	32	0	0	12.0	88.0	0	0	16.3
Serbia (incl. Kosovo)	RS	9 856	0	1.7	8.1	59.6	10.8	19.8	22.7
Slovakia	SK	5 425	0	0.1	3.2	82.4	12.5	1.8	21.3
Slovenia	SI	2 047	0	0.1	7.3	92.7	0	0	19.0
Spain	ES	45 989	0.8	21.2	76.0	2.0	0	0	11.8
Sweden	SE	9 341	3.1	82.7	14.2	0	0	0	8.1
Switzerland	CH	7 786	0.2	2.0	16.2	81.7	0	0	15.5
United Kingdom	UK	62 027	0.5	5.8	80.3	13.4	0	0	13.0
Total		**538 185**	**0.4**	**7.4**	**32.0**	**51.8**	**4.6**	**3.8**	**16.8**
			7.8				**8.3**		

Note: Turkey is not included in the calculation due to lacking air quality data.

Table 5.4 shows the evolution of the population exposure in the last years. However, only population exposure for 2007 and 2008 have been earlier calculated, not for 2009. Thus, the interannual difference cannot be presented. The exposure tables for 2007 and 2008 are presented here for the first time. (In Denby et al., 2011b only the exposure tables based on the 10x10 km resolution were presented.) For all the three years, the same mapping method is used. The results for West-Balkan countries are strongly influenced by the limited number of measurement stations in this area.

Table 5.4 Evolution of percentage population living in above target value (left) and population-weighted concentration (right) in the years 2007-2010 – $PM_{2.5}$, annual average. Resolution: 1x1 km.

Country		Population above TV 25 µg.m^{-3} [%]				Population-weighted conc. [µg.m^{-3}]			
		2007	2008	2009	2010	2007	2008	2009	2010
Albania	AL	1.6	1.6		53.4	20.8	19.6		25.1
Andorra	AD	0	0		0	11.5	11.3		12.4
Austria	AT	0	0		0	16.3	16.4		17.7
Belgium	BE	0	0		0	16.6	17.1		18.8
Bosnia-Herzegovina	BA	12.8	10.9		47.2	21.7	20.3		22.2
Bulgaria	BG	68.8	68.4		60.9	28.8	28.4		24.5
Croatia	HR	0.2	0		1.0	19.5	18.5		20.0
Cyprus	CY	77.6	79.6		0	25.0	25.3		21.8
Czech Republic	CZ	8.0	8.3		15.7	17.5	17.7		21.5
Denmark	DK	0	0		0	11.5	11.1		11.4
Estonia	EE	0	0		0	8.8	8.9		8.9
Finland	FI	0	0		0	7.7	7.4		7.8
France	FR	0	0		0	14.9	14.7		16.2
Germany	DE	0	0		0	14.0	14.1		16.3
Greece	GR	18.5	18.4		6.3	22.0	21.7		20.0
Hungary	HU	0	0		6.7	19.3	19.4		20.3
Iceland	IS	0	0		0	7.1	7.1		6.9
Ireland	IE	0	0		0	8.5	9.6		10.3
Italy	IT	12.4	12.3		6.0	19.0	19.1		17.5
Latvia	LV	0	0	not	0	15.3	16.4	not	14.7
Liechtenstein	LI	0	0	mapped	0	15.5	15.5	mapped	15.3
Lithuania	LT	0	0		0	13.8	15.5		15.6
Luxembourg	LU	0	0		0	13.9	14.5		15.8
Macedonia, FYR of	MK	61.5	61.0		73.8	24.4	23.6		27.5
Malta	MT	0	0		0	14.9	14.9		13.8
Monaco	MC	0	0		0	16.5	16.5		14.9
Montenegro	ME	12.6	12.6		64.6	21.4	19.9		24.6
Netherlands	NL	0	0		0	16.9	17.0		17.6
Norway	NO	0	0		0	8.6	8.2		8.8
Poland	PL	20.6	21.0		53.1	20.8	21.1		26.4
Portugal	PT	0	0		0	11.5	10.9		10.5
Romania	RO	28.5	27.7		7.8	22.4	21.8		17.0
San Marino	SM	0	0		0	18.2	18.2		16.3
Serbia (incl. Kosovo)	RS	69.4	64.7		30.6	26.6	25.4		22.7
Slovakia	SK	12.4	11.5		14.3	20.2	20.6		21.3
Slovenia	SI	0	0		0	18.5	18.0		19.0
Spain	ES	0	0		0	14.1	13.6		11.8
Sweden	SE	0	0		0	9.2	8.8		8.1
Switzerland	CH	0	0		0	14.9	14.8		15.5
United Kingdom	UK	0	0		0	12.2	12.5		13.0
Total		**7.8**	**7.6**		**8.3**	**16.3**	**16.3**		**16.8**

5.1.3 Uncertainties

Uncertainty estimated by cross-validation

Using RMSE as the most common indicator, the *absolute mean uncertainty* of the combined final map at areas 'in between' the station measurements can be expressed in µg.m^{-3}. Table 5.2 shows that the absolute mean uncertainty of the combined final map of $PM_{2.5}$ annual average expressed as RMSE is 3.4 µg.m^{-3} for the rural areas and 3.1 µg.m^{-3} for the urban areas. Alternatively, one can express this uncertainty in relative terms by relating the absolute RMSE uncertainty to the mean air pollution indicator value for all stations. This *relative mean uncertainty* of the combined final map of PM_{10} annual average is 25.0 % for rural areas and 16.8 % for urban areas. These relative uncertainty values fulfil the data quality objectives for models as set in Annex I of the air quality directive 2008/50/EC (EC, 2008). Table 7.6 summarises both the absolute and relative uncertainties of these three years. The decrease of uncertainties in 2010 is probably caused by an increased number of $PM_{2.5}$ stations.

Figure 5.2 shows the cross-validation scatter plots, obtained according Section 2.3 of De Smet et al. (2010), for both the rural and urban areas. The R^2 indicates that for the rural areas about 74 % and for the urban areas about 81 % of the variability is attributable to the interpolation.

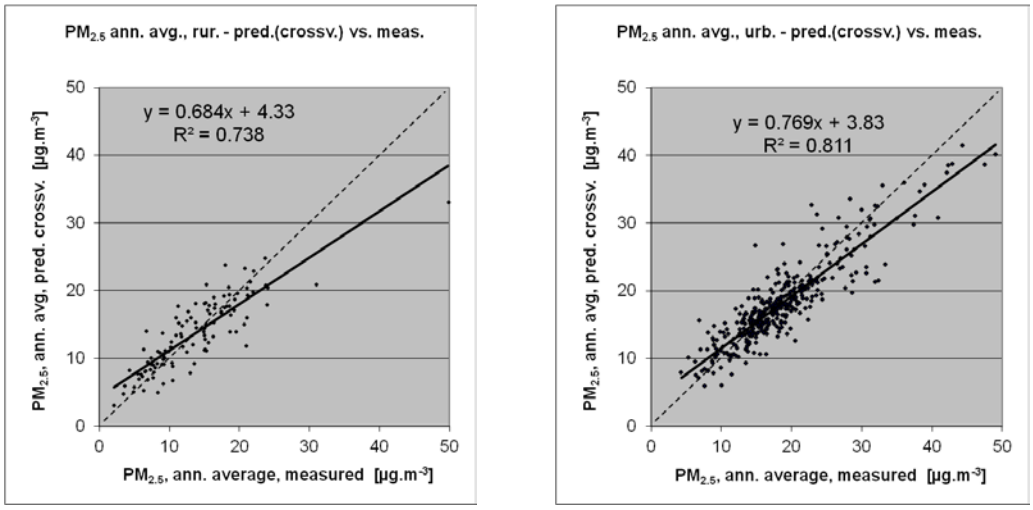

Figure 5.2 Correlation between cross-validation predicted values (y-axis) and measurements (x-axis) for the $PM_{2.5}$ annual average for 2010 for rural (left) and urban (right) areas. R^2 and the slope a (from the linear regression equation $y = a \cdot x + c$) should be as close 1 as possible, the intercept c should be as close 0 as possible

The scatter plots indicate that in areas with high concentrations the interpolation methods tend to underestimate the levels. For example, in rural areas an observed value of 25 µg.m^{-3} is estimated in the interpolations to be about 21 µg.m^{-3}, about 15 % too low. This underestimation at high values is an inherent feature of all spatial interpolations. It can be reduced by either using a higher number of the stations at improved spatial distribution, or introducing a closer regression by using other supplementary data.

Comparison of point measurement values with the predicted grid value

In addition to the above point observation - point prediction cross-validation, a simple comparison has been made between the point observation values and interpolated prediction values averaged in a 10x10 km resolution grid for the separate rural and urban map. This point-grid comparison indicates to what extent the predicted value of a grid cell represents the corresponding measured values at stations located in that cell. The results of the point observation - point prediction cross-validation of Figure 5.2 compared to those of the point-grid validation are summarised in Table 5.4. The table shows a better correlated relation between station measurements and the interpolated values of the corresponding grid cells (i.e. higher R^2, smaller intercept and slope closer to 1) at both rural and urban

map areas than it does at the point cross-validation predictions. That is because the simple comparison between point measurements and the gridded interpolated values shows the uncertainty at the actual station locations (points), while the point observation – point prediction cross-validation simulates the behaviour of the interpolation at positions without actual measurements within the area covered by measurements. The uncertainty at measurement locations is caused partly by the smoothing effect of the interpolation and partly by the spatial averaging of the values in the 10x10 km grid cells. The level of smoothing, which leads to underestimation in areas with high values, is weaker in areas where measurements exist than in areas where a measurement point is not available. For example, in rural areas the predicted interpolation gridded value will be about 23 µg.m^{-3} at the corresponding station point with the measured value of 25 µg.m^{-3}, i.e. an underestimation of about 8 %. This is less than the underestimation of 15 % for such a location without a measurement value, discussed in the previous subsection.

Table 5.4 Linear regression equation and coefficient of determination R^2 from the scatter plots of (i) the predicted point values based on cross-validation and (ii) the aggregated predictions into 10x10 km grid cells versus the measured point values for $PM_{2.5}$ indicator annual average for rural and urban areas of 2010.

	rural areas		urban areas	
	equation	R^2	equation	R^2
i) cross-validation prediction (Fig 5.2)	y = 0.684x + 4.33	0.738	y = 0.769x + 3.83	0.811
ii) 10x10 km grid prediction	y = 0.852x + 1.87	0.948	y = 0.815x + 2.85	0.908

Probability of Target Value exceedance map

The probability of target value exceedance map was created for the $PM_{2.5}$ indicator in similar fashion to the PoE maps for PM_{10} indicators. This map at 10x10 km resolution is presented in Figure 5.3, with the Target Value (TV) of 25 µg.m^{-3}.

The areas with the highest probability of TV exceedance include the region of southern Poland – north-eastern Czech Republic with the industrial zones of Krakow, Katowice and Ostrava, the central part of Poland, and the Po valley in northern Italy with Turin and Milan. In south-eastern Europe, where relatively few measurement stations are located, increased PoE do occur (for example, in some urban areas or larger agglomerations with mostly high traffic density and heavy industry). This includes Craiova and Bucharest in Romania. In the other parts of Europe, there exists little likelihood of exceedance.

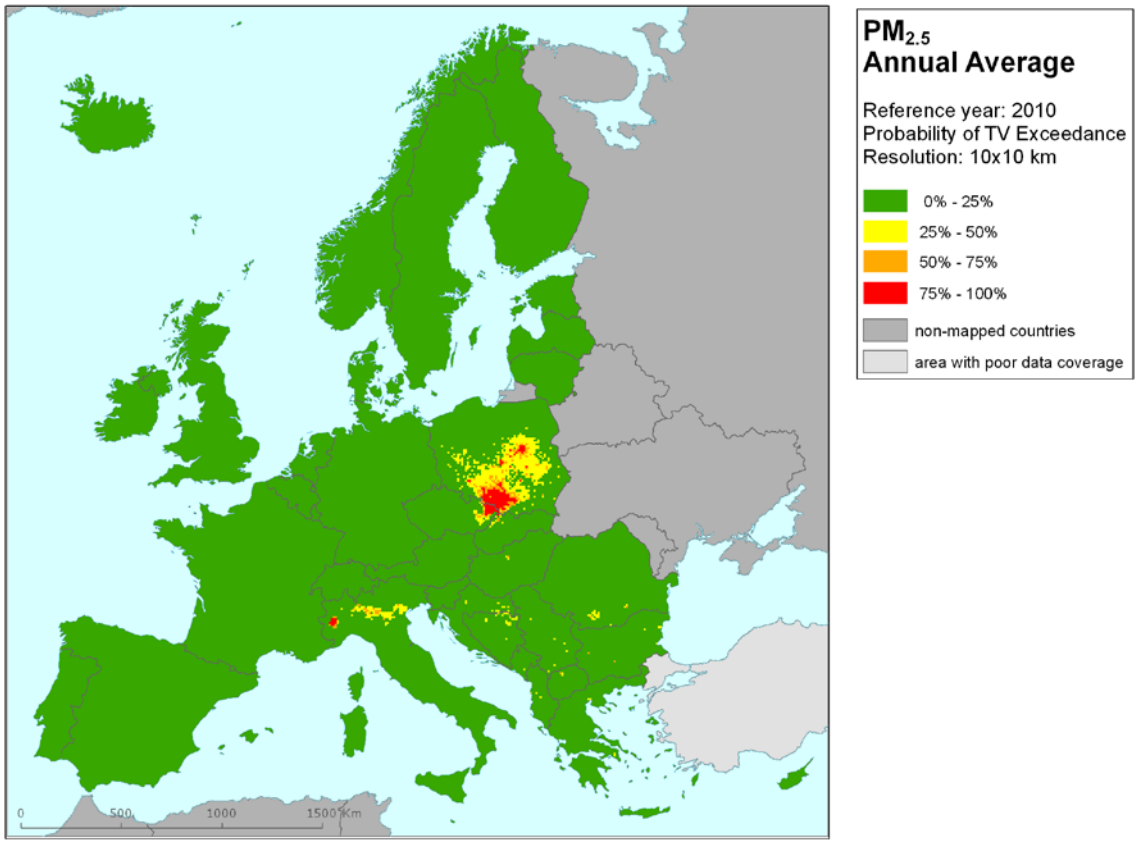

Figure 5.3 Map with the probability of the limit value exceedance for $PM_{2.5}$ annual average ($\mu g.m^{-3}$) for 2010 on European scale calculated on the 10 x 10 km grid resolution. Interpolation uncertainty is considered only.

6 Ozone maps

For ozone, the two health-related indicators (26th highest daily maximum 8-hour running mean and SOMO35) and the two vegetation-related indicators (AOT40 for crops and AOT40 for forests) are considered. The separate urban and rural health-related indicator fields are calculated at a resolution of 10x10 km. The final health-related indicator maps are then created by combining rural and urban areas on the basis of the 1x1 km resolution gridded population density map, as described in Chapter 2. We present the maps on a 10x10 km grid resolution. The vegetation-related indicator maps are calculated and presented for rural areas only (assuming urban areas do not cover vegetation) and on a grid of 2x2 km resolution, covering the same mapping domain as at the human health indicators. This resolution serves the needs of the EEA Core Set Indicator 005 on ecosystem exposure to ozone. Map projection is the standard EEA ETRS89-LAEA5210.

6.1 26th highest daily maximum 8-hour average

6.1.1 Concentration map

Figure 6.1 presents the combined final map for 26th highest daily maximum 8-hour average as a result of combining the separate rural and urban interpolated map following the procedures as described in more detail in De Smet et al. (2011) and Horálek et al. (2007). Both separate maps were created by combining the measured ozone concentrations with supplementary data in a linear regression model, followed by the interpolation of its residuals by ordinary kriging. The supplementary data used in the regression model for rural areas are EMEP model output, altitude and surface solar radiation for rural areas and EMEP model output, wind speed and surface solar radiation for urban areas, respectively. (The relevant linear regression models have been identified in the earlier reports and indicated as O.Ear and UO.Ewr respectively).

Table 6.1 presents the estimated parameters of the linear regression models and of the residual kriging, including the statistical indicators of both the regression and the kriging. The fit of the 2010 regression relationship, expressed as the adjusted R^2, is 0.56 for rural areas and 0.50 for urban areas. These values are worse than in 2009 (0.59 and 0.54), but better than at almost all other previous years: 2008 (0.41 and 0.43), 2007 (0.51 and 0.48), 2006 (0.40 and 0.43) and 2005 (0.45 and 0.51), (De Smet et al. 2012, 2011, 2010 and 2009 and Horálek et al. 2008). The numbers show that over the years the fit of the regressions are reasonably of the same order of magnitude at both the rural and the urban areas. RMSE and MPE are the cross-validation indicators, showing the quality of the resulting map. Section 5.1.3 discusses in more detail the RMSE analysis and comparison with results of 2005 – 2009.

Table 6.1 Parameters of the linear regression models (Eq. 2.2) and of the ordinary kriging variograms (nugget, sill, range) - and their statistics - of ozone indicator 26th highest daily maximum 8-hour mean for 2010 in the rural (left) and urban (right) areas as used the for combined final map, i.e. linear regression model O.Ear (left), resp. UO.Ewr (right) followed by interpolation of its residuals using ordinary kriging (OK, coded 'a').

linear regr. model + OK on its residuals	**rural areas (O.Ear-a)** **coeff.**	**urban areas (UO.Ewr-a)** **coeff.**
c (constant)	14.3	39.8
a1 (EMEP model 2010)	0.71	0.59
a2 (altitude GTOPO)	0.0087	
a3 (wind speed 2010)		-3.53
a4 (s. solar radiation 2010)	1.08	1.00
adjusted R^2	**0.56**	**0.50**
standard error [µg.m^{-3}]	**10.49**	**11.96**
nugget	30	60
sill	69	37
range [km]	100	200
RMSE [µg.m^{-3}]	**9.02**	**9.18**
MPE [µg.m^{-3}]	**0.05**	**0.04**

In the combined final map of Figure 6.1 the red and purple areas and stations do exceed the target value (TV) of 120 µg.m^{-3} (to be met by 2010). Note that in Directive 20008/50/EC the target value is defined as 120 µg/m^3 not to be exceeded on more than 25 days per calendar year *averaged over three years.*

As one can observe in a few areas of the map, the high measurement values do not seem to influence the interpolation results despite their clustering. The main reasons are (i) that the map presented here is an aggregation of 1 km^2 values to 10 km^2 resolution and this aggregation smoothes out the elevated values (ii) the smoothing effect kriging has in general.

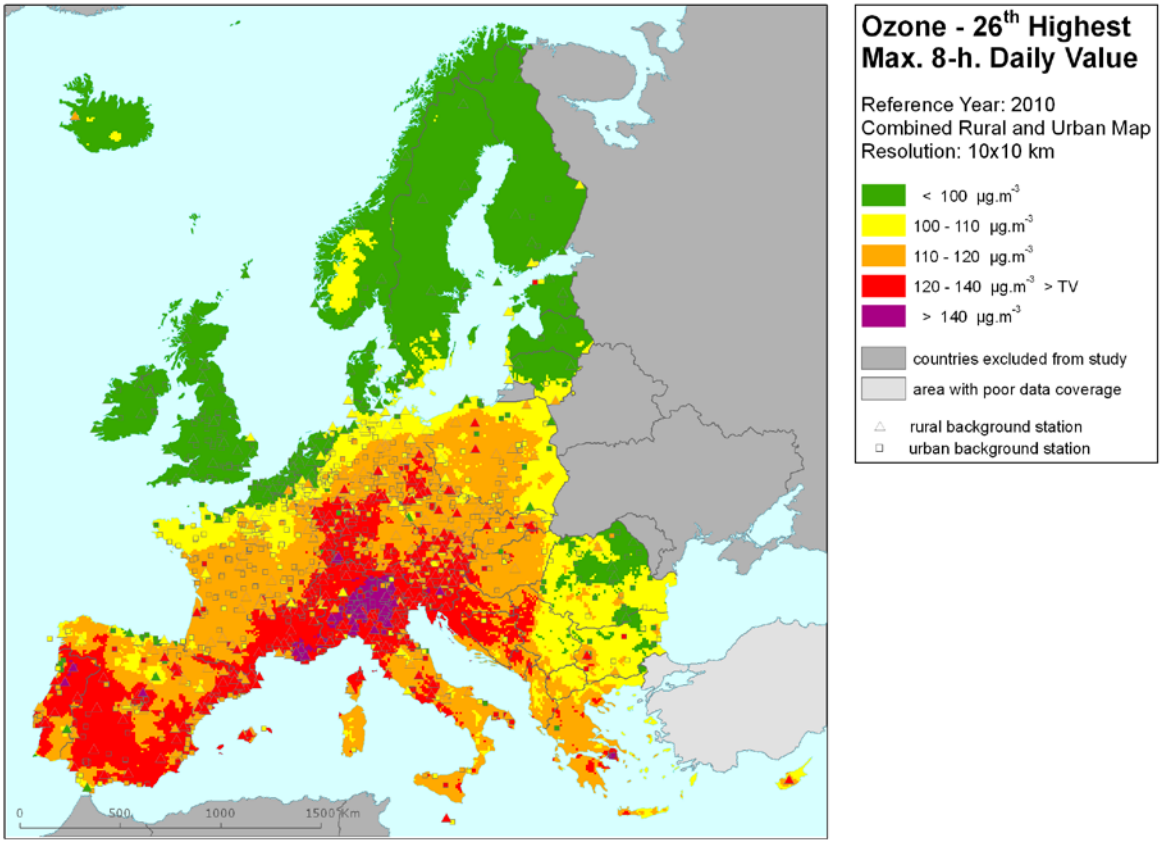

Figure 6.1 Combined rural and urban concentration map of ozone health indicators 26th highest daily maximum 8-hour value in µg.m^{-3} for the year 2010. Its target value is 120 µg.m^{-3}. Resolution: 10x10 km.

Figure 6.2 presents the interannual difference between 2010 and 2009 for 26th highest daily maximum 8-hour value. Red areas show an increase of ozone concentration, while blue areas show a decrease. The highest increases can be seen in France, north-western Switzerland and northern Portugal. Considerable decreases are visible in south-eastern Europe – especially in Romania, Bulgaria, Serbia, FYR of Macedonia and Cyprus. These decreases are influenced by the limited number of observations in these countries.

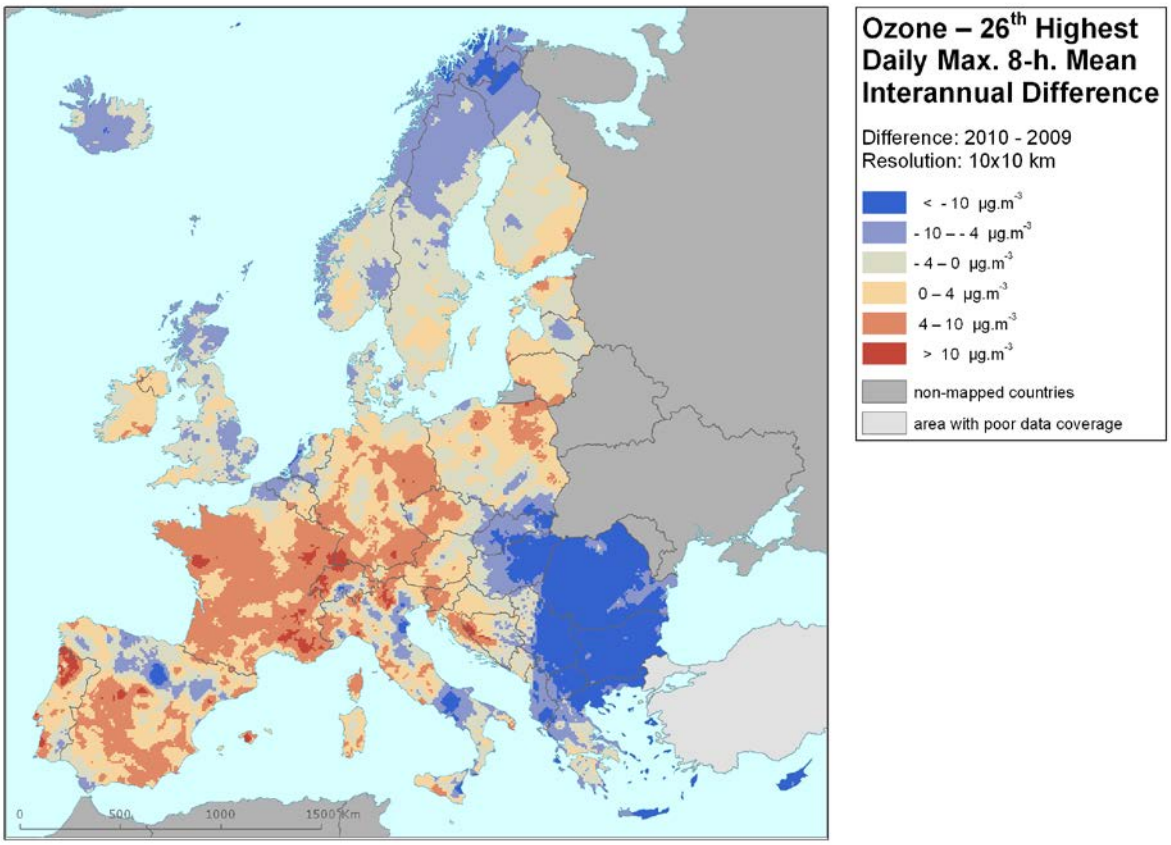

Figure 6.2 Interannual difference between mapped concentrations for 2010 and 2009 – ozone, 26th highest daily maximum 8-hour value. Units: µg.m-3.

6.1.2 Population exposure

Table 6.2 gives, for 26th highest daily maximum 8-hour running mean, the population frequency distribution for a limited number of exposure classes, as well as the population-weighted concentration for individual countries and for Europe as a whole. In Table 6.3 the evolution of population exposure in the last five years is presented.

It has been estimated that in 2010 some 16.4 % of the European population lived in areas where the ozone concentration exceeded the target value (TV of 120 µg.m-3) of the 26th highest daily maximum 8-hour mean. This is a minor increase compared to 2009 (16 %) 2008 (15 %). Similar to previous years there are no exceedances in 2010 in Benelux and Scandinavia, the UK, Ireland and Iceland. Countries with a similar percentage of inhabitants exposed to concentrations exceeding the target value in 2009 and 2010 are Croatia (19 %) Italy (52 %) and the small states with no or few measurement stations – San Marino (12 %) and Monaco (100 %).

Table 6.2 Population exposure and population weighted concentration – ozone, 26th highest daily maximum 8-hour mean for the year 2010.

Country		Population	2010 Percent [%]					Population-weighted conc.
			< TV			> TV		
		x 1000	< 100 µg.m^{-3}	100 - 110 µg.m^{-3}	110 - 120 µg.m^{-3}	120 - 140 µg.m^{-3}	> 140 µg.m^{-3}	[µg.m^{-3}]
Albania	AL	3 204	0	66.4	33.2	0.4	0	109.2
Andorra	AD	85	0	0	0	100	0	122.7
Austria	AT	8 375	0	0	74.5	25.5	0.1	118.6
Belgium	BE	10 840	68.4	29.2	2.4	0	0	97.7
Bosnia & Herzegovina	BA	3 760	26.0	34.6	21.0	18.5	0	108.3
Bulgaria	BG	7 564	23.2	72.2	4.4	0.2	0	102.5
Croatia	HR	4 426	0.6	20.1	60.9	18.5	0	115.2
Cyprus	CY	819	0	86.1	13.9	0	0	107.1
Czech Republic	CZ	10 507	0	5.7	93.7	0.6	0	113.9
Denmark	DK	5 535	97.3	2.7	0	0	0	91.3
Estonia	EE	1 340	65.8	34.2	0	0	0	97.3
Finland	FI	5 351	100.0	0.0	0	0	0	92.3
France	FR	64 694	10.9	32.9	34.7	21.4	0.1	111.5
Germany	DE	81 802	2.7	33.7	49.1	14.5	0.0	112.9
Greece	GR	11 305	0.5	17.3	44.3	37.9	0	118.0
Hungary	HU	10 014	8.0	23.4	66.8	1.7	0	111.4
Iceland	IS	318	99.6	0.4	0	0	0	78.3
Ireland	IE	4 468	100.0	0	0	0	0	85.0
Italy	IT	60 340	0.4	15.1	33.1	34.7	16.7	124.5
Latvia	LV	2 248	98.3	1.7	0	0	0	92.8
Liechtenstein	LI	36	0	0	0	100	0	121.4
Lithuania	LT	3 329	87.0	13.0	0	0	0	96.5
Luxembourg	LU	502	0	3.4	93.4	3.2	0	112.0
Macedonia, FYR of	MK	2 053	0	89.2	10.5	0.3	0	106.8
Malta	MT	414	0	93.3	6.1	0.7	0	106.6
Monaco	MC	35	0	0	0	100	0	122.8
Montenegro	ME	616	1.9	66.1	26.3	5.6	0	107.1
Netherlands	NL	16 575	93.0	7.0	0	0	0	90.6
Norway	NO	4 858	98.9	1.1	0.0	0	0	88.7
Poland	PL	38 167	15.5	54.4	30.1	0.1	0	106.5
Portugal	PT	10 638	18.2	18.9	39.7	22.5	0.6	112.1
Romania	RO	21 462	80.9	17.8	1.3	0.0	0	92.8
San Marino	SM	32	0	0	88.4	11.6	0	116.2
Serbia (incl. Kosovo)	RS	9 856	38.3	47.9	9.1	4.6	0	103.2
Slovakia	SK	5 425	0	23.1	76.0	0.9	0	112.4
Slovenia	SI	2 047	0	0	50.4	49.5	0.1	122.1
Spain	ES	45 989	8.8	10.7	51.5	29.0	0	115.2
Sweden	SE	9 341	97.3	2.7	0	0	0	91.4
Switzerland	CH	7 786	0	0	0.7	95.7	3.6	125.1
United Kingdom	UK	62 027	99.8	0.2	0	0	0	81.4
Total		**538 185**	**31.0**	**22.6**	**30.0**	**14.5**	**1.9**	**106.7**
			83.6			**16.4**		

Note: Turkey is not included in the calculation due to lack of air quality data.

Table 6.3 Evolution of percentage population living in above target value (left) and population weighted concentration (right) in the years 2006-2010 – O_3, 26th highest daily maximum 8-hour mean. Resolution: 1x1 km.

Country		Population above TV 120 µg.m^{-3} [%]						Population-weighted conc. [µg.m^{-3}]					
		2006	2007	2008	2009	2010	diff. '10 - '09	2006	2007	2008	2009	2010	diff. '10 - '09
Albania	AL	24.9	67.6	6.6	13.2	0.4	-12.8	117.4	126.9	115.3	114.7	109.2	-5.5
Andorra	AD	26.8	18.9	78.2	13.5	100	86.5	120.1	118.6	122.0	115.6	122.7	7.1
Austria	AT	84.8	67.3	13.7	14.5	25.5	11.0	124.7	122.8	114.8	116.4	118.6	2.1
Belgium	BE	94.1	0	0	0	0	0	126.0	98.9	103.6	101.5	97.7	-3.7
Bosnia-Herzegovina	BA	34.9	63.8	7.5	25.7	18.5	-7.2	117.3	122.5	113.7	114.5	108.3	-6.2
Bulgaria	BG	0.8	34.2	6.6	16.3	0.2	-16.1	105.0	115.7	114.4	112.0	102.5	-9.5
Croatia	HR	79.6	85.8	8.8	19.2	18.5	-0.7	124.3	124.7	115.5	115.6	115.2	-0.3
Cyprus	CY	1.2	23.8	0.2	50.9	0	-50.9	102.1	116.9	115.2	120.8	107.1	-13.6
Czech Republic	CZ	95.6	59.1	6.8	6.6	0.6	-6.0	126.1	121.0	114.6	113.5	113.9	0.4
Denmark	DK	0	0	0	0	0	0	104.9	95.2	102.6	95.5	91.3	-4.2
Estonia	EE	0	0	0	0	0	0	105.3	94.1	96.3	90.8	97.3	6.4
Finland	FI	0	0	0	0	0	0	100.2	89.0	94.3	90.6	92.3	1.7
France	FR	61.4	14.2	5.6	9.6	21.5	11.9	121.8	109.0	107.3	107.3	111.5	4.2
Germany	DE	88.0	13.1	10.6	2.0	14.5	12.6	125.6	113.3	113.5	108.8	112.9	4.1
Greece	GR	34.6	76.7	84.5	59.4	37.9	-21.5	114.7	126.5	131.1	122.8	118.0	-4.8
Hungary	HU	69.3	85.9	28.6	85.6	1.7	-83.8	121.6	125.0	117.5	124.2	111.4	-12.8
Iceland	IS	0	0	0	0	0	0	93.9	81.1	90.8	81.4	78.3	-3.2
Ireland	IE	0	0	0	0	0	0	90.0	84.2	92.1	84.9	85.0	0.0
Italy	IT	88.8	71.6	55.2	57.3	51.4	-5.9	134.7	129.5	123.2	125.8	124.5	-1.3
Latvia	LV	0	0	0	0	0	0	103.8	95.8	94.9	91.9	92.8	0.9
Liechtenstein	LI	100	21.8	9.4	17.8	100	82.2	126.2	119.9	119.4	118.9	121.4	2.5
Lithuania	LT	0	0	0	0	0	0	109.6	98.1	102.0	95.8	96.5	0.6
Luxembourg	LU	100	0	0	0	3.2	3.2	130.0	111.7	112.1	108.6	112.0	3.4
Macedonia, FYR of	MK	15.0	29.7	78.4	16.6	0.3	-16.3	110.2	121.1	121.0	111.3	106.8	-4.5
Malta	MT	4.9	2.7	1.6	0	0.7	0.7	115.8	109.1	108.4	107.7	106.6	-1.1
Monaco	MC	100	100	100	100	100	0	132.0	127.3	123.1	127.2	122.8	-4.4
Montenegro	ME	23.7	35.4	12.3	14.5	5.6	-8.9	114.2	122.3	118.1	111.7	107.1	-4.6
Netherlands	NL	38.8	0	0	0	0	0	116.2	94.1	98.4	94.7	90.6	-4.1
Norway	NO	0	0	0	0	0	0	101.7	91.3	99.0	94.0	88.7	-5.3
Poland	PL	53.0	12.3	1.9	0.4	0.1	-0.3	120.3	112.9	109.7	107.8	106.5	-1.4
Portugal	PT	46.5	5.0	0.0	18.5	23.2	4.7	119.3	111.0	102.7	112.4	112.1	-0.3
Romania	RO	0.6	36.7	3.1	8.0	0.0	-8.0	105.8	116.9	110.1	108.8	92.8	-16.0
San Marino	SM	22.9	100	14.1	13.8	11.6	-2.3	120.4	130.4	119.0	118.1	116.2	-1.9
Serbia (incl. Kosovo)	RS	6.3	62.2	20.2	38.2	4.6	-33.6	108.6	122.5	117.3	115.8	103.2	-12.6
Slovakia	SK	66.5	69.2	24.0	88.3	0.9	-87.4	122.2	122.2	116.4	122.7	112.4	-10.3
Slovenia	SI	100	99.9	22.7	38.2	49.6	11.4	131.7	126.6	116.9	119.7	122.1	2.4
Spain	ES	42.5	24.6	16.8	18.1	29.0	10.9	116.4	115.4	110.7	113.1	115.2	2.2
Sweden	SE	0.1	0	0	0	0	0	104.3	93.5	97.6	94.2	91.4	-2.8
Switzerland	CH	100.0	53.6	11.1	15.4	99.3	83.9	132.1	120.1	116.8	117.3	125.1	7.7
United Kingdom	UK	0.0	0	0	0	0	0	98.0	83.3	93.1	86.8	81.4	-5.4
Total		**51.4**	**27.1**	**15.0**	**16.0**	**16.4**	**0.4**	**118.0**	**110.7**	**109.8**	**108.1**	**106.7**	**-1.4**

Increases in countries are observed for 2010 compared to 2009, they can be categorized into three cases:

- Countries with a minor increase in the population exposed to levels above the TV: Luxembourg, Portugal.
- Countries with population exposures above the TV in 2009 that show a small increase in 2010 of about 10 %: Austria, France, Germany, Slovenia and Spain.
- Countries with remarkably large increases in the percentage of national population exposed: Switzerland (from 15 % in 2009 to 99 % in 2010) and small states

Liechtenstein (from 18 to 100 %) and Andorra (from 14 to 100 %). Results in these later two small countries might be influenced by the limited number of observations.

For the decreases in national population exposures of 2010 compared to those of 2009, one observes three cases as well:

- Countries of south-eastern Europe: Albania, Montenegro, Serbia, Romania, Bulgaria, FYR of Macedonia and Greece. Results in these countries might be influenced by the limited number of observations.
- Countries showing a large decrease to almost non-exceedance: Slovakia (from 88 % in 2009 to 2 % in 2010), Hungary (from 86 % in 2009 to 2 % in 2010) and Cyprus (from 50.9 % in 2009 to 0% in 2010). Also in these cases, the limited number of stations can play a role.
- Other countries with some decreases not likely related to a limited number of observations: Italy (from 57 % in 2009 to 51 % in 2010) and Czech Republic (from 7 % in 2009 to 1 % in 2010). In 2010, Italy again had most of its population in the areas above TV, while the Czech Republic showed almost no exceedances.

The population-weighted concentrations of Andorra, Italy, Liechtenstein, Monaco, Slovenia and Switzerland have been estimated, for 2010, to be above the TV. About 50 % of the Slovenians, 51 % of the Italians, more than 99 % of the Swiss population and all citizens of Andorra, Liechtenstein and Monaco were exposed to average levels above the TV. Part of the population in Portugal (0.6 %) and Switzerland (4 %) and more substantially in Italy (almost 17 %) were estimated to be exposed to ozone levels of more than 140 $\mu g.m^{-3}$. As the current mapping methodology tends to underestimate high values due to interpolation smoothing, these actual numbers will most likely be higher. Most of the countries showed a decrease in their population-weighted concentrations in 2010 compared to 2009, however, increases most notably occurred in Switzerland, Estonia, France, Germany and Andorra.

The overall European population-weighted ozone concentration in terms of the 26^{th} highest daily maximum 8-hour mean was estimated for the year 2010 to be 107 $\mu g.m^{-3}$. That is a decrease compared to previous years.

6.1.3 Uncertainties

Uncertainty estimated by cross-validation

The basic uncertainty analysis is provided by cross-validation. Table 6.1 shows RMSE values of 9.0 $\mu g.m^{-3}$ for the rural areas and 9.2 $\mu g.m^{-3}$ for the urban areas of the combined final map. For previous years the values were for rural and urban areas respectively: 8.2 and 9.3 (2009) 8.7 and 8.8 $\mu g.m^{-3}$ (2008), 8.8 and 8.9 $\mu g.m^{-3}$ (2007), 11.2 and 10.2 $\mu g.m^{-3}$ (2006) and 12.3 and 10.0 $\mu g.m^{-3}$ (2005) (De Smet et al. 2012, 2011, 2010 and 2009, Table 6.1; Horálek et al. 2008, Tables A3.3, A3.12). The relative mean uncertainty of the 2010 ozone map is 7.8 % for rural areas and 8.2 % for urban areas. The previous years had for rural and urban areas respectively: 7.2 % and 8.4 % (2009), 7.6 % and 7.9 % (2008), 7.5 % and 7.9 % (2007), 8.9% and 8.4 % (2006), 10.3 % and 8.9 % (2005). Table 7.7 summarises both the absolute and relative uncertainties over these past six years.

Figure 6.3 shows the cross-validation scatter plots for both the rural and urban areas of the 2010 map. The R^2, an indicator for the interpolation correlation with the observations, shows that for the rural areas about 68 % and for the urban areas about 71 % of the variability is attributable to the interpolation. Corresponding values for the 2009 map (69 % and 64 %), 2008 map (56 % and 61 %), 2007 map (71 % and 66 %), the 2006 map (49 % and 53 %) and the 2005 map (51 % and 50 %), show a highest urban fit. They also show that the 2010 rural interpolations are in line with the quality of 2009 and 2007 and fit better than in the years 2005, 2006 and 2008.

The scatter plots indicate that the higher values are underestimated and the lower values somewhat overestimated by the interpolation method; a typical smoothing effect inherent to interpolation method of the linear regression and its residuals kriging. For example, in rural areas (Figure 6.3, left panel) an observed value of 150 µg.m^{-3} is estimated in the interpolation as 141 µg.m^{-3}, which is 6 % too low.

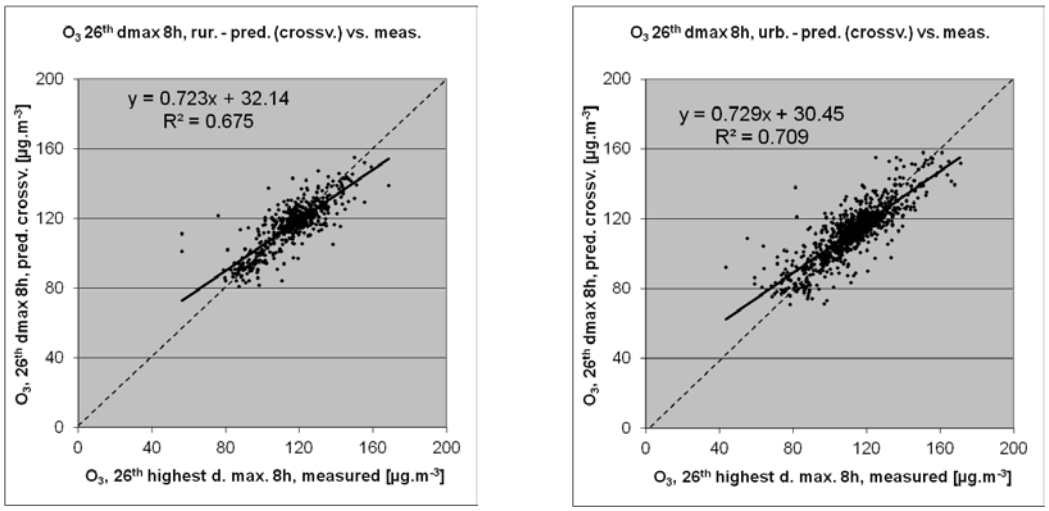

Figure 6.3 Correlation between cross-validation predicted values (y-axis) and measurements (x-axis) for the ozone indicator 26th highest daily maximum 8-hour mean for rural (left) and urban (right) areas in 2010.

Comparison of point measurement values with the predicted grid value

In addition to the point observation - point prediction cross-validation, a simple comparison was made between the point observation values and interpolated predicted grid values. The results of the cross-validation compared to the gridded validation examination are summarised in Table 6.4. The uncertainty at measurement locations is caused partly by the smoothing effect of interpolation and partly by the spatial averaging of the values in the 10x10 km grid cells The level of smoothing, which leads to underestimation in areas with high values, is weaker in areas where measurements exist than in areas where a measurement point is not available. For example, in rural areas the predicted interpolation grid value will be about 146 µg.m^{-3} at the corresponding station point with the observed value of 150 µg.m^{-3}, i.e. an underestimation of about 3 %. This is less than the underestimation of 6 % for such a location without a measurement value, discussed in the previous subsection.

Table 6.4 Linear regression equation and coefficient of determination R^2 from the scatter plots of (i) the predicted point values based on cross-validation and (ii) aggregation into 10x10 km grid cells versus the measured point values for the ozone indicator 26th highest daily maximum 8-hour mean for rural and urban areas of 2010.

	rural areas		urban areas	
	equation	R^2	equation	R^2
i) cross-validation prediction (Fig 6.3)	y = 0.723x + 32.14	0.675	y = 0.729x + 30.45	0.709
ii) 10x10 km grid prediction	y = 0.890x + 12.74	0.948	y = 0.792x + 23.44	0.825

Probability of Target Value exceedance map

A gridded map of 10x10 km resolution showing the probability of target value exceedance is in Figure 6.4. It was constructed on the basis of the 10x10 km gridded concentration map (Figure 6.1, derived from the 1x1 km resolution results), the 10x10 km gridded uncertainty map and the target value (TV) of 120 µg.m^{-3}. Section 4.1.3 explains the significance of the colour classes in the map.

The PoE map for 2010 was compared with 2005 – 2009. It becomes evident that after the year 2006 with its temporary increase in PoE to levels above 50 % and even above 75 % in large parts of

specifically central Europe, a decrease took place in the levels of PoE in 2007 – 2010, to levels in many areas well below those of 2005. In 2010, most of the red areas (large PoE) in the southern and south-western regions of Europe did not change compared to 2009. On the contrary, the red areas extended somewhat in Switzerland, south-western Germany and south-eastern France.

In eastern and south-eastern Europe there were clear decreases, going red and orange (large PoE) to yellow and green (moderate PoE). This decrease was driven by a large decrease in concentrations at several rural stations in this area, but also by very low values at two new Romanian rural stations (RO0138A, RO0210A, both about 56 $\mu g.m^{-3}$). The small number of rural stations in this area means high sensitivity of the map to the values measured at these stations.

On the Iberian Peninsula enlarged areas were estimated with large PoE (red). The increase in PoE to levels above 50 % in this area continued. A minor increase was visible also in central Europe, changing from green to yellow.

The meteorologically induced variations from year to year, combined with methodological uncertainties and the limited number of years considered here do not allow for conclusions on whether or not there is any significant tendency in this ozone indicator. For that purpose, one would need a longer time series and reduced uncertainties.

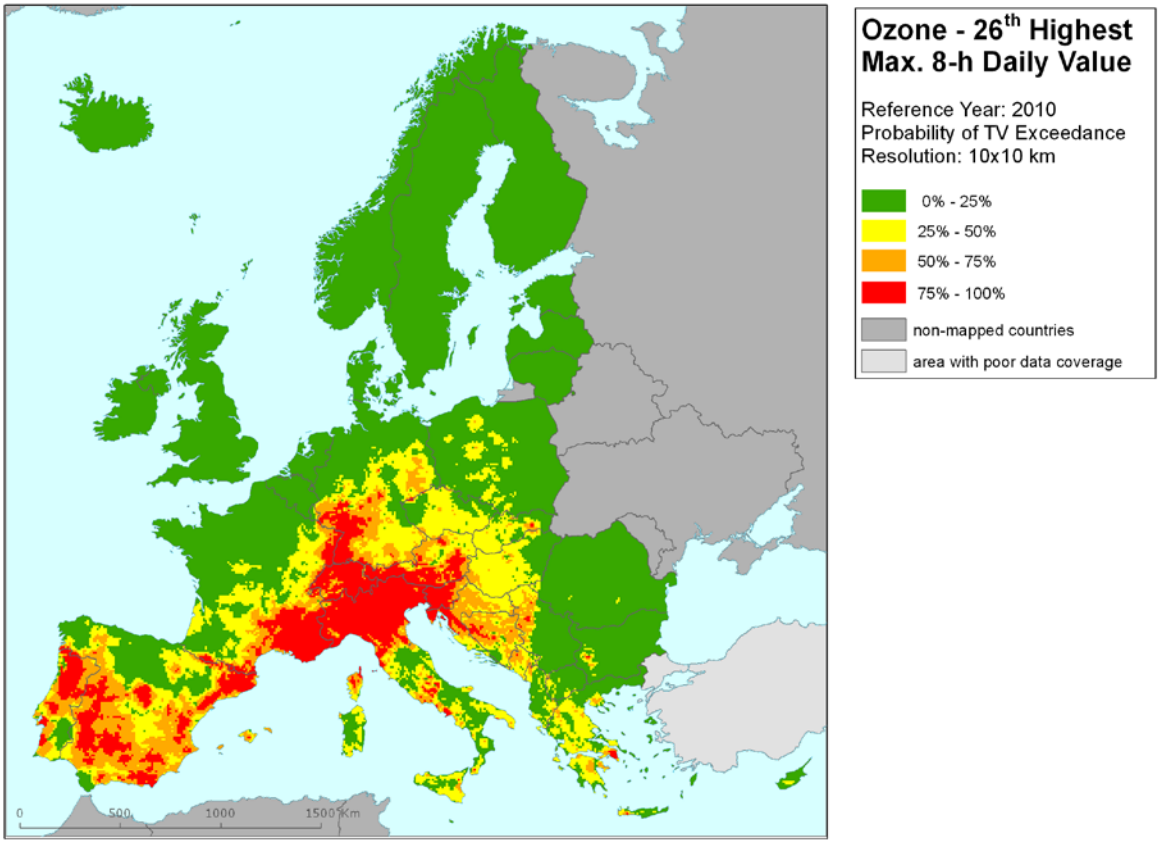

Figure 6.4 Map with the probability of the target value exceedance for ozone indicator 26th highest daily maximum 8-hour average ($\mu g.m^{-3}$) for 2010 on European scale calculated on the 10 x 10 km grid resolution. Interpolation uncertainty is considered only, no other sources of uncertainty.

6.2 SOMO35

6.2.1 Concentration map

Figure 6.5 presents the combined final map for SOMO35 as result of combining the separate rural and urban interpolated map following the procedure as described in De Smet et al. (2011) and Horálek et al. (2007).

As one can observe in a few areas of the map, the high or low measurement values do not seem to influence the interpolation results despite their clustering. The main reason is that the map presented here is an aggregation of 1 km^2 values to 10 km^2 resolution and this aggregation smoothes out the values one would more likely be able to distinguish in the higher resolution map, especially in the case of urban stations representing the urban areas. Another less prominent reason is the smoothing effect kriging has in general.

The supplementary data used in the regression models are the same as for 26th highest daily maximum 8-hour mean, i.e. EMEP model output, altitude and surface solar radiation for rural areas and EMEP model output, wind speed and surface solar radiation for urban areas. (The relevant linear regression models are indicated as O.Ear and UO.Ewr for urban areas.)

Table 6.5 presents the estimated parameters of the linear regression models and of the residual kriging, including the statistical indicators of both the regression and the kriging. The fit of the regression is expressed by the adjusted R^2 and standard error. The adjusted R^2 in 2010 for the rural areas is 0.59 and for the urban areas 0.54. This is quite a similar fit to 2009 (0.60 and 0.53) and 2007 (both 0.58) and somewhat better than in 2008 (0.49 and 0.44), 2006 (0.42 and 0.38) and 2005 (0.51 and 0.49) (De Smet et al. 2011 and 2010, Table 6.4; Horálek et al. 2008, Tables A3.1 and A3.11). RMSE and MPE are the cross-validation indicators showing the quality of the resulting map. Section 6.2.3 discusses in more detail the RMSE analysis and comparison with results of 2005 - 2009.

Table 6.5 Parameters of the linear regression models (Eq. 2.2) and of the ordinary kriging variograms (nugget, sill, range) - and their statistics - of ozone indicator SOMO35 for 2010 in the rural (left) and urban (right) areas as used for final mapping, i.e. rural linear regression model O.Ear (left), resp. UO.Ewr (right) followed by the interpolation on its residuals using ordinary kriging (OK, coded with 'a').

linear regr. model + OK on its residuals	**rural areas (O.Ear-a)** **coeff.**	**urban areas (UO.Ewr-a)** **coeff.**
c (constant)	-2367	-2041
a1 (EMEP model 2010)	0.80	0.79
a2 (altitude GTOPO)	1.73	
a3 (wind speed 2010)		-37.38
a4 (s. solar radiation 2010)	372.15	296.71
adjusted R^2	**0.59**	**0.54**
standard error [µg.m^{-3}.d]	**1665**	**1462**
nugget	1.4E+06	9.0E+05
sill	1.2E+06	4.6E+05
range [km]	100	250
RMSE [µg.m^{-3}.d]	**1604**	**1270**
MPE [µg.m^{-3}.d]	**-6**	**4**

SOMO35 is not subject to one of the EU air quality directives and there are no limit or target values defined that might allow for mapping the probability of exceedances.

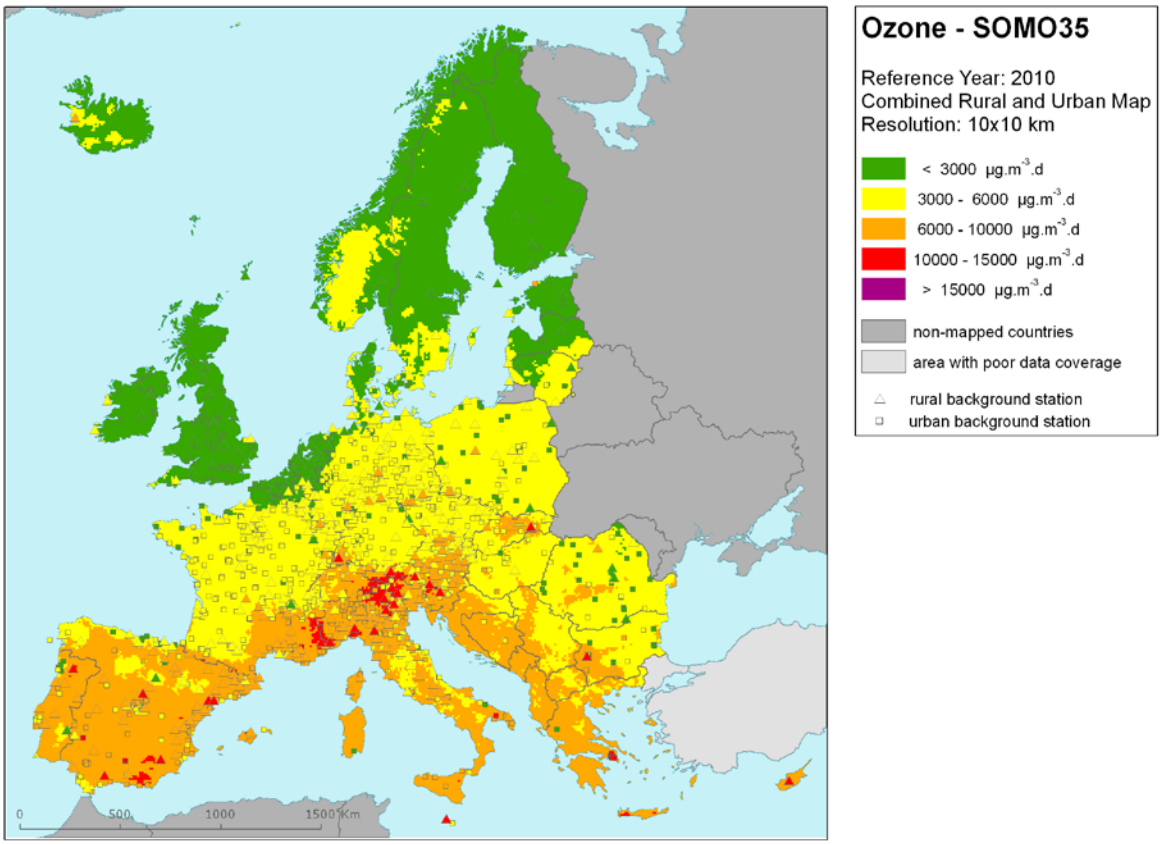

Figure 6.5 Combined rural and urban concentration map of ozone indicators SOMO35 in µg.m^{-3}.days for the year 2010. Resolution: 10x10 km.

Figure 6.6 presents the interannual difference between 2010 and 2009 for SOMO35. Red areas show an increase of ozone concentration, while blue areas show a decrease. A considerable decrease is visible in south-eastern Europe – especially in Romania, Bulgaria, Serbia and FYR of Macedonia. The limited number of observations in concerned countries influences this decrease.

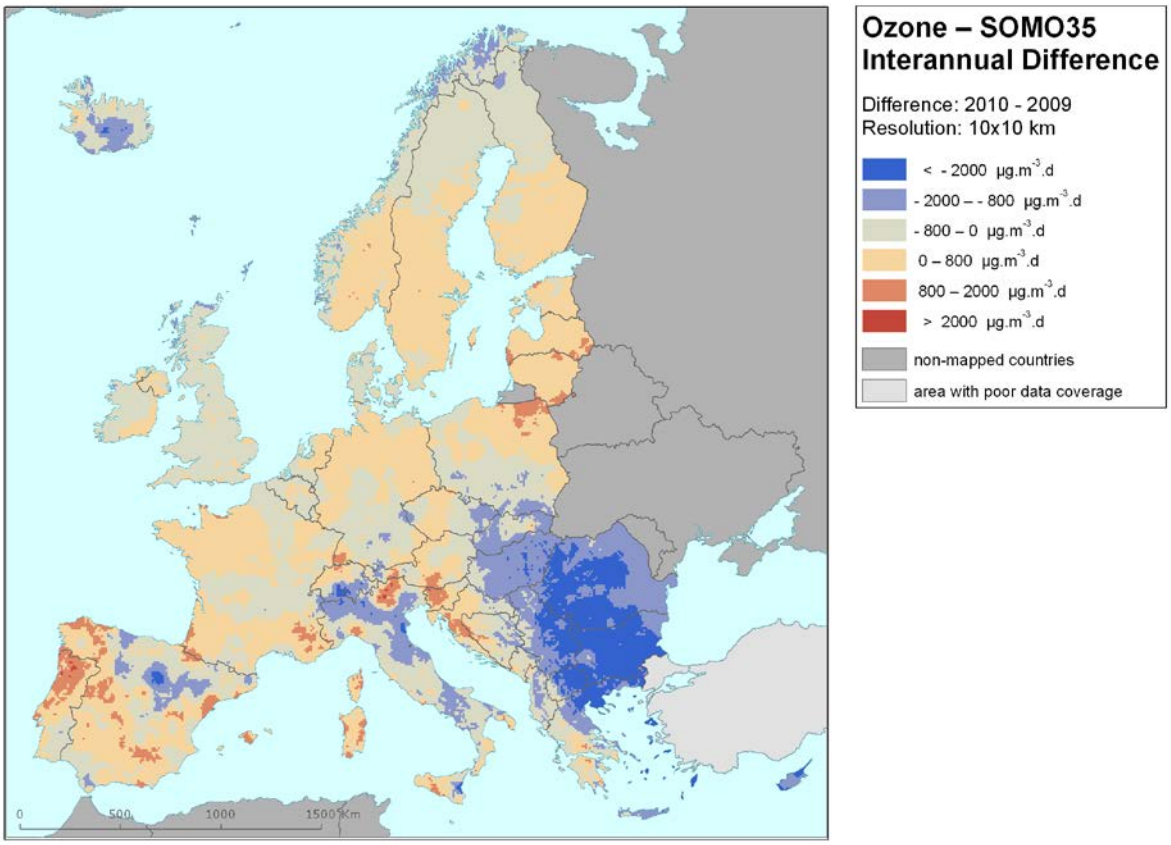

Figure 6.6 Interannual difference between mapped concentrations for 2010 and 2009 – ozone, SOMO35. Units: µg.m^{-3}.days.

6.2.2 Population exposure

Table 6.6 gives for SOMO35 the population frequency distribution for a limited number of exposure classes, as well as the population-weighted concentration for individual countries and for Europe as a whole. In the Table 6.7 the evolution of population exposure in the last five year is presented.

It has been estimated that in 2010 about 16 % of the European population lived in areas with SOMO35 values above 6000 µg.m^{-3}.d. This is a decrease of 8 % compared to 2009. In 2010, many of the northern and north-western European countries had rather similar numbers of people living in areas experiencing more than 6000 µg.m^{-3}.d. Other areas do show decreases of different extents and ranges, with the exception of Portugal (which shows a small increase). In Italy and Greece, more than half of the population continued to be exposed to levels above 6000 µg.m^{-3} in 2010. In Slovakia and Hungary, a steep decrease in the percentage of people exposed was observed, from more than 75 % in 2009 to less than 10 % in 2010. A clear decrease in the population exposed was also observed in the whole of south-eastern Europe, i.e. Albania, Serbia, FYR of Macedonia, Romania, Bulgaria and Greece.

Comparing the national frequency distributions of 2010 with that of 2009, shifts were observed in the percentage of inhabitants per class per country that coincide more or less with shifts in SOMO35 map colours between 2010 and 2009. As in the case of the 26th highest daily maximum 8-hour average, a decrease of the values in south-eastern Europe occurred (namely in Romania, Bulgaria, Serbia and Hungary).

We observe in 2010 compared to 2009 a slight (further) European overall decrease in population exposed to ozone levels above 10 000 µg.m^{-3}.d. In 2010, limited areas of Austria, Bulgaria, France, Greece, Italy and Switzerland exhibited these elevated SOMO35 values (red pixels on the map).

Table 6.6 Population exposure and population-weighted concentration – ozone, SOMO35, year 2010.

Country		Population	2010 Percent [%]					Population-weighted conc.
			< 3000	3000 - 6000	6000 - 10000	10000 - 15000	> 15000	
		x 1000	µg.m^{-3}.d	µg.m^{-3}.d	µg.m^{-3}.d	µg.m^{-3}.d	µg.m^{-3}.d	[µg.m^{-3}.d]
Albania	AL	3 204	0	65.4	34.6	0	0	5 705
Andorra	AD	85	0	0	96.7	3.3	0	7 095
Austria	AT	8 375	0	87.9	12.0	0.2	0	4 991
Belgium	BE	10 840	91.5	8.5	0	0	0	2 394
Bosnia & Herzegovina	BA	3 760	0.7	72.4	26.9	0	0	4 856
Bulgaria	BG	7 564	3.0	91.9	5.0	0.0	0	4 209
Croatia	HR	4 426	0	74.5	25.5	0	0	5 469
Cyprus	CY	819	0	0	100	0	0	7 014
Czech Republic	CZ	10 507	0	99.8	0.2	0	0	4 139
Denmark	DK	5 535	89.7	10.3	0	0	0	2 249
Estonia	EE	1 340	66.7	33.3	0	0	0	2 584
Finland	FI	5 351	100.0	0.0	0	0	0	1 826
France	FR	64 694	22.4	64.3	13.2	0.0	0	4 139
Germany	DE	81 802	12.8	86.9	0.4	0	0	3 659
Greece	GR	11 305	0	15.9	84.0	0.1	0	7 414
Hungary	HU	10 014	3.0	95.9	1.2	0	0	4 428
Iceland	IS	318	98.1	1.9	0	0	0	766
Ireland	IE	4 468	99.5	0.5	0	0	0	1 393
Italy	IT	60 340	0	39.0	60.6	0.4	0	6 349
Latvia	LV	2 248	92.3	7.7	0	0	0	2 254
Liechtenstein	LI	36	0	94.4	5.6	0	0	5 034
Lithuania	LT	3 329	72.6	27.4	0	0	0	2 574
Luxembourg	LU	502	0	100.0	0	0	0	3 521
Macedonia, FYR of	MK	2 053	0	89.5	10.5	0	0	5 110
Malta	MT	414	0	0	100	0	0	6 497
Monaco	MC	35	0	0	100	0	0	7 840
Montenegro	ME	616	0	68.2	31.8	0	0	5 295
Netherlands	NL	16 575	99.5	0.5	0	0	0	1 889
Norway	NO	4 858	95.5	4.5	0	0	0	1 814
Poland	PL	38 167	38.1	61.9	0.0	0	0	3 281
Portugal	PT	10 638	13.8	53.7	32.2	0.2	0	5 231
Romania	RO	21 462	60.2	39.3	0.5	0	0	2 986
San Marino	SM	32	0	89.0	11.0	0	0	5 290
Serbia	RS	9 856	27.9	64.1	8.0	0	0	3 996
Slovakia	SK	5 425	0	93.6	6.4	0	0	4 693
Slovenia	SI	2 047	0	62.9	36.6	0.5	0	6 027
Spain	ES	45 989	3.5	47.5	48.9	0.1	0	6 091
Sweden	SE	9 341	93.3	6.7	0	0	0	2 001
Switzerland	CH	7 786	0	86.5	13.3	0.2	0	5 129
United Kingdom	UK	62 027	99.4	0.6	0	0	0	1 061
Total		**538 185**	**33.6**	**50.1**	**16.2**	**0.1**	**0**	**3 915**
			83.7		**16.3**			

Note: Turkey is not included in the calculation due to lacking air quality data.

The total European population-weighted ozone concentration in terms of SOMO35 was estimated to be 3915 µg.m^{-3}.d, which is less than 2009's value of 4275 µg.m^{-3}.d.

Table 6.7 Evolution of percentage population living in above 6000 µg.m^{-3} (left) and population-weighted concentration (right) in the years 2006-2010 – ozone, SOMO35. Resolution: 1x1 km.

Country		Population above 6000 µg.m^{-3}.d [%]						Population-weighted conc. [µg.m^{-3}.d]					
		2006	2007	2008	2009	2010	diff. '10 - '09	2006	2007	2008	2009	2010	diff. '10 - '09
Albania	AL	75.3	95.8	100	97.6	34.6	-63.0	7193	7817	7668	6754	5705	-1049
Andorra	AD	29.3	100	29.6	100	100	0	6587	7121	6319	7186	7095	-91
Austria	AT	40.1	56.7	12.5	13.4	12.1	-1.2	6237	5874	5099	5050	4991	-59
Belgium	BE	0.3	0	0	0	0	0	4017	2235	2520	2599	2394	-205
Bosnia-Herzegovina	BA	55.5	67.2	37.4	33.8	26.9	-6.9	6571	6938	5972	5536	4856	-680
Bulgaria	BG	28.2	39.2	47.7	32.7	5.0	-27.6	4896	6064	5797	5686	4209	-1477
Croatia	HR	85.7	83.2	35.8	32.5	25.5	-7.0	6928	6756	5899	5491	5469	-22
Cyprus	CY	25.6	98.1	100.0	100	100	0	5759	7739	8027	8788	7014	-1773
Czech Republic	CZ	47.3	11.8	1.7	0.8	0.2	-0.6	6097	5123	4576	4487	4139	-348
Denmark	DK	0.0	0	0	0	0	0	3578	2440	3080	2440	2249	-191
Estonia	EE	0	0	0	0	0	0	3594	2061	2363	1762	2584	822
Finland	FI	0.0	0	0	0	0	0	3141	1332	1938	1623	1826	202
France	FR	18.3	12.0	4.7	13.2	13.3	0.0	4972	3686	3563	4025	4139	114
Germany	DE	8.2	1.1	0.5	0.4	0.4	0.0	4860	3648	3822	3507	3659	152
Greece	GR	74.6	98.0	99.9	98.8	84.1	-14.8	6657	8330	8969	8330	7414	-916
Hungary	HU	36.3	87.2	25.5	89.9	1.2	-88.7	5738	6547	5751	6631	4428	-2203
Iceland	IS	0	0	0	0	0	0	2265	1168	2224	833	766	-67
Ireland	IE	0	0	0	0	0	0	2453	1412	2096	1487	1393	-93
Italy	IT	96.0	86.7	66.1	75.3	61.0	-14.3	8205	7506	6386	6986	6349	-637
Latvia	LV	0	0	0	0	0	0	3734	2262	2347	1837	2254	417
Liechtenstein	LI	51.4	9.1	6.4	12.2	5.6	-6.6	6258	4826	4930	5271	5034	-237
Lithuania	LT	0.0	0	0	0	0	0	4535	2744	3059	2291	2574	283
Luxembourg	LU	1.2	0	0	0	0	0	5090	3424	3557	3500	3521	20
Macedonia, FYR of	MK	32.7	35.6	100	41.5	10.5	-31.1	6297	6690	7133	6229	5110	-1119
Malta	MT	100	100	100	100	100	0	7797	7209	6582	6634	6497	-137
Monaco	MC	100	100	100	100	100	0	8903	8381	7246	8325	7840	-485
Montenegro	ME	35.5	71.8	100	37.1	31.8	-5.3	6554	7379	7120	6237	5295	-943
Netherlands	NL	0	0	0	0	0	0	3245	1816	2104	1922	1889	-33
Norway	NO	2.9	0.0	0	0	0	0	3496	1705	2514	2000	1814	-187
Poland	PL	27.3	1.4	0.7	0.5	0.0	-0.5	5416	4179	3951	3747	3281	-466
Portugal	PT	24.8	14.8	8.6	28.9	32.5	3.6	5257	4863	3851	5003	5231	228
Romania	RO	19.5	41.4	17.9	28.3	0.5	-27.8	4798	5882	5039	5044	2986	-2058
San Marino	SM	22.9	100	14.1	15.3	11.0	-4.3	6321	7296	5863	5860	5290	-569
Serbia (incl. Kosovo)	RS	27.1	65.1	74.9	60.6	8.0	-52.6	5239	6768	6378	6118	3996	-2122
Slovakia	SK	51.9	57.8	19.5	75.6	6.4	-69.2	6261	6098	5455	6348	4693	-1655
Slovenia	SI	98.5	68.1	37.2	36.6	37.1	0.5	7480	6671	5761	5775	6027	252
Spain	ES	50.6	61.0	32.6	57.7	49.0	-8.7	5813	5992	5110	5983	6091	108
Sweden	SE	0.0	0	0	0	0	0	3635	1795	2387	2100	2001	-99
Switzerland	CH	40.5	12.7	8.6	14.3	13.5	-0.9	6321	5114	4619	5139	5129	-10
United Kingdom	UK	0.0	0	0	0	0	0	2676	1174	2044	1433	1061	-372
Total		**29.5**	**28.1**	**19.6**	**24.6**	**16.3**	**-8.3**	**5167**	**4411**	**4275**	**4275**	**3915**	**-360**

6.2.3 Uncertainties

Uncertainty estimated by cross-validation

The basic uncertainty analysis is given by cross-validation. In Table 6.5 the absolute mean uncertainty (RMSE) in 2010 was 1604 µg.m^{-3}.d for the rural areas and 1270 µg.m^{-3}.d for the urban areas. This means that for rural areas a progressive reduction in uncertainty compared to its previous years is confirmed. The uncertainties at rural and urban areas in previous years were: 1635 and 1475 µg.m^{-3}.d (2009), 1609 and 1293 µg.m^{-3}.d (2008), 1801 and 1260 µg.m^{-3}.d (2007), 2077 and 1472 µg.m^{-3}.d (2006) and 2173 and 1459 µg.m^{-3}.d (2005). The relative mean uncertainty of the 2010 map of

SOMO35 is 29.5 % for both and urban areas. The previous years had for rural and urban areas respectively: 29.7 % and 33.1 % (2009), 30.7 % and 31.3 % (2008), 33.3 % and 29.5 % (2007), 31.6 % and 29.2 % (2006) and 35.5 % and 32 % (2005), meaning that the 2010 relative uncertainties for both rural and urban areas are at the lower end of the range. Table 7.7 summarises both the absolute and the relative uncertainties over these past six years.

Figure 6.7 shows the cross-validation scatter plots for interpolated values at both rural and urban areas. R^2 for rural areas and urban areas in 2010 indicates that, respectively, about 62 % and 65 % of the variability is attributable to the interpolation. The corresponding values for the 2009 maps (63 % and 62 %), 2008 maps (63 % and 54 %), 2007 maps (63 % and 67 %), the 2006 maps (47 % and 49 %) and 2005 maps (55 % and 58 %), illustrate a somewhat similar fit for the years 2007 – 2010.

The scatter plots show again that in areas with high concentrations the interpolation methods tend to deliver underestimated predictions, although some overestimation or lower values of urban areas is also likely. For example, in urban areas (Figure 6.7, right panel) an observed value of 10 000 µg.m^{-3}.d is estimated in the interpolation as about 8100 µg.m^{-3}.d. That is 19 % too low, leading in general to high underestimations at high SOMO35 values. Vice versa at low values an overestimation will occur, e.g. at a measured 2000 µg.m^{-3}.d the interpolation will predict some 2800 µg.m^{-3}.d, which is about 39 % too high.

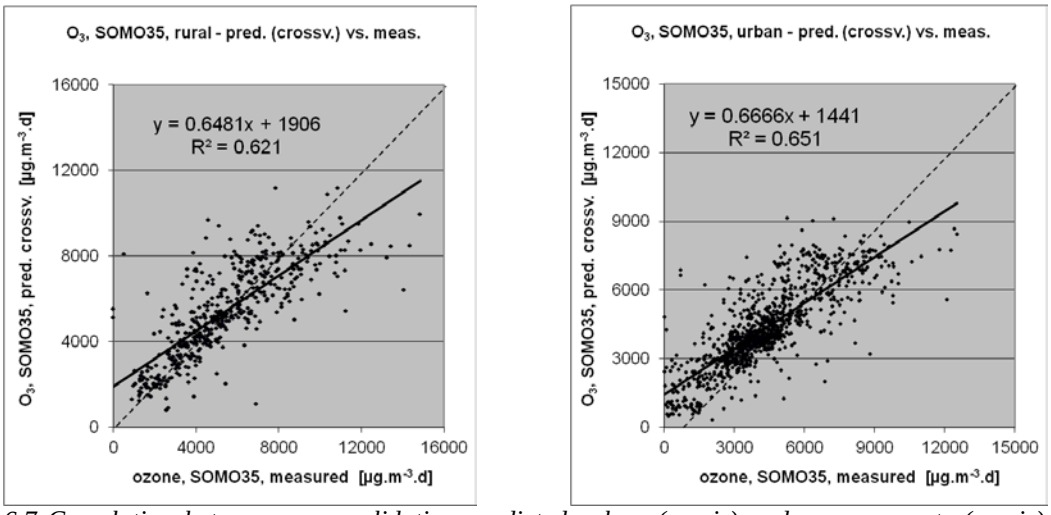

Figure 6.7 Correlation between cross-validation predicted values (y-axis) and measurements (x-axis) for the ozone indicator SOMO35 for rural (left) and urban (right) areas in 2010.

Comparison of point measurement values with the predicted grid value

Additional to the point observation - point prediction cross-validation, a simple comparison was made between the point measurements and interpolated predicted grid values averaged in on a grid of 10x10 km resolution the separate rural and urban maps. This point-grid comparison indicates to what extent the predicted value of a grid cell represents the corresponding measured values at stations located in that cell. The results of the point observation - point prediction cross-validation of Figure 6.7, compared to those of the point-grid validation are summarised in Table 6.8. The table shows a better correlated relationship (i.e. higher R^2, smaller intercept, slope closer to 1) between station measurements and the interpolated values of the corresponding grid cells (case ii) at both rural and urban map areas than it does for the point cross-validation predictions (case i). This is because the simple comparison between point measurements and the gridded interpolated values shows the uncertainty of predictions where there are actual station locations, while the point observation – point prediction cross-validation simulates the behaviour of the interpolation at positions without actual measurements but within the area covered by measurements. The uncertainty at measurement locations is caused partly by the smoothing effect of the interpolation and partly by the spatial averaging of the values into 10x10 km grid cells. The degree of smoothing leading to underestimation in areas with high values is weaker when measurements exist, than when no measurement exists. For

example, in urban areas the predicted interpolation grid value will be about 8500 µg.m^{-3}.d at a corresponding station point with an observed value of 10 000 µg.m^{-3}.d, i.e. an underestimation of about 15 %. This underestimation is weaker than the 19%, discussed in the previous subsection, which was simulating the situation where no measurement exists.

Table 6.8 Linear regression equation and coefficient of determination R^2 from the scatter plots of (i) the predicted point values based on cross-validation and (ii) aggregation into 10x10 km grid cells versus the measured point values for the ozone indicator SOMO35 for rural and urban areas of 20109.

	rural areas		urban areas	
	equation	R^2	equation	R^2
i) cross-validation prediction (Fig 5.5)	y = 0.648x + 1906	0,621	y = 0.667x + 1441	0,651
ii) 10x10 km grid prediction	y = 0.795x + 1111	0,874	y = 0.732x + 1161	0,774

No Limit Value or Target Value is set for the WHO recommended ozone health indicator SOMO35, therefore no probability of exceedance map has been prepared.

6.3 AOT40 for crops and for forests

The ecosystem based accumulative ozone indicators described in this section are specifically prepared for calculation of EEA Core Set Indicator 005 (CSI005, http://themes.eea.europa.eu/indicators). For the estimation of the vegetation and forested area exposure to accumulated ozone the maps in this section are created on a grid of 2x2 km resolution, instead of the 10x10 km grid used for the human health indicators. This resolution is selected as a compromise between calculation time and accuracy in the impact assessment done for ozone within CSI005. It serves as a refinement of the exposure frequency distribution outcomes of the overlay with 100x100 m resolution CLC2000 land cover classes.

6.3.1 Concentration maps

The interpolated maps of AOT40 for crops and AOT40 for forests were created for rural areas only, combining AOT40 data derived from rural background station observations with supplementary data sources EMEP model output, altitude and surface solar radiation. The relevant linear regression model is referred to as O.Ear. Note that supplementary data sources are the same as for the human health related ozone indicators.

Table 6.9 presents the estimated parameters of the linear regression models and of the residual kriging, including their statistical indicators of the regression and kriging. The fit of the regression is expressed by adjusted R^2 and the standard error. The adjusted R^2 is in 2010 for AOT40 for crops 0.59 and for AOT40 for forests 0.63, i.e. quite a similar fit as in 2009 (0.64 and 0.61) and better fit than in 2008 (0.40 and 0.49) and in 2007 (0.49 and 0.59) (De Smet et al. 2012, 2011 and 2010, Table 6.7). RMSE and MPE are the cross-validation indicators, showing the quality of the resulting map. Section 5.3.3 discusses in more detail the RMSE analysis and comparison with results of 2005 – 2009.

Table 6.9 Parameters of the linear regression models (Eq2.1) and of the ordinary kriging variograms (nugget, sill, range) - and their statistics - of ozone indicators AOT40 for crops (left) and for forests (right) for 2010 in the rural areas as used for final mapping, i.e. rural linear regression model O.Ear followed by the interpolation on its residuals using ordinary kriging (OK, coded with 'a').

linear regr. model + OK on its residuals	AOT40 for crops (O.Ear-a) coeff.	AOT40 for forests (O.Ear-a) coeff.
c (constant)	-6705	-16303
a1 (EMEP model 2010)	0.57	0.42
a2 (altitude GTOPO)	3.29	7.52
a3 (s. solar radiation 2010)	1062.1	2328.9
adjusted R^2	**0.59**	**0.63**
standard error [µg.m^{-3}]	**5779**	**9080**
nugget	1.5E+07	3.5E+07
sill	1.7E+07	3.8E+07
range [km]	140000	110000
RMSE [µg.m^{-3}]	**5198**	**8384**
MPE [µg.m^{-3}]	**149**	**244**

Figure 6.8 presents the final map of AOT40 for crops. The areas and stations in the map that exceed the target value (TV) of 18 mg.m^{-3}.h are marked in red and purple. It is applicable to rural areas only, as it is based on rural background station observations. It represents the indicator for vegetation exposure to ozone while assuming there is no relevant vegetation in urban areas. The map was compared to its counterparts from 2009, 2008 and 2007 and an increase in the extent of areas with the highest AOT40 levels (red and purple) was found specifically in the south-western regions of Europe.

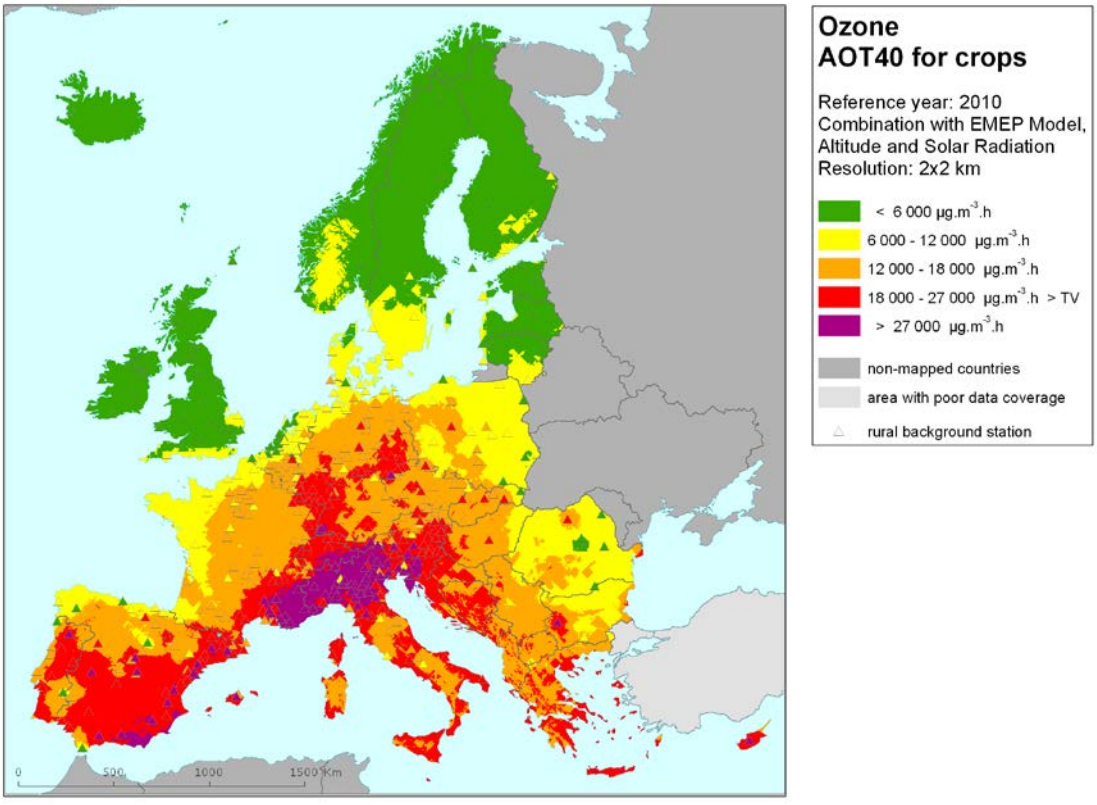

Figure 6.8 Rural concentration map of ozone vegetation indicator AOT40 for crops for the year 2010. Units: µg.m^{-3}.hours. Resolution: 2x2km.

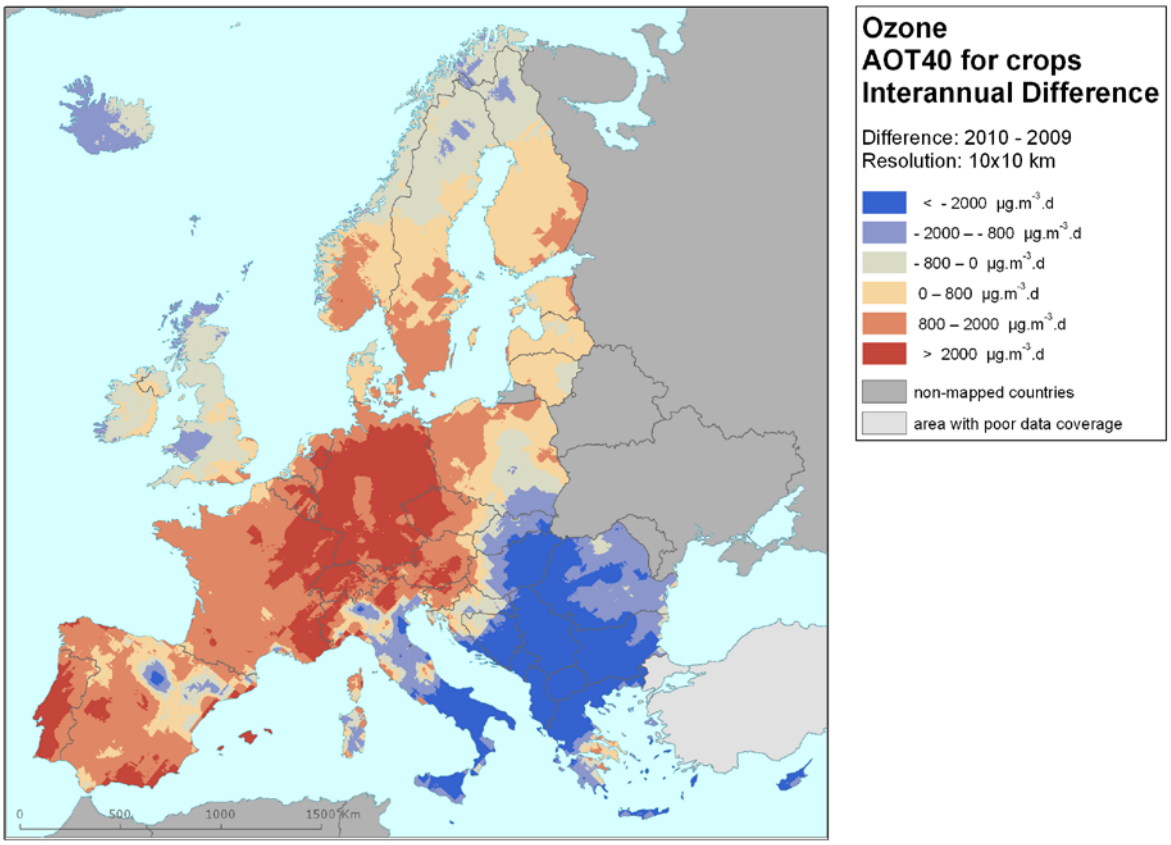

Figure 6.9 Interannual difference between mapped concentrations for 2010 and 2009 – ozone, AOT40 for crops. Units: µg.m^{-3}.hours.

Figure 6.9 presents the interannual difference between 2010 and 2009 for AOT40 for crops. Red areas show an increase of ozone concentration, while blue areas show a decrease. The highest increases can be seen in Germany, Switzerland, north-eastern France and Portugal. Contrary to that, considerable decreases are visible in south-eastern Europe – especially in Romania, Bulgaria, Serbia, FYR of Macedonia, Montenegro, Albania, southern Italy and Cyprus. This decrease might be influenced by the limited number of observations in relevant countries.

Figure 6.10 presents the final map of AOT40 for forests. Like Figure 6.8, it concerns a map for rural areas. It is based on rural background station observations only, representing an indicator for vegetation exposure to ozone. For AOT40 for forests there is no TV defined.

In Figure 6.9, the interannual difference between 2010 and 2009 for AOT40 for forests is shown. Again, the main decrease is visible in south-eastern Europe – especially in Romania, Bulgaria, Serbia, FYR of Macedonia, Montenegro, Albania, southern Italy and Cyprus. The limited number of measuring stations in the relevant countries might influence the extent of the area in decrease.

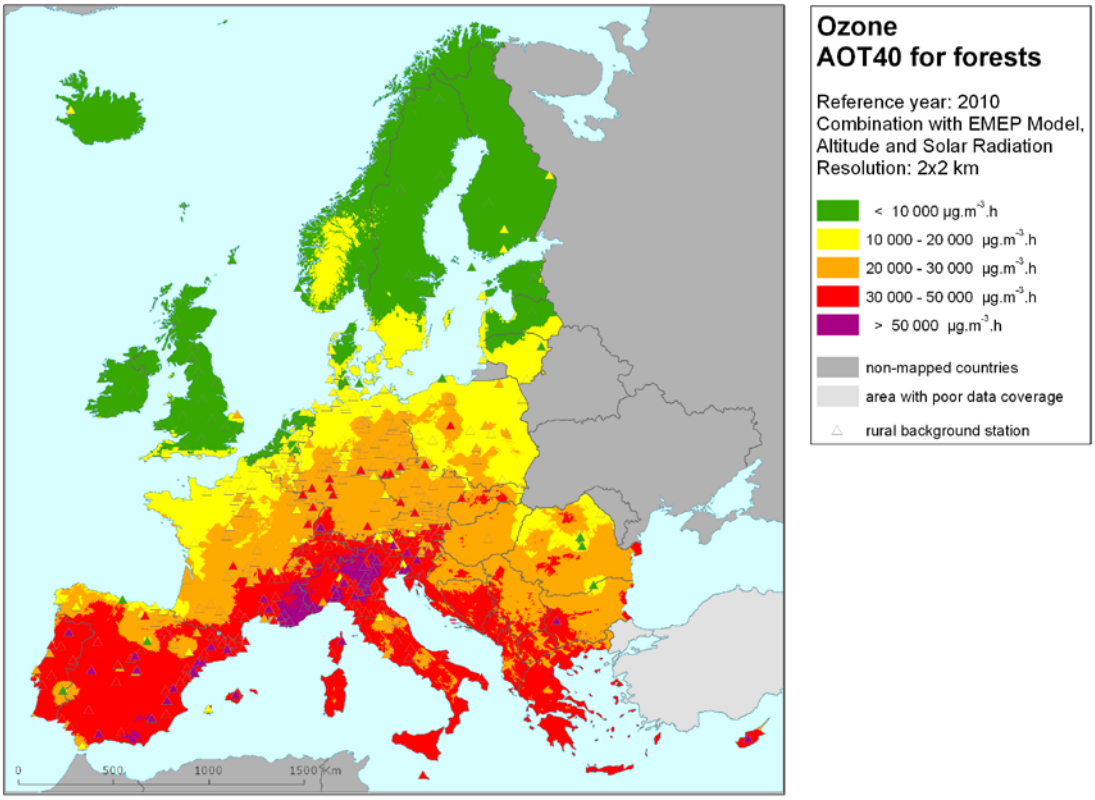

Figure 6.10 Rural concentration map of ozone vegetation indicator AOT40 for forests for the year 2010. Units: µg.m^{-3}.hours. Resolution: 2x2km.

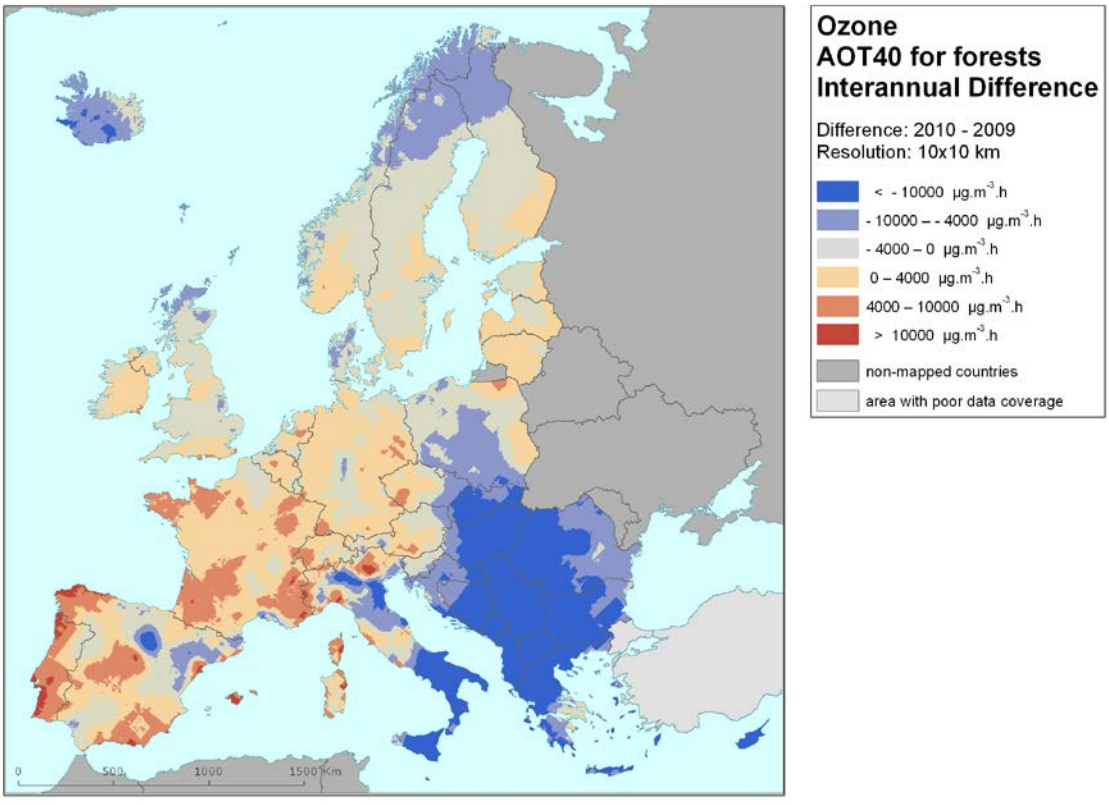

Figure 6.11 Interannual difference between mapped concentrations for 2010 and 2009 – ozone, AOT40 for crops. Units: µg.m^{-3}.hours. Resolution: 2x2km.

6.3.2 Vegetation exposure

Agricultural crops

The rural map with ozone indicator AOT40 for vegetation, i.e. agricultural crops, as given in Figure 6.8, has been combined with the land cover CLC2000 map. Following a similar procedure as described in Horálek et al. (2007) the exposure of agricultural areas, defined as the Corine Land Cover level-1 class *2 Agricultural areas* (encompassing the level-2 classes *2.1 Arable land, 2.2 Permanent crops, 2.3 Pastures* and *2.4 Heterogeneous agricultural areas)* has been calculated at the country-level.

Table 6.10 gives the absolute and relative agricultural area for each country and for four European regions where the target value (TV) and long-term objective (LTO) for ozone are exceeded. The frequency distribution of the agricultural area per country over the exposure classes is presented as well.

The table indicates the country grouping with corresponding colours of the region; *Northern Europe*: Sweden, Finland, Norway, Estonia, Lithuania, Latvia and Denmark. *North-western Europe*: United Kingdom, Ireland, Iceland, the Netherlands, Belgium, Luxembourg and France north of 45 degrees latitude. *Central and Eastern Europe*: Germany, Poland, Czech Republic, Slovakia, Hungary, Austria, Liechtenstein, Bulgaria and Romania. *Southern Europe*: Albania, Bosnia-Herzegovina, France south of 45 degrees latitude, Portugal, Spain, Italy, San Marino, Slovenia, Croatia, Greece, Cyprus, F.Y.R. of Macedonia, Montenegro, Serbia and Malta.

Table 6.10 illustrates that in 2010, some 21 % of all European agricultural land was exposed to ozone exceeding the target value (TV) of 18 $mg.m^{-3}.h$. This is a decrease in the total area with agricultural crops above the TV (and as such considered to suffer from adverse effects to ozone exposure) compared to 2009 (26 %). It is lower, however, than 2008 (38 %), 2007 (36 %) and well below that of 2006 (70 %), see Table 6.12 (and also below that of 2005 (49%), see Horálek et al., 2008). Considering the long-term objective (LTO, 6 $mg.m^{-3}.h$) the area in excess (85 %) was higher than in 2009 (81%) and 2007 (78 %), but lower than in 2008 (96 %) and 2006 (98 %). Two European countries (i.e. one less than in 2009) did have ozone levels not being in excess of the LTO, namely Ireland and Iceland. In many countries of central and southern Europe, more than half of their total agricultural area experienced exposures above the less stringent TV.

Table 6.12 (left) presents for comparison the percentages of area in exceedance of the target value for the years 2006 – 2010. In southern Europe, about 57 % of the total agricultural area exceeded the target value in 2010. This is within the range of what it was in 2009 (60 %), 2008 (64 %) and 2007 (55 %) and substantially below the amounts of 2006 (94 %). For 2010, 2009, 2008 and 2007 (and also for 2005) no area was mapped in excess of the target value in northern Europe; only in 2006 about 4 % of its area was in excess. In the north-western region the area exceeding the target value is about 33 % in 2010, which is a steep increase compared to the period of 2007 – 2009, when the area exceeded was only 0.1 – 2 %, although it is still below the 50 % of 2006. For the central and eastern region, the total area where ozone exceeds the target value decreased considerably from 2006 to 2007: from 77 % to 50 % (after increase from 44% in 2005). From that time, it has further reduced to 47 % in 2008, 17 % in 2009 and 11 % in 2010.

Compared to 2006, the frequency distribution of agricultural area over the exposure classes showed a clear shift towards lower exposures in 2007 leading to a decreased total area exceeded (to a distribution more similar to that of 2005, see Horálek et al., 2008). In 2008, this tendency continued with an approximately similar area percentage in excess of the TV, however, a shift in area percentages with lower exposure levels in 2007 to somewhat higher levels in 2008 (but still below the target value) also occurred. Compared to 2007 – 2008, we observed in 2009 – 2010 an increased area with lower exposure level, leading to a lower TV exceedance.

Table 6.10 Agricultural area exposure and exceedance (Long Term Objective, LTO and Target Value, TV) for ozone, AOT40 for crops, year 2010.

Country	Agricultural Area, 2010					Percentage of agricultural area, 2010 [%]				
	tot. area	> LTO (6 mg.m^{-3}.h)		> TV (18 mg.m^{-3}.h)		< 6 mg.m^{-3}.h	6 - 12 mg.m^{-3}.h	12 - 18 mg.m^{-3}.h	18 - 27 mg.m^{-3}.h	> 27 mg.m^{-3}.h
	[km^2]	[km^2]	[%]	[km^2]	[%]					
Albania	7184	7184	100	286	4.0	0	0.03	96.0	4.0	0
Austria	27462	27462	100	11235	40.9	0	0	59.1	40.7	0.3
Belgium	17652	17299	98.0	0	0	2.0	36.9	61.1	0	0
Bosnia-Herzegovina	19316	19316	100	8929	46.2	0	0	53.8	46.2	0
Bulgaria	57388	57216	99.7	2649	4.6	0.3	67.2	27.9	4.6	0
Croatia	24135	24135	100	14960	62.0	0	0	38.0	57.1	4.9
Cyprus	4290	4290	100	3739	87.2	0	0	12.8	85.1	2.1
Czech Republic	45550	45550	100	3629	8.0	0	0.6	91.4	8.0	0
Denmark (w~out Faroes)	32247	28109	87.2	0	0	12.8	87.0	0.2	0	0
Estonia	14684	343	2.3	0	0	97.7	2.3	0	0	0
Finland	28833	2238	7.8	0	0	92.2	7.8	0	0	0
France	328466	328466	100	38976	11.9	0	33.0	55.1	9.6	2.3
Germany	213519	213519	100	52087	24.4	0	14.2	61.4	24.2	0.2
Greece	51575	51575	100	22738	44.1	0	3.5	52.4	44.1	0.0
Hungary	63086	63086	100	4518	7.2	0	20.7	72.1	7.2	0
Iceland	2380	0	0	0	0	100	0	0	0	0
Ireland	46395	0	0	0	0	100	0	0	0	0
Italy	155658	155658	100	105739	67.9	0	0	32.1	41.9	26.0
Latvia	28286	1587	5.6	0	0	94.4	5.6	0	0	0
Liechtenstein	47	47	100	46.6	100	0	0	0	100	0
Lithuania	40045	12787	31.9	0	0	68.1	31.9	0	0	0
Luxembourg	1411	1411	100	379	26.8	0	0	73.2	26.8	0
Macedonia, FYR of	9506	9506	100	126	1.3	0	3.7	94.9	1.3	0
Malta	125	125	100	125	100	0	0	0	100	0
Monaco	0.52	0.52	100	0.5	100	0	0	0	0	100
Montenegro	2396	2396	100	633	26.4	0	0	73.6	26.4	0
Netherlands	24900	19940	80.1	0	0	19.9	71.0	9.0	0	0
Norway	15674	684	4.4	0	0	95.6	4.4	0	0	0
Poland	200499	199411	99.5	0	0	0.5	76.2	23.2	0	0
Portugal	42568	42568	100	17653	41.5	0	4.0	54.5	41.5	0
Romania	134891	131591	97.6	28	0.0	2.4	84.7	12.8	0.0	0
San Marino	43	43	100	43	100	0	0	0	100	0
Serbia (incl. Kosovo)	48503	48503	100	1411	2.9	0	8.9	88.2	2.9	0
Slovakia	24339	24339	100	58	0.2	0	14.8	85.0	0.2	0
Slovenia	7127	7127	100	7127	100	0	0	0	79.0	21.0
Spain	252314	252281	99.99	153219	60.7	0.0	7.9	31.4	58.5	2.2
Sweden	38624	18842	49	0	0	51.2	48.8	0	0	0
Switzerland	11784	11784	100	11558	98.1	0	0	1.9	94.5	3.6
United Kingdom	141974	18400	13	0	0	87.0	13.0	0	0	0
Total	**2164873**	**1848819**	**85.4**	**461891**	**21.3**	**14.6**	**27.6**	**36.5**	**18.7**	**2.6**
France N of 45N	260777	260777	100	16905	6.5	0	37.4	56.1	6.4	0
France S of 45N	67688	67688	100	22067	32.6	89.0	11.0	0	0	0
Northern	198393	64590	32.6	0	0					
North-western	495488	317828	64.1	17284	3.5					
Central & eastern	778564	774006	99.4	85809	11.0					
Southern	692427	692395	100.0	358796	51.8					
Total	**2164873**	**1848819**	**85.4**	**461888**	**21.3**					

Note: Countries not included due to lack of land cover data: Andorra, Turkey.

Forests

The rural map with ozone indicator AOT40 for forests, as given in Figure 6.9, was combined with the land cover CLC2000 map as done for crops. Following a similar procedure as described in Horálek et al. (2007) the exposure of forest areas, defined as CORINE Land Cover level-2 class *3.1. Forests*, has been calculated at the country-level.

Table 6.11 gives the absolute and relative forest area where the *Reporting Value* (RV of 20 $mg.m^{-3}.h$, as Annex III of the ozone directive defines it) in combination with the *Critical Level* (*CL* of 10 $mg.m^{-3}.h$, as defined in the UNECE Mapping Manual) are exceeded. This is done for each country, for four European regions and for Europe as a whole. The table presents the frequency distribution of the forest area per country over the exposure classes as well. The Reporting Value of the ozone directive was exceeded in 2010 at 49 % of the total European forest area. Table 6.12 (right) presents for comparison the percentages of area which exceed the Reporting Value for the years 2006 – 2010. The RV for 2010 is about the same as in 2009 (49%), 2008 (50 %) and 2007 (48 %), while in 2006 it was almost 70 % (and in 2005 about 60 %, see Horálek et al., 2008). This means that the area of forest exposed to levels above the accumulated ozone RV diminished in 2007 – 2010 to an area of 20 percentage points below that of 2006 (and 10 percentage points below that of 2005).

In 2006 about all of the European forest areas were exposed to exceedances of the Critical Level (CL) of 10 $mg.m^{-3}.h$ (while in 2005 it was the case for three-quarters of the forest areas). This extensive portion shrank in 2007 to 62 %, but in 2008 it increased to 80 %. In 2009, the forest area exposed to exceedances of the CL was reduced to a level of 67 % and in 2010 to a level of 63%.

In 2010 almost all European countries had forests exposed to accumulated ozone concentrations above the CL and many of those had forests experiencing exposures in excess of the less stringent RV. Finland, Estonia, Sweden, Iceland and Ireland continued to experience accumulated ozone levels over forests that were below the RV and a further reduced part of their forests experienced levels exceeding the CL. In 2010, the list of countries without areas above the RV, but with CL exceedances was extended with Denmark and reduced with Belgium.

As in previous years, in 2010, the southern European region had AOT40 levels where approximately all forested areas were exposed to exceedances of the CL.

The central and eastern regions show, for the period of 2005 – 2010, a continued 100 % exceedance of the CL. The area with exceedances of the RV (Table 6.12) showed a peak of 100 % in 2006, followed by a reduction to about 86 % in 2007 and a subsequent increase of about 10 % in 2008 to 95 % (which comes close to the 96 % of 2005, see Horálek et al., 2008). In 2009, the area in excess of the RV was 88 %. In 2010 it is 76 %. In the north-western region, the area exceeding the CL increased from 84 % in 2005 to practically the whole area (98 %) in 2006. In 2007, it dropped again to 78 %, but in 2008 it increased to almost all forested area (94 %). In 2009, it was 81 % and in 2010 it is 82 %, close to the excess of 2007. Concerning the north-western European forested area above the RV, there was a prominent drop from 80% in 2006 to 28% in 2007 (after an increase from 69% in 2005) that continued in 2008 to 23 %, but increased again in 2009 to 30 % and to 60 % in 2010. Specifically in the northern region of Europe, the area in exceedance peaked considerably in 2006: the area above the CL enlarged from 40 % in 2005 to 100 % in 2006 and reduced thereafter to 12 % in 2007 and increased in 2008 to 51 %. In 2009, some 23 % of the northern European forest area exceeded the CL, in 2010 it was about 13 %. The RV (Table 6.12) decreases in northern Europe from 23 % in 2006 (after an increase from none in 2005) to none in 2007 – 2010. In comparison with 2006, the frequency distribution of the whole European forested area over the exposure classes shows for 2007 a clear shift to lower exposures. In 2008 a shift was observed of areas exposed in 2007 to the highest exposures to its neighbouring lower class interval and for the areas exposed in 2007 to the lowest exposure class to its neighbouring higher class interval. In 2009 and 2010 the distribution showed similarity with that of 2007. The total area with AOT40 levels below the CL diminished by 18 % in 2008 (20 %) compared to 2007 (38 %) but increased again in 2009 up to 33 % and in 2010 to 37 %; the total forested area submitted to levels below the RV stabilised in the period 2007 – 2010 around a value of 50 %.

Table 6.11 Forest area exposure and exceedance (critical level, CL and reporting value, RV) for ozone, AOT40 for forests, year 2010.

Country	Area of forests, 2010					Percentage of forest area, 2010 [%]				
	tot. area	> CL (10 mg.m^{-3}.h)		> RV (20 mg.m^{-3}.h)		< 10 mg.m^{-3}.h	10 - 20 mg.m^{-3}.h	20 - 30 mg.m^{-3}.h	30 - 50 mg.m^{-3}.h	> 50 mg.m^{-3}.h
	[km^2]	[km^2]	[%]	[km^2]	[%]					
Albania	7817	7817	100	7817	100	0	0	12.8	87.2	0
Austria	37608	37608	100	37493	99.7	0	0.3	41.6	58.1	0.01
Belgium	6104	6000	98.3	2058	33.7	1.7	64.6	33.7	0	0
Bosnia-Herzegovina	22962	22962	100	22962	100	0	0	20.2	79.8	0
Bulgaria	34845	34845	100	34167	98.1	0	1.9	58.8	39.2	0.01
Croatia	20197	20197	100	20197	100	0	0	39.5	60.5	0.02
Cyprus	1552	1552	100	1552	100	0	0	3.9	89.3	6.8
Czech Republic	25484	25484	100	24569	96.4	0	3.6	93.5	2.9	0
Denmark	3694	2054	55.6	0	0	44.4	55.6	0	0	0
Estonia	20778	629	3.0	0	0	97.0	3.0	0	0	0
Finland	193325	98	0.1	0	0	99.9	0.1	0	0	0
France	144853	144801	100.0	123539	85.3	0.0	14.7	54.0	23.9	7.4
Germany	103828	103744	99.9	87180	84.0	0.1	16.0	78.2	5.8	0
Greece	23563	23563	100	23563	100	0	0	10.9	88.9	0.2
Hungary	17351	17351	100	16074	92.6	0	7.4	89.1	3.6	0
Iceland	314	0	0	0	0	100	0	0	0	0
Ireland	2913	3	0.1	0	0	99.9	0.1	0	0	0
Italy	78836	78836	100	78836	100	0	0	7.1	73.7	19.2
Latvia	26960	7078	26.3	0	0	73.7	26.3	0	0	0
Liechtenstein	66	66	100	66	100	0	0	31.2	68.8	0
Lithuania	18663	15779	84.5	0	0	15.5	84.5	0	0	0
Luxembourg	903	903	100	857	94.9	0	5.1	94.9	0	0
Macedonia, FYR of	8630	8630	100	8630	100	0	0	11.8	88.2	0
Malta	2	2	100	2	100	0	0	0	100	0
Monaco	1	1	100	1	100	0	0	0	0	100
Montenegro	5785	5785	100	5785	100	0	0	11.0	89.0	0
Netherlands	3100	2156	69.6	0	0	30.4	69.6	0	0	0
Norway	104935	17677	16.8	0	0	83.2	16.8	0	0	0
Poland	91851	91851	100	25095	27.3	0	72.7	27.3	0.04	0
Portugal	24319	24319	100	24242	99.7	0	0.3	10.6	89.0	0.01
Romania	69787	69690	99.9	56365	80.8	0.1	19	72.4	8.4	0
San Marino	6	6	100	6	100	0	0	0	100	0
Serbia (incl. Kosovo)	26687	26687	100	26687	100	0	0	65.4	34.6	0
Slovakia	19300	19300	100	17526	90.8	0	9.2	70.7	20.1	0
Slovenia	11476	11476	100	11476	100	0	0	3.6	96.4	0.02
Spain	91885	91885	100	85695	93.3	0	6.7	23.7	67.8	1.8
Sweden	249922	36713	14.7	0	0	85.3	14.7	0	0	0
Switzerland	12513	12513	100	12513	100	0	0	7.9	87.4	4.7
United Kingdom	19660	2163	11.0	0	0	89.0	11.0	0	0	0
Total	**1532473**	**972222**	**63.4**	**754952**	**49.3**	**36.6**	**14.2**	**25.7**	**21.7**	**1.8**
France N of 45N	89502	89450	99.9	70257	78.5	0.1	21.4	66.0	12.2	0.3
France S of 45N	55346	55346	100	53278	96.3	89.0	11.0	0	0	0
Northern	618277	80028	12.9	0	0					
North-western	122496	100676	82.2	73172	59.7					
Central & eastern	412634	412451	99.96	311048	75.4					
Southern	379062	379062	100	370728	97.8					
Total	**1532469**	**972218**	**63.4**	**754948**	**49.3**					

Note: Countries not included due to lack of land cover data: Andorra, Turkey.

Table 6.12 Evolution of percentage agricultural area above target value for AOT40 for crops (left) and percentage forested area above reporting value for AOT40 for forests (right) in the years 2006-2010.

Country		AOT40 for crops						AOT40 for forests					
		Agricultural area above TV [%]						Forested area above RV [%]					
		2006	2007	2008	2009	2010	diff. '10 - '09	2006	2007	2008	2009	2010	diff. '10 - '09
Albania	AL	100	100	87.3	100	4.0	-96.0	100.0	100	100	100	100	0
Austria	AT	100	81.8	67.3	4.0	40.9	36.9	100.0	100	100	100	99.7	-0.3
Belgium	BE	98.0	0	0	0	0	0	99.8	7.9	0	0	33.7	33.7
Bosnia-Herzegovina	BA	62.7	100	80.0	90.3	46.2	-44.1	100.0	100	100	100	100	0
Bulgaria	BG	44.5	99.6	2.4	64.4	4.6	-59.8	100.0	100	100	100	98.1	-1.9
Croatia	HR	82.2	100	95.8	85.5	62.0	-23.5	100.0	100	100	100	100	0
Cyprus	CY	99.0	100	0.0	100	87.2	-12.8	100.0	100	100	100	100	0
Czech Republic	CZ	100	83.0	99.0	0.0	8.0	8.0	100.0	100	100	100	96.4	-3.6
Denmark	DK	5	0	0	0	0	0	91.7	0.9	1.7	1.7	0	-1.7
Estonia	EE	0	0	0	0	0	0	52.6	0	0	0	0	0
Finland	FI	0	0	0	0	0	0	2.1	0	0	0	0	0
France	FR	78.0	3.4	10.2	10.2	11.9	1.7	97.0	50.9	48.0	52.2	85.3	33.1
Germany	DE	94.7	3.6	62	0.0	24.4	24.4	99.8	76.9	92.8	81.0	84.0	3.0
Greece	GR	95.2	97.4	79.0	95.2	44.1	-51.1	100	100	100	100	100	0
Hungary	HU	93.4	100	82.8	83.6	7.2	-76.4	100	100	100	100	92.6	-7.4
Iceland	IS	*no d.*	0	0	0	0	0	*no d.*	0	0	0	0	0
Ireland	IE	0	0	0	0	0	0	0	0	0	0	0	0
Italy	IT	100.0	84.0	83.8	91.2	67.9	-23.3	100	100	100	100	100	0
Latvia	LV	0	0	0	0	0	0	39.9	0	0	0	0	0
Liechtenstein	LI	100	7.7	100	0	100	100	100	100	100	100	100	0
Lithuania	LT	0	0	0	0	0	0	55.1	0	0	0	0	0
Luxembourg	LU	100	0	0	0	26.8	26.8	100	64.8	7.4	100	94.9	-5.1
Macedonia, FYR of	MK	100	100	99.8	100	1.3	-98.7	100	100	100	100	100	0
Malta	MT	99	99.1	100	100	100	0	100	100	100	100	100	0
Monaco	MC	100	92.3	0	100	100	0	100	100	100	100	100	0
Montenegro	ME	*no d.*	100	94.2	100	26.4	-73.6	*no d.*	100	100	100	100	0
Netherlands	NL	53.3	0	0	0	0	0	87.7	0	0	0	0	0
Norway	NO	*no d.*	0	0	0	0	0	*no d.*	0.2	0.0	0	0	0
Poland	PL	94.4	21.2	38.9	0	0	0	100	65.3	81.7	70.0	27.3	-42.6
Portugal	PT	87.7	0	2	0	41.5	41.5	100	91.1	89.1	95.7	99.7	4.0
Romania	RO	10.4	97.0	9.9	21.5	0	-21.5	98.8	100	99.6	100	80.8	-19.2
San Marino	SM	100	100	100	100	100	0	100	100	100	100	100	0
Serbia (incl. Kosovo)	RS	*no d.*	100	67.4	100	2.9	-97.1	*no d.*	100	100	100	100	0
Slovakia	SK	99.1	99.7	78.7	58.4	0.2	-58.2	100	100	100	100	90.8	-9.2
Slovenia	SI	100	100	95.6	73.1	100	26.9	100	100	100	100	100	0
Spain	ES	93.3	27.2	58.5	35.1	60.7	25.6	99.4	94.3	89.8	88.4	93.3	4.9
Sweden	SE	12.6	0	0	0	0	0	31.2	0.0	0	0	0	0
Switzerland	CH	*no data*		67.4	10.0	98.1	88.1	*no data*		100	99.9	100	0.1
United Kingdom	UK	14.4	0	0	0	0	0	11.0	0	0	0	0	0
Total		**69.1**	**35.7**	**37.8**	**26.0**	**21.3**	**-4.7**	**69.4**	**48.4**	**50.2**	**49.2**	**49.3**	**0.1**
Northern		3.6	0	0	0	0	0	22.9	0.0	0	0.0	0	0
North-western		49.4	0.1	2.0	2.0	33.0	31.0	79.8	27.8	23.3	29.9	59.7	29.8
Central & eastern		76.8	50.3	47.2	17.4	11.0	-6.4	99.7	86.1	94.0	88.5	75.4	-13.1
Southern		93.9	55.3	63.5	60.4	56.8	-3.6	99.7	94.2	93.1	92.8	97.8	5.0

Note: Lack of land cover data in 2006: CH, IS, ME, NO, RS; in 2007: CH.

6.3.3 Uncertainties

Uncertainty estimated by cross-validation

In Table 6.9 the absolute mean uncertainty (RMSE) obtained by cross-validation is 5198 µg.m^{-3}.h for the AOT40 for crops and 8384 µg.m^{-3}.h for the AOT40 for forests. It indicates that the year 2010 has slightly higher absolute mean uncertainties for the crops than in 2009 (5138 µg.m^{-3}.h), while lower than in the previous years: 5283 µg.m^{-3}.h (2008), 5876 µg.m^{-3}.h (2007), 7674 µg.m^{-3}.h (2006) and 7700 µg.m^{-3}.h (2005). For forests it is lower than the values 9311 µg.m^{-3}.h (2009), 8750 µg.m^{-3}.h (2008), 10190 µg.m^{-3}.h (2007), 11990 µg.m^{-3}.h (2006) and 12500 µg.m^{-3}.h (2005). The relative mean uncertainties of the 2010 maps of ozone indicators AOT40 for crops and AOT40 for forests were both about 31%. For crops, that is lower than in 2009 (38 %), 2007 (40 %) and 2005 (41 %) and roughly the same as in 2008 (31 %) and 2006 (30%). For forests, the relative RMSE is less than all previous years 2009 (34 %), 2008 (34 %), 2007 (37 %), 2006 (34 %) and 2005 (41%). Table 7.7 summarises both the absolute and the relative uncertainties over these past six years.

Figure 6.12 shows the cross-validation scatter plots of the AOT40 for both crops and forests. R^2 indicates that for AOT40 for crops about 67 % and for AOT40 for forests about 69 % of the variability is attributable to the interpolation. The corresponding values for the 2009 maps (69 % and 68 %), 2008 maps (53 % and 56 %), 2007 maps (63 % and 67 %), the 2006 maps (47 % and 49 %) and 2005 maps (55 % and 58 %), indicates a somewhat increased level of interpolation performance at the 2009 and 2010 maps compared to those of previous years.

The cross-validation scatter plots show again that in areas with higher accumulated ozone concentrations the interpolation methods tend to deliver underestimated predicted values. For example, in agricultural areas (Figure 6.12, left panel) an observed value of 30 000 µg.m^{-3}.h is estimated in the interpolation as about 25 000 µg.m^{-3}.h, i.e. an underestimation of about 16 %. In addition, an overestimation at the lower end of predicted values occurred. One could reduce this under- and overestimation by extending the number of measurement stations and by optimising the spatial distribution of those stations, specifically in areas with elevated values.

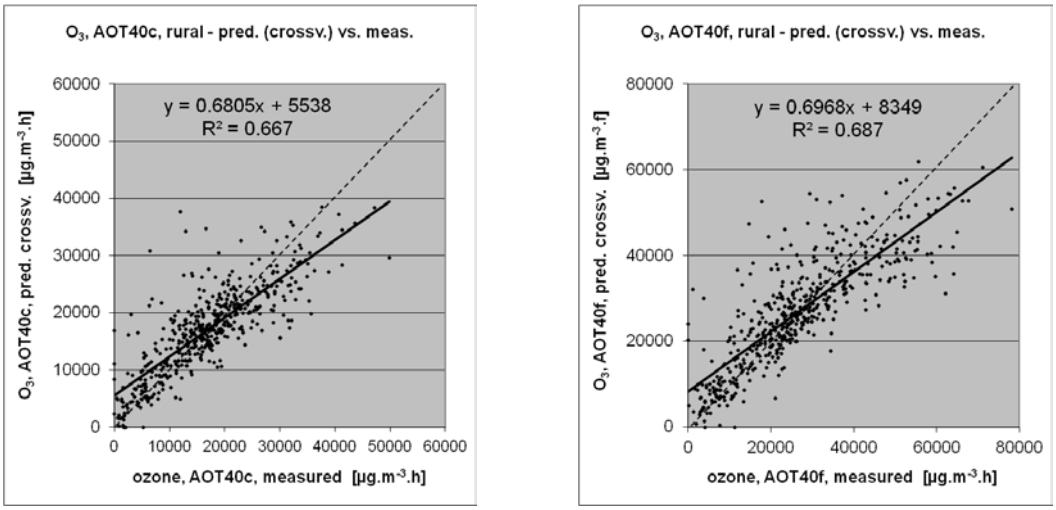

Figure 6.12 Correlation between cross-validation predicted values (y-axis) and measurements (x-axis) for the ozone indicators AOT40 for crops (left) and AOT40 for forests (right) for rural areas in 2010.

Comparison of point measurement values with the predicted grid value

In addition to the point observation - point prediction cross-validation, a simple comparison was made between the point measurements and interpolated predicted grid values on the grid of 2 km^2 resolution. The results of the cross-validation compared to the gridded validation are summarised in Table 6.13.

The table shows for both receptors a better correlation between the station measurements and the averaged interpolated predicted values of the corresponding grid cells (case ii) than it does at the point cross-validation predictions (case i) of Figure 6.12. Case ii) represents the uncertainty in the predicted gridded interpolation map at the actual station locations (points) itself, whereas the point observation – point prediction cross-validation of case i) simulates the behaviour of the interpolation at point positions without actual measurements within the area covered by measurements. The uncertainty at measurement locations has partly its cause in the smoothing effect of interpolation and partly in the spatial averaging of the values in the 2x2 km grid cells. In such situations the degree of smoothing leading to underestimation at areas with high values is smaller than it is in case no measurement is present in such areas. For example, in agricultural areas a predicted interpolation grid value will be about 28 000 µg.m^{-3}.h at a corresponding station point with an observed value of 30 000 µg.m^{-3}.h, i.e. an underestimation of about 7 %. This is lower than the likely underestimation of about 16% in areas where no measurements exist, as discussed in the previous subsection.

Table 6.13 Linear regression equation and coefficient of determination R^2 from the scatter plots of (i) the predicted point values based on cross-validation and (ii) aggregation into 2x2 km grid cells versus the measured point values for ozone indicators AOT40 for crops (left) and AOT40 for forests (right) for rural areas in 2010.

	AOT40 for crops		AOT40 for forests	
	equation	R^2	equation	R^2
i) cross-validation prediction (Fig 6.12)	y = 0.681x + 5538	0.667	y = 0.697x + 8349	0.687
ii) 2x2 km grid prediction	y = 0.820x + 3109	0.893	y = 0.840x + 4399	0.915

The AOT40 for crops with a target value of 18 000 µg.m^{-3}.h would allow us to prepare a probability of exceedance map. However, we limited the preparation of such maps to the human health related indicators, thus not involving the accumulative ozone indicators used in the EEA CSI005 (itself not demanding such maps).

7 Concluding exposure and uncertainty estimates

Mapping and exposure results

This paper presents the interpolated maps for 2010 on the PM_{10}, $PM_{2.5}$ and ozone human health related air pollution indicators, together with their frequency distribution of the estimated population exposures and exceedances. It concerns the annual average and the 36th highest daily mean for PM_{10}, annual average for $PM_{2.5}$, and the 26th highest daily maximum 8-hour value and the SOMO35 for ozone. Interpolated maps on the vegetation/ecosystem based ozone indicators AOT40 for crops and AOT40 for forests are additionally presented, including their frequency distribution of estimated land area exposures and exceedances. A mapping approach similar to previous years (De Smet et al. 2011 and references cited therein, Denby et al. 2011b) on observational data was used. For the first time, interannual difference maps are presented, for PM_{10} and ozone indicators.

Human health PM_{10} indicators

Table 7.1 summarises for both *human health PM_{10} indicators* the average concentration the European inhabitant is exposed to, i.e. the population-weighted concentration and the number of Europeans exposed to PM_{10} concentrations above their limit values (LV) for the years 2005 to 2010. The table presents the results obtained from both the 10x10 km resolution fields, as used in previous data years up to 2007 and the 1x1 km resolution grid as tested with the 2006 data in Horálek et al (2010), recomputed for 2007 and implemented fully on the 2008 data and onwards. This indicates that the underestimated predictions of PM_{10} values caused by merging rural and urban predictions at 10x10 km resolution have been resolved better when using the higher 1x1 km grid resolution. In other words, an increased merging resolution contributes to a quantitatively better population exposure estimate due to better-resolved spatially smaller urbanised patterns in the map.

Table 7.1 Percentage of the total European population exposed to PM_{10} concentrations above the limit values (LV) and the population-weighted concentration for the human health PM_{10} indicators annual average and 36th highest daily average for 2005 to 2010.

PM10			2005	2006	2007	2008	2009	2010
Annual average								
Population-weighted concentration	(µg.m^{-3})	10x10 merger	26.3	27.1	25.3			
		1x1 merger		28.5	26.2	24.8	24.6	24.3
Population exposed > LV (40 µg.m^{-3})	(% of total)	10x10 merger	9.3	7.7	5.7			
		1x1 merger		10.32	6.796	5.8	6.0	5.2
36th max. daily average								
Population-weighted concentration	(µg.m^{-3})	10x10 merger	43.8	45.4	42.4			
		1x1 merger		47.8	44.11	41.3	41.2	41.87
Population exposed > LV (50 µg.m^{-3})	(% of total)	10x10 merger	28.1	28.5	22.0			
		1x1 merger		35.7	26.19	19.4	16.5	20.64

The population exposed to *annual mean* concentrations of PM_{10} above the limit value of 40 µg.m^{-3} is at least 5 % of the total population in 2010, slightly less than in 2009. Furthermore, it is estimated that European inhabitants living in background (neither hot-spot nor industrial) areas – without regard to urban or rural – are, as in 2009, exposed on average to the annual mean PM_{10} concentration of about 24 µg.m^{-3}. In comparison with the previous three years, the number of people living in the areas above the LV tends to go down slightly. It is not possible to talk about a trend when taking into account (i) the meteorologically induced variations and (ii) the uncertainties involved in the interpolation. Longer time series and reduced uncertainties will be needed before any conclusions on a possible trend can be drawn.

In 2010 at least 20 % of the European population lived in areas where the PM_{10} limit value of 50 µg.m^{-3} for the *36th highest daily mean* is exceeded, being some 4 % higher than in 2009, 1 % higher

than in 2008, 6 % lower than in 2007, and 15 % lower than in 2006. The overall European population-weighted concentration of the 36th highest daily mean for the background areas is estimated at about 42 µg.m^{-3}, which is the slightly more than in 2008 and 2007. Compared to 2006 and 2007 it is less. Comparing the observed (and also predicted) exceedances for both PM_{10} indicators, one can conclude that the daily limit value is the most stringent throughout the years.

Human health $PM_{2.5}$ indicator

Table 7.2 summarises for *human health $PM_{2.5}$ indicator* (annual average) the population-weighted concentration and the number of Europeans exposed to $PM_{2.5}$ concentrations above its target value (TV) for the years 2007 to 2010 (without 2009, for which nor the map nor the population exposure were prepared).

Table 7.2 Percentage of the total European population exposed to $PM_{2.5}$ concentrations above the target value (TV) and the population-weighted concentration for the human health $PM_{2.5}$ indicator annual average for 2007 to 2010.

PM2.5			2007	2008	2009	2010
Annual average						
Population-weighted concentration	(µg.m^{-3})	10x10 merger	15.5	15.6		
		1x1 merger	16.3	16.3		16.8
Population exposed > TV (25 µg.m^{-3})	(% of total)	10x10 merger	6.2	6.2		
		1x1 merger	7.8	7.6		8.3

The proportion exposed to annual mean concentrations of $PM_{2.5}$ above the target value of 25 µg.m^{-3} is at least 8 % of the total population in 2010, which is slightly more than in 2007 and 2008. Furthermore, it is estimated that European inhabitants living in background (neither hot-spot nor industrial) areas – without regard to urban or rural – are exposed on average to the annual mean $PM_{2.5}$ concentration of about 17 µg.m^{-3}. In comparison with the previous years, the number of people living in the areas above the TV seems to increase slightly.

Human health ozone indicators

Table 7.3 summarises the levels of both *human health ozone indicators* that European inhabitants are exposed to, i.e. population-weighted concentrations. Furthermore, it presents the number of Europeans exposed to concentrations above the target value (TV) of the 26th highest daily maximum 8-hour mean and above a level of 6 mg.m^{-3}.d for the SOMO35 for the years 2005 to 2010.

Table 7.3 Percentage of the total European population exposed to ozone concentrations above the target value (TV) for the 26th highest daily maximum 8-hour average and an indicative chosen threshold for SOMO35, including their population-weighted concentrations for2005 to 2010.

Ozone			2005	2006	2007	2008	2009	2010
26th highest daily max. 8-hr average								
Population-weighted concentration	(µg.m^{-3})	10x10 merger	112.9	119.6	112.1			
		1x1 merger		118.2	110.7	109.8	108.1	106.7
Population exposed > TV (120 µg.m^{-3}.h)	(% of total)	10x10 merger	37.8	55.5	33.5			
		1x1 merger		51.4	27.1	15.0	16.0	16.4
SOMO35								
Population-weighted concentration	(µg.m^{-3})	10x10 merger	5047	5485	4679			
		1x1 merger		5167	4411	4275	4275	3915
Population exposed > 6 mg.m^{-3}.d	(% of total)	10x10 merger	33.9	37.4	32.6			
		1x1 merger		29.5	28.07	19.6	24.6	16.3

The table presents the results obtained with the merging resolution of 10x10 km, as used at previous data years up to 2007, and the 1x1 km merging resolution as tested on the 2006 data in Horálek et al (2010) and implemented fully on the 2008 data and onwards. It provides an indication that the

underestimation of ozone values when merged with the 10x10 km grid resolution has been resolved better when using a higher 1x1 km grid resolution. In other words, an increased merging resolution contributes to a quantitatively better population exposure estimate due to better-resolved spatially smaller urbanised patterns in the map.

For the ozone indicator *26th highest daily maximum 8-hour mean* it is estimated that at least 16 % of the population lived in 2010 in areas above the ozone target value (TV) of 120 µg.m^{-3}, which was similar to that of 2009. The overall European population-weighted ozone concentration in terms of the 26th highest daily maximum 8-hour mean in the background areas is estimated at almost 107 µg.m^{-3} and is therefore close to that of 2009 (108 µg.m^{-3}). Compared to the previous years 2005 – 2007, one could conclude that 2006 is a year with elevated ozone concentrations, leading to increased exposure levels compared to the other five years. Additionally, the population exposed to ozone level above the target value is in 2008 – 2010 substantially lower than in the preceding period 2007 – 2005.

A similar tendency is observed for the *SOMO35*: In 2006 – 2007 almost one-third of the population lived in areas where a level of 6 mg.m^{-3}.d$^{(*)}$ was exceeded, with the highest level in 2006. In 2008 it concerns only one-fifth of the population, a quarter in 2009, and one-sixth in 2010. The population-weighted SOMO35 concentrations shows quite a similar pattern in time, with a decrease in 2010 in south-eastern Europe.

(*) Note that the 6 mg.m^{-3}.d does not represent a health-related legally binding 'threshold'. In this and previous papers it concerns a somewhat arbitrarily chosen threshold to facilitate the discussion of the observed distributions of SOMO35 levels in their spatial and temporal context. This choice is based on a comparison of the 26th highest daily max. 8-hour means versus the SOMO35 of the ozone concentration measurements at all background stations in The Netherlands. The SOMO35 is estimated to be about 4 mg.m^{-3}.d when no Dutch population is exposed to ozone concentrations above the target value of the 26th h.d.m.8-hour mean. The Netherlands has in general relative low ozone concentrations compared to most other European countries. Over the years we applied the level of 6 mg.m^{-3}.d in our discussions of the annual results for two reasons: (i) to compensate for a possible underestimation of the SOMO35, and (ii) to match with a class interval limit of the SOMO35 map (Figure 6.5).

Agricultural and forest ozone indicators

Exposure indicators describing the *agricultural and forest areas exposed to accumulated ozone* concentrations above defined thresholds are summarised in Table 7.4. Those thresholds are the target value (TV) of 18 mg.m^{-3}.h and the long-term objective (LTO) of 6 mg.m^{-3}.h for the AOT40 for crops, and the Reporting Value (RV) of 20 mg.m^{-3}.h and the Critical Level (CL) of 10 mg.m^{-3}.h for the AOT40 for forests.

Table 7.4 Percentages of the total European agricultural and forest area exposed to ozone concentrations above their thresholds: target value (TV) and long-term objective (LTO) for AOT40 for crops, and Critical Level (CL) and Reporting Value (RV) for AOT40 for forests for2005 to 2010.

Ozone		2005	2006	2007	2008	2009	2010
AOT40 for crops							
Agricultural area % > TV (18 mg.m^{-3}.h)	(% of total)	48.5	69.1	35.7	37.8	26.0	21.3
Agricultural area % > LTO (6 mg.m^{-3}.h)	(% of total)	88.8	97.6	77.5	95.5	81.0	85.4
AOT40 for forests							
Forest area exposed > RV (20 mg.m^{-3}.h)	(% of total)	59.1	69.4	48.4	50.2	49.2	49.3
Forest area exposed > CL (10 mg.m^{-3}.h)	(% of total)	76.4	99.8	62.1	79.6	67.4	63.4

In 2010, 21% of all agricultural land (*crops*) was exposed to accumulated ozone concentrations exceeding the target value (TV) and 85 % was exposed to levels in excess of the long-term objective (LTO). Compared to the previous five years one could conclude that 2006 was a year with elevated ozone concentrations, leading to increased exposure levels above the target value and that they subsided in the period 2007 – 2010 to levels clearly below those of 2005. On the other hand, the percentage of the total area exposed to levels above the long-term objective (LTO) is in 2007 lowest compared to all the other years.

For the ozone indicator AOT40 for *forests* the level of 20 $mg.m^{-3}.h$ (Reporting Value, RV) was in 2010 exceeded in almost half of the European forest area, which is similar to 2007 – 2009 and clearly below the percentages of the years 2005 and 2006. The forest area exceeding the Critical Level was in 2010 about 63 %, which is roughly the same as in 2007 (62 %), slight below 2009 (67 %), well below 2008 and 2005 with 76 – 80 % exceedance, and 2006 when all forest area was exceeded.

The temporal pattern of the AOT40 for forests exceedances shows some similarity with those of the AOT40 for crops, despite their different definitions. This annual variability is heavily dependent on meteorological variability.

Uncertainty results

Next to the creation of European wide interpolated air pollutant maps and exposure tables, we evaluated the uncertainty of the presented concentration maps and maps with estimated probability of threshold exceedance for the human health indicators. As exactly the same method and data sources have been applied over the years 2005 to 2010, a change in uncertainty is in principle related to the data content itself. However, for the 2008 data we implemented for the first time an increased resolution (from a 10x10 km into 1x1 km grid field) at the merging of the separate human health indicator interpolated maps (on 10x10 km grid) into one combined final 1x1 km gridded indicator map. The merging made use of the 1x1 km population density map. (The subsequent exposure estimates however, have been based on the 10x10 km grid fields, aggregated from the 1x1 km grids of the merging result). The increased merging resolution should in principle improve the accuracy in the concentration maps, including the subsequent exposure estimates. Denby et al. (2008) discusses a diversity of uncertainty factors potentially involved, including their possible levels of influence. More background information on causes of uncertainties and their assessment can be found in Malherbe et al (2012). The paper recommends options to reduce uncertainties systematically. Horálek et al. (2010) explored specific options to reduce interpolation uncertainty related to the spatial resolutions applied at the different process steps of the mapping method. This paper concludes and justifies the implementation of the increased merging grid as the most significant uncertainty reduction measure, against the least additional computational demands.

Table 7.5 summarises the absolute and relative mean interpolation uncertainties of the PM_{10} maps for the six-year sequence. The uncertainties in 2007 are slightly lower for the most of the indicators than in the other five years; this is probably given by the better fit of the linear regression with supplementary data in 2007 compared to the other years. The higher uncertainty levels for urban areas in the years 2008 - 2010, compared to the years 2007 – 2005, are caused specifically by addition of Turkish urban background stations reported only since 2008.

Table 7.5 Absolute mean uncertainty (RMSE, $\mu g.m^{-3}$) and relative mean uncertainty (RMSE relative to mean indicator value, in %) for the total European rural and urban areas for PM_{10} annual average and the 36th highest daily average for the years 2005 – 2010.

PM10			2005	2006	2007	2008	2009	2010
Annual average								
rural areas	abs. mean uncertainty	RMSE ($\mu g.m^{-3}$)	5.5	5.8	4.6	5.0	4.6	4.5
	rel. mean uncertainty	(%)	*25.9*	*26.6*	*23.5*	*27.2*	*23.9*	*22.7*
urban areas	abs. mean uncertainty	RMSE ($\mu g.m^{-3}$)	5.5	6.1	5.0	6.3	6.7	6.6
	rel. mean uncertainty	(%)	*20.0*	*20.9*	*18.4*	*22.4*	*23.0*	*22.5*
36th max. daily average								
rural areas	abs. mean uncertainty	RMSE ($\mu g.m^{-3}$)	9.7	9.9	8.0	8.8	8.0	8.6
	rel. mean uncertainty	(%)	*26.3*	*26.6*	*23.5*	*28.2*	*24.1*	*24.4*
urban areas	abs. mean uncertainty	RMSE ($\mu g.m^{-3}$)	9.9	11.7	9.1	12.7	13.2	12.2
	rel. mean uncertainty	(%)	*21.4*	*23.5*	*19.6*	*24.4*	*26.7*	*23.7*

Table 7.6 presents the uncertainty results for $PM_{2.5}$ maps for the years 2007 – 2010 (without non-mapped year 2009). Both absolute and relative uncertainties show decrease in 2010, in comparison with the previous years.

Table 7.6 Absolute and relative mean uncertainty for the total European rural and urban areas for $PM_{2.5}$ annual average, for the years 2007 – 2010.

PM2.5			2007	2008	2009	2010
Annual average						
rural areas	abs. mean uncertainty	RMSE (µg.m^{-3})	3.3	3.5	not	3.4
	rel. mean uncertainty	(%)	*27.4*	*29.8*	mapped	*25.0*
urban areas	abs. mean uncertainty	RMSE (µg.m^{-3})	4.1	3.6	not	3.1
	rel. mean uncertainty	(%)	*23.7*	*20.0*	mapped	*16.8*

The relative mean interpolation uncertainty of the ozone maps in Table 7.7 at the rural areas decreased slightly for the most of the indicators in 2010, compared to previous years. The exception is the 26th highest daily maximum 8-hour average with a slight increase in relative uncertainty. The relative uncertainties of the health indicators for the urban areas decreased in 2010 somewhat compared to previous years. In the case of AOT40 for crops where the absolute uncertainty increases and simultaneously the relative uncertainty decreases, the absolute mean of the indicator (taken across Europe) has increased relatively more than its absolute RMSE.

Table 7.7 Absolute and relative mean uncertainty for the total European areas for ozone the 26th highest daily maximum 8-hour average, SOMO35, AOT40 for crops and for forests, for the years 2005 – 2010.

Ozone			2005	2006	2007	2008	2009	2010
26th highest daily max. 8-hr average								
rural areas	abs. mean uncertainty	RMSE (µg.m^{-3})	12.3	11.2	8.8	8.7	8.2	9.0
	rel. mean uncertainty	(%)	*10.3*	*8.9*	*7.5*	*7.6*	*7.2*	*7.8*
urban areas	abs. mean uncertainty	RMSE (µg.m^{-3})	10.0	10.2	8.9	8.8	9.3	9.2
	rel. mean uncertainty	(%)	*8.9*	*8.4*	*7.9*	*7.9*	*8.4*	*8.2*
SOMO35								
rural areas	abs. mean uncertainty	RMSE (µg.m^{-3}.d)	2173	2077	1801	1609	1635	1604
	rel. mean uncertainty	(%)	*35.5*	*31.6*	*33.3*	*30.7*	*29.7*	*29.5*
urban areas	abs. mean uncertainty	RMSE (µg.m^{-3}.d)	1459	1472	1260	1293	1475	1270
	rel. mean uncertainty	(%)	*32.0*	*29.2*	*29.5*	*31.3*	*33.1*	*29.5*
AOT40 for crops								
rural areas	abs. mean uncertainty	RMSE (µg.m^{-3}.h)	7677	7674	5876	5283	5138	5198
	rel. mean uncertainty	(%)	*40.7*	*29.6*	*39.6*	*31.3*	*37.7*	*30.8*
AOT40 for forests								
rural areas	abs. mean uncertainty	RMSE (µg.m^{-3}.h)	12474	11990	10190	8750	9304	8384
	rel. mean uncertainty	(%)	*41.5*	*33.6*	*37.1*	*34.0*	*33.9*	*31.4*

The scatter plots of the interpolation results versus the measurements show that for both the PM_{10} and the ozone indicators, in areas with high values, an underestimation of the predicted values occurs. This also leads to a considerable underestimation at locations without measurements and at areas with the higher concentrations. This effect occurs most prominently for the ozone indicators. We expect that the underestimation would reduce when an improved fit of the linear regression with (other) supplementary data could be obtained. For example, in the near future more contributions from satellite imagery data and interpretation techniques could be expected. An option is to extend the number of measurement stations and/or using additional mobile stations (e.g. in measurement campaigns). For further reading on this subject, we refer to Denby et al. (2009), Gerharz et al. (2011) and Gräler et al. (2012).

Probability of exceedance

Maps with the probability of exceedance of Limit Values and Target Value have been prepared for the human health indicators of PM_{10}, $PM_{2.5}$, and ozone, respectively. These probability maps, with a class distribution as defined in Table 4.5, are derived from combining the indicator map and its uncertainty map following the same method throughout the years 2005 to 2010. The differences in the maps between years depend on annual fluctuations in concentration levels, supplementary data and their involved uncertainties (Denby et al. 2009, Gerharz et al. 2011, and Gräler et al. 2012). Some disruption or 'jump' could be expected between the data of 2005 – 2007 and 2008 – 2010. This would be caused by the increased merging resolution applied for the first time on the 2008 data. As Horálek et al. (2010) indicated, it should improve the population exposure estimates, specifically for population living in urban areas (that profit most of this methodological refinement). Nevertheless, as the maps are spatially merged into 10x10 km grid resolution, the influence of the urban pollution into the final map is smaller than was in the methodology used until 2007. Thus, it is needed to bear in mind that the spatial average of a 10x10 km grid cell can show low probability of exceedance even though some smaller (e.g. urban) areas inside such a grid cell would show high probability of exceedance (using finer grid cell resolution).

In 2010 for the annual average PM_{10}, the patterns in the spatial distribution of the different probability of exceedance (PoE) classes over Europe were similar to those of 2009. However, the region of southern Poland – north-eastern Czech Republic with the industrial zones of Katowice and Ostrava showed a larger area with high PoE values in comparison with 2009. Contrary to that, the Po valley in Italy showed a lower probability of exceedance, in comparison with 2009.

The 36^{th} highest daily means of PM_{10} do show an increase in the spatial extents and PoE levels throughout central and south-eastern Europe, in comparison with PoE of 2008 and 2009. An increase in the spatial extents and PoE levels throughout central and south-eastern Europe occurred in 2010. In particular, large areas of Poland, Slovakia, Hungary, Serbia, Bulgaria, Greece and Cyprus have increased PoE. The Po valley in northern Italy has quite a similar PoE pattern to 2009. Western Belgium and north-western France have decreased levels of PoE.

PoE map for $PM_{2.5}$ is presented for the first time. The areas with the highest probability of TV exceedance include the region of southern Poland – north-eastern Czech Republic (with the industrial zones of Krakow, Katowice and Ostrava), the central part of Poland, and the Po valley in northern Italy with Turin and Milan. In south-eastern Europe, where relatively few measurement stations are located, increased PoE do occur in some urban areas or larger agglomerations. In the other parts of Europe, there exists little likelihood of exceedance.

Interpreting 2010 and its preceding five years, one can conclude for ozone that in 2006 the probability of exceedance (PoE) increased temporarily in most parts of Europe. In 2007 – 2010, a decrease took place in the levels of PoE, to levels in many areas well below those of 2005. In 2010, most of the areas with large PoE in the southern and south-western regions of Europe did not change compared to 2009. Simultaneously, the areas with large PoE extended somewhat in Switzerland, south-western Germany, south-eastern France and on the Iberian Peninsula. Furthermore, the increase in PoE on the Iberian Peninsula continued to levels above 50 %. In eastern and south-eastern Europe there were clear decreases of PoE of ozone target value.

References

AirBase, European air quality database, http://airbase.eionet.europa.eu

Cressie N (1993). Statistics for spatial data. Wiley series, New York.

De Leeuw F, Ruyssenaars P (2011). Evaluation of current limit and target values as set in the EU Air Quality Directive. ETC/ACM Technical Paper 2011/3. http://acm.eionet.europa.eu/reports/ETCACM_TP_2011_3_evaluationAQ_LV_LT

Denby B, Schaap M, Segers A, Builtjes P, Horálek J (2008). Comparison of two data assimilation methods for assessing PM_{10} exceedances on the European scale. Atmospheric Environment 42, 7122–7134.

Denby B, De Leeuw F, De Smet P, Horálek J (2009). Sources of uncertainty and their assessment in spatial mapping, ETC/ACC Technical Paper 2008/20. http://acm.eionet.europa.eu/reports/ETCACC_TP_2008_20_spatialAQ_uncertainties

Denby B, Gola G, De Leeuw F, De Smet P, Horálek J (2011a). Calculation of pseudo PM2.5 annual mean concentrations in Europe based on annual mean PM10 concentrations and other supplementary data. ETC/ACC Technical Paper 2010/9. http://acm.eionet.europa.eu/reports/ETCACC_TP_2010_9_pseudo_PM2.5_stations

Denby B, Horálek J, de Smet P, de Leeuw F (2011b). Mapping annual mean $PM_{2.5}$ concentrations in Europe: application of pseudo $PM_{2.5}$ station data. ETC/ACM Technical Paper 2011/5. http://acm.eionet.europa.eu/reports/ETCACM_TP_2011_5_spatialPM2.5mapping

De Smet P, Horálek J, Coňková M, Kurfürst P, de Leeuw F, Denby B (2009). European air quality maps of ozone and PM10 for 2006 and their uncertainty analysis. ETC/ACC Technical Paper 2008/8. http://acm.eionet.europa.eu/reports/ETCACC_TP_2008_8_spatAQmaps_2006

De Smet P, Horálek J, Coňková M, Kurfürst P, de Leeuw F, Denby B (2010). European air quality maps of ozone and PM10 for 2007 and their uncertainty analysis. ETC/ACC Technical Paper 2009/9. http://acm.eionet.europa.eu/reports/ETCACC_TP_2009_9_spatAQmaps_2007

De Smet P, Horálek J, Coňková M, Kurfürst P, de Leeuw F, Denby B (2011). European air quality maps of ozone and PM10 for 2008 and their uncertainty analysis. ETC/ACC Technical Paper 2010/10. http://acm.eionet.europa.eu/reports/ETCACC_TP_2010_10_spatAQmaps_2008

De Smet P, Horálek J, Schreiberová M, Kurfürst P, de Leeuw F (2012). European air quality maps of ozone and PM10 for 2009 and their uncertainty analysis. ETC/ACM Technical Paper 2011/11. http://acm.eionet.europa.eu/reports/ETCACM_TP_2011_11_spatAQmaps_2009

EBAS, Database of atmospheric chemical composition and physical properties http://ebas.nilu.no/

EC (2008). Directive 2008/50/EC of the European Parliament and of the Council of 21 May 2008 on ambient air quality and cleaner air for Europe. OJ L 152, 11.06.2008, 1-44. http://eur-lex.europa.eu/LexUriServ/LexUriServ.do?uri=OJ:L:2008:152:0001:0044:EN:PDF

ECMWF: Meteorological Archival and Retrieval System (MARS). It is the main repository of meteorological data at ECMWF (European Centre for Medium-Range Weather Forecasts). http://www.ecmwf.int/

EEA (2012). Corine land cover 2000 (CLC2000) raster data. 100x100m gridded version 16 (04/2012). http://www.eea.europa.eu/data-and-maps/data/corine-land-cover-2000-raster-2

EEA (2011). Guide for EEA map layout. EEA operational guidelines. August 2011, version 4. http://www.eionet.europa.eu/gis/docs/GISguide_v4_EEA_Layout_for_map_production.pdf

EEA (2008). ORNL Landscan 2008 Global Population Data conversion into EEA ETRS89-LAEA5210 1km grid resolution (eea_r_3035_1_km_landscan-eurmed_2008, by Hermann Peifer of EEA; contact person Paul Hasenohr, EEA).

Eurostat (2012). Total population for European states for 2010. http://epp.eurostat.ec.europa.eu/tgm/table.do?tab=table&language=en&pcode=tps00001&tableSelection=1&footnotes=yes&labeling=labels&plugin=1

Fagerli H, et al (2012). Transboundary acidification, eutrophication and ground level ozone in Europe in 2010. EMEP Report 1/2012. http://emep.int/publ/reports/2012/status_report_1_2012.pdf

Gerharz L, Gräler B, Pebesma E (2011). Measurement artefacts and inhomogeneity detection, ETC/ACM Technical Paper 2011/8. http://acm.eionet.europa.eu/reports/ETCACM_TP_2011_8_artefacts_inhom_detection

Gräler B, Gerharz L, Pebesma E (2012). Spatio-temporal analysis and interpolation of PM_{10} measurements in Europe, ETC/ACM Technical Paper 2011/10. http://acm.eionet.europa.eu/reports/ETCACM_TP_2011_10_spatio-temp_AQinterpolation

Horálek J, Kurfürst P, Denby B, de Smet P, de Leeuw F, Brabec M, Fiala J (2005). Interpolation and assimilation methods for European scale air quality assessment and mapping. Part II: Development and testing new methodologies. ETC/ACC Technical paper 2005/8. http://acm.eionet.europa.eu/docs/ETCACC_TechnPaper_2005_8_SpatAQ_Part_II.pdf

Horálek J, Denby B, de Smet PAM, de Leeuw FAAM, Kurfürst P, Swart R, van Noije T (2007). Spatial mapping of air quality for European scale assessment. ETC/ACC Technical paper 2006/6. http://acm.eionet.europa.eu/reports/ETCACC_TechnPaper_2006_6_Spat_AQ

Horálek J, de Smet PAM, de Leeuw FAAM, Denby B, Kurfürst P, Swart R, (2008). European air quality maps including uncertainty analysis. ETC/ACC Technical paper 2007/7. http://acm.eionet.europa.eu/reports/ETCACC_TP_2007_7_spatAQmaps_ann_interpol

Horálek J, de Smet PAM, de Leeuw FAAM, Coňková M, Denby B, Kurfürst P (2010). Methodological improvements on interpolating European air quality maps. ETC/ACC Technical Paper 2009/16. http://acm.eionet.europa.eu/reports/ETCACC_TP_2009_16_Improv_SpatAQmapping

JRC (2009). population density data 2009. Population density disaggregated with Corine land cover 2000. 100x100 m grid resolution, EEA version pop01clcv5.tif of 24 Sep 2009. http://www.eea.europa.eu/data-and-maps/data/population-density-disaggregated-with-corine-land-cover-2000-2

Malherbe L, Ung A, Colette A, Debry E (2012). Formulation and quantification of uncertainties in air quality mapping, ETC/ACM Technical Paper 2001/9. http://air-climate.eionet.europa.eu/reports/ETCACM_TP_2011_9_AQmapping_uncertainties

Mareckova K, Wankmüller R, Whiting R, Pinteris M (2012). Inventory Review 2012. Review of emission data reported under the LRTAP Convention and NEC Directive. Stage 1 and 2 Review. EEA/CEIP Technical Report. http://www.ceip.at/fileadmin/inhalte/emep/pdf/2012/InventoryReport2012_forWeb.pdf

Mol W, van Hooydonk P (2012). European exchange of monitoring information and state of the air quality in 2010. ETC/ACM Technical Paper 2012/1. http://acm.eionet.europa.eu/reports/ETCACM_TP_2012_1_EoI_AQ_meta_info2010

ORNL (2008). ORNL LandScan high resolution global population data set. http://www.ornl.gov/sci/landscan/landscan_documentation.shtml

Simpson D, Fagerli H, Jonson JE, Tsyro S, Wind P, Tuovinen J-P (2003). Transboundary acidification and eutrophication and ground level ozone in Europe: Unified EMEP model description. EMEP Status Report 1/03 Part I. MNP, Oslo, Norway. http://www.emep.int/publ/reports/2003/emep_report_1_part1_2003.pdf

Simpson D, Bergstöm R, Fagerli H, Tsyro S, Valdebenito Á, Wind P (2012). Chapter 9 Model Updates. In: Transboundary Acidification, Eutrophication and Ground Level Ozone in Europe in 2010, EMEP Report 1/2012. http://emep.int/publ/reports/2012/status_report_1_2012.pdf

UNECE (2004). Mapping Manual 2004. Manual on methodologies and criteria for Modelling and Mapping Critical Loads ands Levels and Air Pollution Effects, Risks and Trends. United Nations – Economic Commission for Europe, LRTAP Convention. http://www.oekodata.com/icpmapping/htm/manual/manual_eng.htm

UN (2010). World Population Prospects - The 2010 Revision, Highlights. United Nations. Department of Economic and Social Affairs, Population Division. New York. http://esa.un.org/unpd/wpp/index.htm